# AN INVESTIGATION INTO THE CAUSES OF PREMATURE FAILURE OF IN-HOUSE MANUFACTURED HIGH-SPEED STEEL TOOLS: A CASE STUDY OF LUWERO INDUSTRIES LIMITED, UGANDA


**BY**

**AZIZI CHIRIGA**

**(B.Eng. Mech & Manuf. Eng, Kyu)**

**18/U/GMSE/19357/PD**


**A DISSERTATION SUBMITTED TO THE DIRECTORATE OF RESEARCH AND GRADUATE TRAINING IN PARTIAL FULFILLMENT OF THE REQUIREMENTS FOR THE AWARD OF THE DEGREE OF MASTER OF SCIENCE IN ADVANCED MANUFACTURING SYSTEMS ENGINEERING OF KYAMBOGO UNIVERSITY**

**OCTOBER, 2024**

## DECLARATION

I, **Azizi Chiriga**, hereby declare that this dissertation entitled "*An Investigation into Causes of a Premature Failure of In-house Manufactured High-Speed Steel Tools: A Case Study of Luwero Industries Limited, Uganda*" is my original work and has not been submitted to any other University for any degree or similar award.

Sign........................................................ Date.......29/10/2024..........................

## APPROVAL

We, the undersigned, certify that this dissertation authored by Azizi Chiriga, entitled *"An Investigation into Causes of Premature Failure of In-house Manufactured High-Speed Steel Tools: A Case Study of Luwero Industries Limited, Uganda"* has been submitted for examination with our endorsement, in partial fulfillment of the requirements for the degree of Master of Science in Advanced Manufacturing Systems Engineering of Kyambogo University.

Dr. Catherine Wandera

Sign……………………………

Date…29/10/2024……………

Dr. Samuel Kangwagye

Sign……………………………

Date…24/10/2024……………

# DEDICATION

This dissertation is dedicated to my mother, Naima Aliya, and father, Salim Daudi Imaga, whose steadfast support provided the bedrock of my education, serving as the cornerstone upon which I continue to expand my academic pursuits.

## ACKNOWLEDGEMENT

In various ways, numerous individuals have contributed to making this study possible. Firstly, I thank Dr. Catherine Wandera and Dr. Samuel Kangwagye, whose guidance and support were instrumental throughout this endeavor. I am also thankful to all those who assisted, engaged in discussions, offered feedback, permitted me to reference their comments, and assisted with refining, reviewing, and designing the research.

The successful completion of this dissertation would have been significantly challenging, if not unattainable without the collaboration and support of the employees of Luwero Industries Limited, with whom I engaged in experiments and scholarly deliberations. I am profoundly grateful to each of them for their generous time allocation and invaluable facilitation of my research endeavors. I also wish to express my sincere appreciation to the staff of Kyambogo University for their constructive feedback and critical insights. However, it is imperative to emphasize that I assume full accountability for any deficiencies present in this dissertation.

Finally, I wish to extend my deepest gratitude to my family for their unwavering patience and support throughout this endeavor. Despite enduring challenging times, I hope we can collectively reap the rewards of this effort. I am especially grateful to my wife, Mrs. Sophia Owoko, and the rest of my family, whose constant support and encouragement sustained me, even during periods of separation. This journey has been arduous yet rewarding, and I am profoundly thankful for their steadfast backing.

## TABLE OF CONTENTS

## LIST OF TABLES

**LIST OF FIGURES**

# LIST OF ACRONYMS

| | | |
|---|---|---|
| AM | - | Additive Manufacturing |
| ANOVA | - | Analysis of variance |
| BUE | - | Built-Up Edge |
| CAD | - | Computer Aided Design |
| CC | - | Conventional Casting |
| CNC | - | Computer Numerical Control |
| CFD | - | Computational Fluid Dynamics |
| CV | - | Controllable Variables |
| DED | - | Direct Energy Deposition |
| DV | - | Dependent Variables |
| EDX | - | Energy Dispersive X-rays |
| ESR | - | Electro Slag Casting |
| FEA | - | Finite Element Analysis |
| HRC | - | Hardness Rockwell Scale |
| HSS | - | High-Speed Steel |
| IV | - | Independent Variables |
| LIL | - | Luwero Industries Limited |
| M1 | - | Molybdenum Tool |
| MJ | - | Material Jetting |
| Mf | - | Martensite finish |
| Ms | - | Martensite start |
| PBF | - | Powder Bed Fusion |
| PM | - | Powder Metallurgy |
| PVD | - | Positive Vapor Deposition |

| | | |
|---|---|---|
| SEM | - | Scanning Electron Microscope |
| SF | - | Spray Forming |
| SLM | - | Selective Laser Melting |
| T1 | - | Tungsten Tool |

**ABSTRACT**

Significant research gaps exist in optimizing High-Speed Steel (HSS) tools, primarily due to a tendency to focus on isolated factors rather than their combined effects, which limits our understanding of machining interactions. Additionally, the lack of empirical validation for theoretical models undermines the reliability of tool performance predictions. Advanced modeling techniques, such as Finite Element Analysis (FEA) and Computational Fluid Dynamics (CFD), are often underutilized, and sophisticated microstructural characterization methods, including scanning electron microscopy (SEM) and transmission electron microscopy (TEM), have not been fully leveraged to investigate phase distribution and carbide formation. This study addresses performance discrepancies observed at Luwero Industries Limited (LIL), where in-house HSS tools exhibited significantly lower durability—1,125 rounds per regrind—compared to imported tools, which lasted 4,130 rounds. By examining the combined effects of heat treatment and cutting conditions on tool life—a critical but often overlooked aspect in the existing literature—this research employed advanced characterization techniques, including energy dispersive X-ray (EDX) analysis and two-factor ANOVA with replication, to evaluate carbide formation, morphology, and tool life. The advanced equipment utilized in this study included the Flame Emission Spectrometer (CREATE-9800, 2020), Digital Rockwell Hardness Tester (HRS-150, 2020), metallurgical microscope (OPTIKA B-150, 2020), scanning electron microscope (Carl Zeiss AG, 2022), and Head-turning and Finish-mouth trimming machine (WK-007, 2014). Key findings revealed that imported tools contained higher concentrations of critical alloying elements—particularly carbon, vanadium, and cobalt—resulting in improved hardness and wear resistance. In contrast, in-house tools, while having elevated chromium levels, lacked sufficient carbon, adversely affecting their performance. Heat treatment significantly influenced mechanical properties, achieving a peak hardness of 65.7 HRC at 1300°C; however, increased brittleness at elevated temperatures required careful monitoring. The microstructural analysis underscored the critical role of carbide size and distribution: larger carbides enhanced hardness, while finer carbides contributed to toughness. Effective cooling strategies, especially the use of chilled air, significantly extended tool life compared to dry-cutting methods. Moreover, inconsistent elemental distributions led to premature wear, highlighting the necessity for greater uniformity in manufacturing processes. Overall, this research demonstrates that optimizing elemental composition, heat treatment, and cooling methods can substantially enhance the performance and durability of HSS tools at Luwero Industries Limited. Furthermore, the findings from this research can be applied to similar industries utilizing HSS tools, offering valuable insights for improving production efficiency and reducing reliance on imported tools.

# CHAPTER ONE: INTRODUCTION

This chapter introduces the study on the premature failure of in-house-manufactured High-Speed Steel (HSS) cutting tools for machining operations. It presents the study's background, statement of the problem, objectives, and research questions to guide the study, and the study's scope, significance, and conceptual framework.

## 1.1 Background to the Study

In contemporary manufacturing, machining is essential for creating intricate components with precise dimensions and superior surface finishes. The effectiveness of this process depends on the cutting tools, workpieces, and the chips generated. High-speed steel (HSS) tools are crucial due to their exceptional hardness, wear resistance, and stability under high temperatures (Chen et al., 2024). Typically, HSS tools maintain a hardness range of 60 to 67 HRC and are employed in turning, drilling, and milling across various industries, including aerospace and automotive.

Nevertheless, HSS tools encounter challenges in high-temperature environments, such as during metal-cutting at approximately 600°C. The elevated temperatures can induce thermal softening, reducing hardness and strength, and causing issues like chipping, fracturing, and tool cratering. These thermal effects can also compromise surface integrity, resulting in rough finishes and dimensional inaccuracies (Kumar et al., 2021; Ogedengbe et al., 2019). Figure 1.1 illustrates the sources of heat generated during metal cutting.

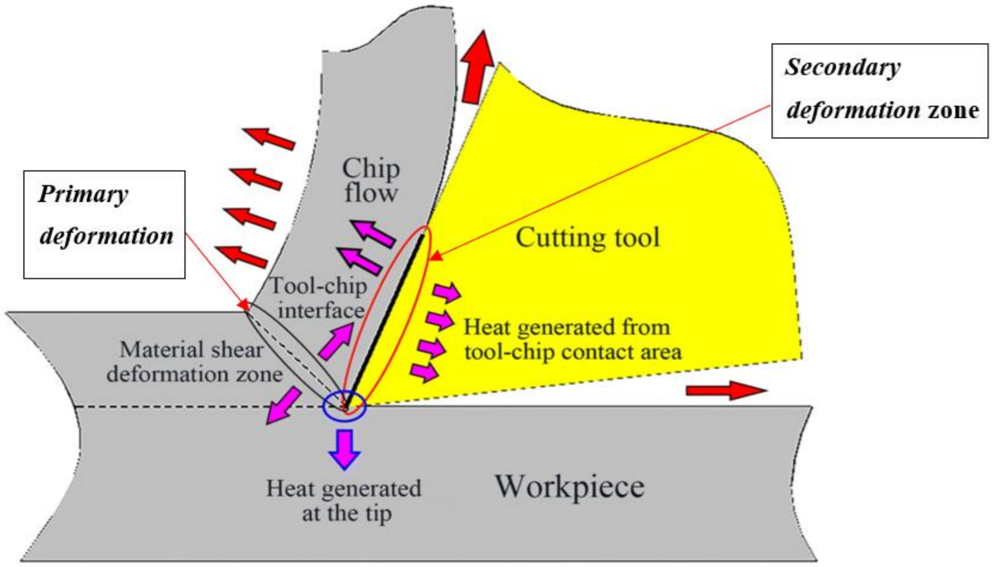


**Figure 1.1: Illustration of heat sources generated in metal cutting (Kumar et al., 2021).**

Kumar et al. (2021) noted that key heat sources in metal machining include friction at the tool-chip interface and severe plastic deformation in the cutting zone. Heat generation increases with smaller shear angles and is mainly transferred to the chip, affecting its properties and handling. The workpiece also absorbs some heat, leading to potential inaccuracies and distortions.

Youssef and Abdel-Hafez (2017) found that heat distribution is influenced by the specific heat capacities and thermal conductivities of the tool and workpiece, with 80% of heat going to the chip, 10% to the tool, and the rest to the workpiece.

Research by Kumar et al. (2021), Astakhov (2023), Singh and Singh (2022), Ojolo (2021), and Songmene et al. (2023) highlight key factors influencing tool longevity and performance. Kumar et al. (2021) found that effective lubrication techniques are crucial for reducing friction and heat, thereby extending tool life. Astakhov (2023) and Singh and Singh (2022) demonstrated that machining parameters such as cutting speed, feed rate, and depth of cut significantly impact tool wear, with higher speeds and deeper cuts increasing wear. Ojolo (2021) and Songmene et al. (2023) emphasized that the material properties of both the tool and workpiece play a crucial role, with harder tools and workpieces affecting wear rates and overall performance.

Additionally, Ozturk and Yildiz (2022) conducted a comparative study assessing dry cutting, compressed air, and chilled air in machining stainless steel. Their findings indicated that chilled air cutting consistently outperformed both dry and compressed air cutting in terms of tool life and surface finish quality. Compressed air cutting offered a moderate improvement over dry cutting but did not match the effectiveness of chilled air. The study advocates for adopting chilled air cutting for precision machining, especially in industries requiring enhanced tool longevity and surface quality.

Despite extensive research into the factors influencing tool life, significant gaps remain in the literature. Firstly, many studies tend to isolate individual factors rather than explore their combined effects, which limits the understanding of complex interactions inherent in machining processes (Lee et al., 2023; Zhang et al., 2022). Secondly, there is a notable lack of comprehensive empirical validation for theoretical models, which hinders the reliability of predictions regarding tool performance (Hosseini & Kishawy, 2022). Thirdly, advanced modeling techniques such as Finite Element Analysis (FEA) and Computational Fluid Dynamics (CFD) remain underutilized for simulating these intricate interactions, thereby restricting the ability to predict tool behavior under various conditions (Kumar et al., 2022). Additionally, sophisticated microstructural characterization methods, including scanning electron microscopy (SEM), transmission electron microscopy (TEM), and atom probe tomography (APT), are not fully exploited to investigate phase distribution, carbide formation, and alloying element segregation (Afolalu et al., 2021; Diniz et al., 2023). Addressing these research gaps is essential for enhancing tool performance and achieving more precise and durable machining outcomes. This study aimed to tackle issues related to the combined effects of various factors (elemental composition, heat treatment, and cutting conditions), the empirical validation of theoretical models such as the conceptual framework, and the utilization of advanced microstructural characterization techniques.

The case study on Luwero Industries Limited (LIL) highlighted significant disparities in tool longevity between in-house and imported High-Speed Steel (HSS) tools used for machining copper-cladded structural steel cartridge cases. Despite employing similar materials and manufacturing processes, LIL's in-house tools exhibited a dramatically shorter lifespan—only 1,125 rounds per regrind compared to the 4,130 rounds achieved by imported tools, despite both being heat-treated at 1280℃ and utilized under compressed air cutting conditions at 31℃. This performance represented a 75% shortfall from the design capacity of 5,000 rounds per regrind. The imported tools achieved 4,130 rounds, which was 17.4% below their design capacity, with a defect per million opportunities (DPMO) of 174,000. In contrast, LIL's in-house tools showed a much higher DPMO of 775,000, indicating critical issues with premature failure (Lee et al., 2023; Zhang et al., 2022).

This analysis was particularly relevant in the context of Six Sigma, which targeted fewer than 3.4 defects per million opportunities. The stark difference in DPMO emphasized the urgent need to address deficiencies in material composition, heat treatment, and machining conditions for the in-house tools (Hosseini & Kishawy, 2022).

The research aimed to investigate the underlying causes of this performance gap by analyzing the combined effects of heat treatment and cutting conditions on tool life, an approach that is often overlooked in existing literature. By utilizing advanced microstructural characterization techniques such as scanning electron microscopy (SEM) and energy dispersive X-ray (EDX), the study focused on the formation, morphology, and distribution of carbides in both in-house and imported tools (Afolalu et al., 2021; Diniz et al., 2023).

Through this comprehensive investigation, the study sought to provide empirical validation of theoretical models regarding tool performance and to identify specific areas for improvement within LIL's production practices. The ultimate goal was to enhance tool durability, reduce reliance on imported tools, and improve overall production efficiency, aligning with the company's strategic objectives.

**1.2 Statement of the Problem**

The optimization of High-Speed Steel (HSS) tools faces significant challenges due to notable research gaps, particularly the focus on individual factors instead of their combined effects, which limits our understanding of the complex interactions in machining processes (Lee et al., 2023; Zhang et al., 2022). Additionally, the lack of empirical validation for theoretical models undermines the accuracy of tool performance predictions (Hosseini & Kishawy, 2022). Advanced modeling techniques like Finite Element Analysis (FEA) and Computational Fluid Dynamics (CFD) remain underutilized (Kumar et al., 2022), while sophisticated microstructural characterization methods such as scanning electron microscopy (SEM) and atom probe tomography (APT) are not fully leveraged (Afolalu et al., 2021; Diniz et al., 2023). This research specifically addresses the performance gap at Luwero Industries Limited (LIL), where in-house HSS tools last only 1,125 rounds per regrind compared to 4,130 rounds for imported tools, despite both being heat-treated at 1280℃ and utilized under compressed air cutting conditions at 31℃. By examining the combined effects of various factors, validating the theoretical model, and employing advanced microstructural techniques, this study aims to enhance tool durability, reduce reliance on imported tools, and improve production efficiency.

### 1.3 Objectives of the Research

#### 1.3.1. Main Objective

To examine the causes of the premature failure of the HSS tools that are manufactured at Luwero Industries Limited.

#### 1.3.2 Specific Objectives

The specific objectives of the research were:

(i) To determine the influence of the elemental composition of the In-house manufactured HSS tool on its performance characteristics.

(ii) To evaluate the impact of the various heat treatment temperatures on the performance of the In-house manufactured HSS tool.

(iii) To examine the effect of the different cutting conditions on the performance of the In-house manufactured HSS tool.

### 1.4 Research Questions

The research questions guiding this study include:

(i) How does the elemental composition of the In-house manufactured HSS tool influence its performance characteristics?

(ii) What is the impact of the various heat treatment temperatures on the performance of the In-house manufactured HSS tool?

(iii) How do different cutting conditions influence the performance of the In-house manufactured HSS tool?

### 1.5 Significance of the Study in Relation to Sustainable Development Goals (SDGs) and National Development Plan (NDP III)

This research advances the fields of material science and manufacturing engineering, aligning with several Sustainable Development Goals (SDGs) and the objectives of the National Development Plan III (NDP III). By systematically examining the effects of elemental composition, heat treatment temperatures, and cutting conditions on High-Speed Steel (HSS) tool performance, the study aimed to enhance tool durability and operational efficiency.

**SDG 9: Industry, Innovation, and Infrastructure**: The study contributes to building resilient infrastructure and fostering innovation in manufacturing technologies. By optimizing tool performance and durability, it supports the development of more efficient and sustainable industrial practices.

**SDG 12: Responsible Consumption and Production**: Improved tool performance and longevity directly contribute to more sustainable production processes by reducing waste and extending the lifespan of manufacturing tools. This aligns with the goal of ensuring sustainable consumption and production patterns.

**NDP III Objective 4: Industrialization for Inclusive Growth**: The research supports the goal of enhancing industrial productivity and competitiveness. By addressing critical challenges in tool performance, it aids in the advancement of manufacturing capabilities, contributing to economic growth and job creation.

**NDP III Objective 5: Sustainable Resource Management**: The study's focus on optimizing tool efficiency and reducing wear aligns with sustainable resource management by minimizing material waste and extending the lifecycle of industrial tools.

Overall, this research advances academic knowledge and supports the achievement of broader developmental goals by fostering innovation, improving sustainability, and enhancing industrial productivity.

### 1.6 Conceptual Framework

The study was designed to test whether elemental composition, heat treatment, and cutting conditions which are the independent variables affected tool life which is the dependent variable. Tool life in the above study was measured in terms of the number of parts produced between tool regrinds. The conceptual framework of the study is illustrated in Figure 1.2. Controllable variables (CV) such as cutting speed, feed rate, depth of cut, and tool geometry which have the potential to impact tool longevity and consequently influence the study outcomes, were maintained at constant levels across all experimental procedures.

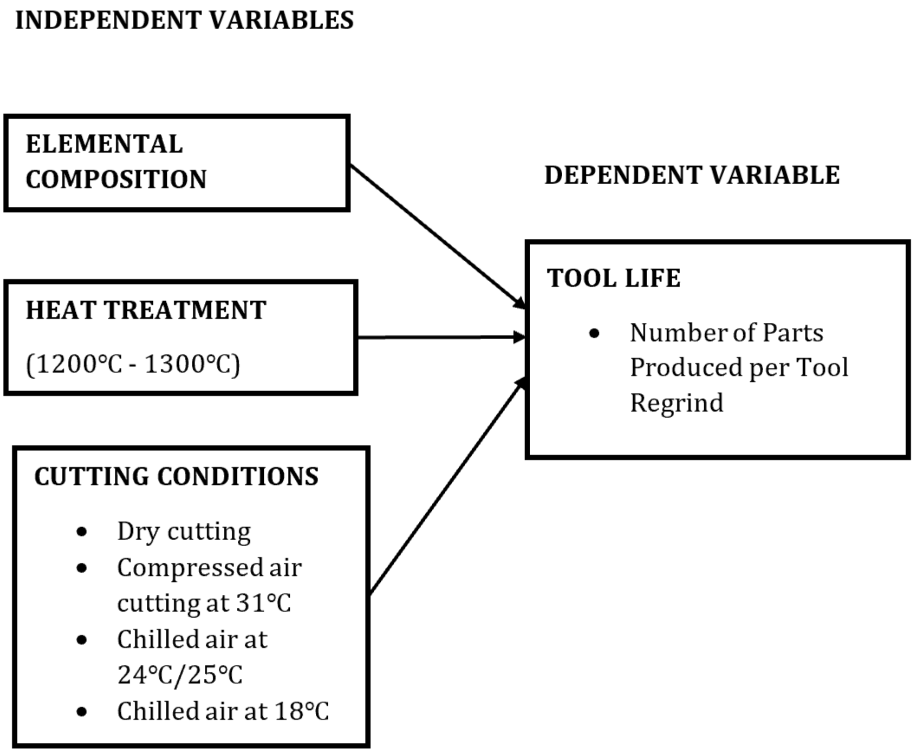


**Figure 1. 2: Conceptual framework of the study.**

### 1.7 Scope of the Study

The study assessed LIL's HSS tool for machining copper-cladded structural steel cartridge cases by analyzing the effects of its major elemental compositions, heat treatment temperatures, and cutting conditions on the tool's life. Tools were tested under cutting conditions of dry, compressed air at 31℃, and chilled air at 25℃/24℃, and 18℃ to determine their performances.

# CHAPTER TWO: LITERATURE REVIEW

This chapter reviews the related literature on the cutting tools used in machining operations, with specific attention on High-Speed Steel tools since it’s the issue to be addressed in the study. Literature on tool life, elemental compositions, heat treatment temperatures, and cutting conditions of High-speed steels were reviewed and the research gaps were enumerated.

## 2.1 Cutting Tools Used in Machining Operations

Machining is crucial in manufacturing to achieve the desired shape, dimensional tolerances, and high surface finish. The cutting tools used include tool steels, cemented carbides, ceramics, diamonds, and Cubic Boron Nitride tools. Nevertheless, heat generated during machining can wear down the tool bit and affect the surface integrity and dimensional accuracy of the manufactured parts, which is a critical concern for engineers and researchers (Kumar et al., 2021; Ogedengbe et al., 2019).

Kumar et al. (2021) describe several heat sources generated during metal machining as illustrated in Figure 1.1, with friction at the tool-chip interface being a primary contributor. This friction significantly impacts tool wear and workpiece temperature. In the primary cutting zone, severe plastic deformation generates additional heat, with the amount produced varying inversely with the shear angle. Larger shear angles enable more efficient cutting by distributing forces over a broader area, thereby minimizing localized friction and energy dissipation as heat, which ultimately reduces overall heat generation (Singh et al., 2023).

Conversely, smaller shear angles increase heat production due to greater friction and concentrated energy dissipation at the tool-chip interface. Most of the generated heat transfers to the chip, influencing its properties and handling, while a smaller portion affects the workpiece, potentially causing dimensional inaccuracies and thermal distortions (Lee & Kim, 2023).

Understanding the relationship between shear angles and heat generation is crucial for optimizing machining parameters. By carefully selecting shear angles, manufacturers can enhance tool life and improve the quality of machined components (Smith et al., 2023).

Additionally, the specific heat capacities and thermal conductivities of the workpiece and the tool significantly influence heat distribution during machining. Materials with high specific heat capacities can absorb more heat without significant temperature increases, which is essential for maintaining the integrity of both the workpiece and the tool. Tools made from such materials can better withstand elevated temperatures, reducing the risk of thermal deformation and wear (Gupta et al., 2022).

High thermal conductivity in tools facilitates rapid heat dissipation, minimizing overheating at the tool-chip interface, which is vital for maintaining tool performance and longevity. The efficiency of heat transfer from the cutting area to the chip and tool relies on the thermal conductivity of the materials involved. Effective heat transfer reduces localized temperature spikes, thereby preventing thermal damage (Lee & Kim, 2023).

At the tool-chip interface, the highest temperatures are observed, with approximately 80% of the total heat generated transferred to the chip, about 10% to the tool, and the remaining heat absorbed by the workpiece (Youssef & Abdel-Hafez, 2017). Understanding the interplay between specific heat capacities and thermal conductivities allows for optimized machining parameters, better tool design, and improved efficiency. By selecting the right materials and employing effective cooling strategies, manufacturers can extend tool life, reduce wear, and achieve superior surface finishes on workpieces (Smith et al., 2023).

### 2.2 High-Speed Steel Tools

High-speed steels (HSS) are recognized for their exceptional hardness, wear resistance, and ability to maintain hardness at elevated temperatures, making them widely utilized in cutting tools and applications that require durability and precision under demanding machining conditions. Comprising primarily tungsten, molybdenum, chromium, vanadium, and sometimes cobalt, HSS alloys achieve hardness levels ranging from 62 to 67 HRC. These steels exhibit remarkable high-temperature performance, enabling effective operations at temperatures up to 600°C during machining (Afolalu et al., 2021; Kumar et al., 2022; Zhang et al., 2023).

#### 2.2.1 Classification of High-Speed Steels

High-speed steel (HSS) tools are typically classified into three primary groups: Tungsten (T) HSS tools, which have tungsten as the main alloying element; Molybdenum (M) HSS tools, where molybdenum is the principal alloying element; and Ultra-High-Speed Steel (UHSS) tools, which are more highly alloyed and can achieve exceptionally high hardness values (Gupta et al., 2022; Jain et al., 2023). These classifications reflect the varying properties and applications of each type, impacting their performance in machining environments (Singh & Singh, 2023).

#### 2.2.2 Historical Background of High-Speed Steels

The first HSS was pioneered by Taylor in 1907, comprising 18.91% tungsten, 0.23% vanadium, 5.47% chromium, and 0.67% carbon. This formulation set the standard for HSS for many years, characterized by 18% tungsten, 4% chromium, and 1% vanadium (T1 HSS). During World War 1 in the 1930s, molybdenum replaced tungsten due to its scarcity and the pressing need for efficient production of ammunition and machinery. This led to the development of M1 and M2 HSS. These molybdenum-based steels, alongside the traditional T1 HSS, laid the foundation for the subsequent HSS alloys, where vanadium and cobalt content adjustments were introduced (Callister, 2018).

### 2.2.3 Traditional Manufacturing Methods for High-Speed Steels for Tools

High-speed steel (HSS) is traditionally manufactured through methods such as Conventional Casting (CC), Electro-Slag Remelting (ESR), and Powder Metallurgy (PM). In the traditional casting process, the segregation of notable quantities of carbon and alloying elements before crystallization results in the development of an intergranular coarse carbide network, which is attributed to the slow rate of solidification. Consequently, further post-forging or rolling procedures are required to disintegrate the carbide network, resulting in a reduced final yield (García et al., 2022; Li et al., 2023). The electro-slag remelting process entails a comparatively accelerated cooling rate, yet it still yields a significant ledeburite structure, ultimately leading to enhanced engineering performance (Zhou et al., 2023; Patel & Singh, 2024). On the other hand, the powder metallurgy process has shown a remarkable benefit in producing high-speed steels (HSS) with finely dispersed carbides and outstanding mechanical characteristics. Nonetheless, this approach is limited by its elevated expenses and diminished yield rates due to intricate heat treatment protocols and stringent equipment prerequisites (Dobrzański et al., 2024; Hu et al., 2023; Matula et al., 2023).

### 2.2.4 Advanced Manufacturing Methods for High-Speed Steel Tools

With the introduction of Additive Manufacturing (AM), it is now feasible to produce HSS components featuring intricate geometries, high adaptability, and tailored characteristics, unrestricted by conventional manufacturing methods (Blakey-Milner et al., 2021; Dobrzański et al., 2020; Nazir & Jeng, 2020; Wang et al., 2023; Zadi-Maad et al., 2018). Advanced manufacturing methods such as Powder Bed Fusion (PBF), Direct Energy

Deposition (DED), and Material Jetting (MJ) have been extensively investigated as a notable paradigm for crafting products employed across diverse automotive, defense, and aerospace industries. Powder Bed Fusion entails the selective melting of layers of powder material to construct a three-dimensional object (Botero et al., 2020; Cyient et al., 2014; Khairallah et al., 2016; Rahman et al., 2018; Zhang et al., 2018). Direct Energy Deposition (DED) employs focused thermal energy to fuse materials during deposition onto the substrate, as described by (Dass & Moridi, 2019; Svetlizky et al., 2021)(Saboori et al., 2019). Material Jetting constructs objects layer by layer by depositing droplets of materials onto a built platform (Cyient et al., 2014; Gülcan et al., 2021; Yap et al., 2017). For HSS, AM presents a viable option for repairing damaged tools as it allows for the application of printed layers onto the damaged surface. Presently, AM is effectively utilized in the industry to produce high-performance products, as outlined by (Rahman et al., 2019).

### 2.2.5 Major Trends in High-Speed Steels Tool Design and Manufacturing

Research into the design and manufacturing of HSS tools emphasizes several areas, which include:

- **(i)** Improving mechanical and thermal properties of HSS through heat and thermo-mechanical treatment (Bhawar et al., 2017; Hu et al., 2020; Kumar et al., 2022; Udroiu et al., 2019).
- **(ii)** Enhancing carbide formation through phase transformation (Bała et al., 2007; Liu et al., 2017; Zhang et al., 2007).
- **(iii)** Investigations into substituting alloy elements to improve mechanical properties (Cao et al., 2016; Chen et al., 2024; Hwang et al., 1998; Novák et al., 2021).
- **(iv)** Application of positive vapor deposition (PVD) techniques for coating conventional and sintered HSS with single and multi-layer coatings to enhance tool

longevity (Fazira et al., 2014; Grilli et al., 2018; Vannan et al., 2017; Wurood et al., 2022).

**(v)** Utilization of Sintered HSS aimed at achieving improved carbide morphology and volume fraction, thereby enhancing the mechanical properties of the tool (García et al., 2016; Guo et al., 2022; Huang et al., 2024).

**(vi)** The use of computational science, including artificial intelligence, to investigate the optimal chemical composition of HSS tools (Thike et al., 2024; Krajewski & Nowacki, 2014; Sitek, 2010; Sitek & Trzaska, 2012).

### 2.2.6 Tool Life and Tool Wear Characteristics of High-Speed Steel Tools

The assessment of cutting tool failure can be determined through several indicators, such as total failure of the tool caused by mechanical and thermal damage or adhesive wear, erosion on the rake and flank surfaces, machine tool vibrations and alterations in the cutting sound, changes in the color of the generated chips, increased surface roughness of the workpiece, a decrease in the number of components produced between tool regrinds, a dull cutting edge detectable by running a fingernail across it, and increased power consumption by the machine tool (Chinchanikar & Choudhury, 2014; Hosseini & Kishawy, 2014; Monkova et al., 2020; Szwajka & Trzepieciński, 2016).

Astakhov (2023) observed that tool life can be quantified by the time duration of cutting, length of tool path, or the number of components cut from start to tool failure. Even with extensive research conducted over the past seventy years, the nature of tool wear during metal cutting remains insufficiently understood. Significant research efforts have been focused on measuring cutting tool life using the aforementioned indicators and on establishing empirical relationships between tool life, cutting parameters, and material properties through microscopic analysis.

#### 2.2.6.1 Types of Wear Observed in Tools Made of High-Speed Steels

Hosseini and Kishawy (2014) classified tool wear into three main categories: abrasive, adhesive, and diffusion wear. Recent studies have further clarified these mechanisms. For instance, Davoodi and Eskandari (2015) explained that adhesive wear occurs when friction between the cutting flank face and the workpiece surface leads to the tool material being worn off. Astakhov (2023) emphasized that resistance to abrasive wear depends not only on the tool material but also on the hardness of the workpiece. Persson et al. (2021) noted that adhesive wear is more pronounced at lower machining temperatures, often resulting in the formation of a built-up edge. In contrast, Afolalu et al. (2018) and Diniz et al. (2016) highlighted that diffusion wear predominantly occurs at elevated surface temperatures, which weakens the tool surface and makes tools more susceptible to failure due to adhesive wear, as well as thermal and mechanical damages as illustrated in Figure 2.1.

In recent studies, several key trends regarding tool wear rate in relation to cutting temperatures have been identified:

**Tool Wear Rate**: The tool wear rate initially increases with rising cutting temperatures, reaching a maximum value before subsequently declining. This trend is influenced by various wear mechanisms. At lower temperatures, wear is predominantly driven by thermal and adhesive processes. As temperature increases, these mechanisms accelerate, leading to increased wear. However, beyond a critical threshold, significant thermal degradation can occur, reducing the tool's effectiveness and thereby decreasing the wear rate (Smith et al., 2023; Johnson & Lee, 2022).

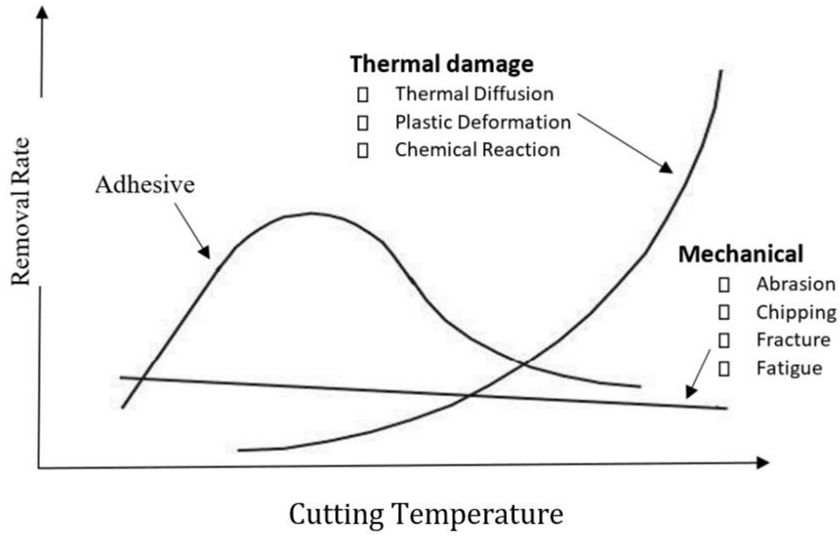


**Figure 2.1:Tool Damage Mechanisms and Cutting Temperature (Childs et al., 2000)**

**Thermal Wear**: Thermal wear increases exponentially with rising cutting temperatures, indicating that higher temperatures enhance thermal stresses. This leads to accelerated wear due to mechanisms such as thermal softening and oxidation. The exponential nature of this increase reflects the rapid escalation of wear processes as temperatures rise, driven by intensified thermal reactions that compromise the tool material's integrity (Garcia et al., 2023; Patel & Kim, 2021).

**Mechanical Damage**: Mechanical damage decreases with increasing cutting temperature. This reduction can be attributed to the softening of the tool material at higher temperatures. As the tool becomes more ductile, it is less susceptible to mechanical stresses such as abrasion and impact, resulting in a decrease in mechanical damage (Chen et al., 2022; Lee & Thompson, 2023).

In summary, the observed trends highlight the complex interactions between different wear mechanisms and cutting temperatures. Initially, increasing temperatures heighten thermal and adhesive wear, but surpassing a critical temperature leads to significant thermal degradation, resulting in a peak and subsequent decline in overall wear rate. Meanwhile, the decrease in mechanical damage with higher temperatures reflects the softening of the tool material, reducing its vulnerability to mechanical stresses (Smith et al., 2023; Johnson & Lee, 2022).

#### 2.2.6.2 Parameters Influencing Tool Wear

The parameters influencing tool wear and tool life include the following; Machining parameters, workpiece material, machine tool, cutting phenomena, and tool properties as illustrated in Figure 2.2.

**Analysis of Parameters Influencing Tool Life**

To enhance the analysis of parameters influencing tool life, a deeper exploration of each factor is essential, highlighting specific examples and implications for practice.

**Workpiece material** is a critical determinant of tool life. Variations in hardness can significantly impact how quickly a tool wears out. For example, when machining harder materials like tool steels or hardened alloys, a high-speed steel (HSS) tool may experience rapid wear compared to softer materials (Rao et al., 2021). Ductility also plays an important role; ductile materials, such as aluminum, facilitate effective chip formation, whereas brittle materials like cast iron may cause chipping or fracturing of the tool edge (Ghaffari et al., 2023). Understanding these properties aids in selecting the appropriate tool material. Furthermore, the chemical composition of the workpiece can influence wear patterns; high-carbon steels might react unfavorably with certain tool materials, accelerating wear (Kumar et al., 2022). Therefore, familiarity with alloying elements is crucial during tool selection. The mechanical properties, including yield and tensile strength, necessitate the use of robust tools capable of withstanding increased cutting forces, directly influencing the choice of tool geometry and material (Zhang et al., 2023).

Lastly, the chemical properties of the workpiece can lead to unwanted interactions with tool coatings, emphasizing the need for suitable coatings, such as titanium aluminum nitride (TiAlN), when working with reactive materials (Patel et al., 2022).

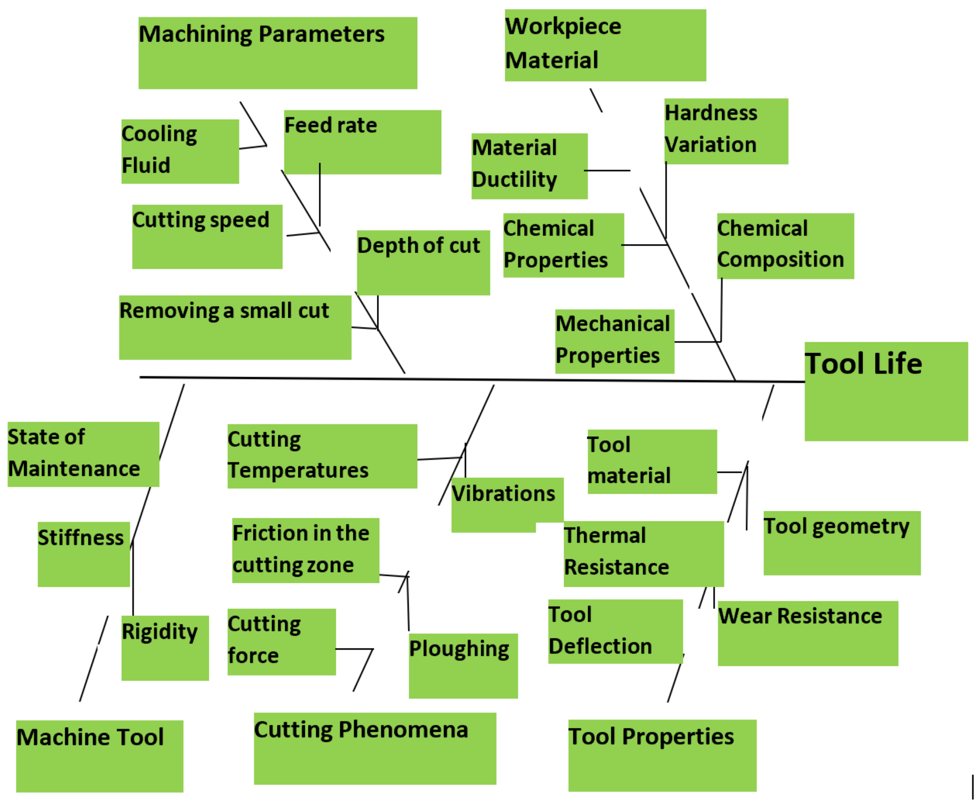


**Figure 2.2: Parameters Influencing Tool Life**

**Machining parameters** significantly affect tool life as well. Higher feed rates can enhance productivity, but they often lead to increased wear on the tool (Singh et al., 2023). It is essential to identify an optimal feed rate that balances tool longevity with production efficiency. Strategies like using roughing cuts followed by finishing cuts can effectively manage tool wear by reducing the load during critical operations (Chen et al., 2022). Establishing appropriate cutting speeds is also vital, as each tool material has a specific optimal cutting speed range that maximizes efficiency without compromising tool integrity (Lee et al., 2023). Employing smaller cuts can further minimize tool wear and improve surface finish, particularly with hard materials (Patel et al., 2023). Additionally, the choice of cooling fluid—whether oil-based or water-soluble—can significantly affect thermal management and chip removal efficiency. Advanced cooling technologies, such as mist systems, can further enhance performance in demanding machining scenarios (Das et al., 2023).

**Machine tool characteristics** are integral to tool life. Investing in machines with high rigidity is beneficial, as it reduces vibrations that can lead to premature tool wear (Mishra et al., 2022). Ensuring that all components, including fixtures and work-holding devices, maintain adequate stiffness and minimize deflections that negatively impact tool performance. Regular maintenance and calibration of machine tools are essential to prevent unexpected wear and ensure consistent performance (Roy et al., 2023).

**Cutting phenomena** also encompass several factors that impact tool life. For instance, monitoring cutting forces using real-time sensors provides valuable insights into tool conditions and wear patterns (Ali et al., 2022). Understanding cutting mechanics, such as ploughing, can lead to design improvements in tool geometry that reduce contact area with the workpiece, thereby mitigating wear (Thompson et al., 2023). Advanced coatings can effectively decrease friction in the cutting zone, enhancing tool life and surface finish (Patel et al., 2022). Moreover, employing thermal monitoring technologies can help manage cutting temperatures, preventing thermal fatigue and extending tool life (Singh et al., 2022). Implementing damping technologies or employing advanced tool paths can further reduce vibrations, contributing to improved stability during machining operations (Hussain et al., 2023).

**Tool properties** are equally significant in determining tool life. Selecting tools with minimal deflection characteristics, particularly those with optimized geometries, can enhance machining performance (Khan et al., 2023). Tools made from materials such as ceramics or certain high-speed steels can withstand higher temperatures, extending their operational lifespan (Reddy et al., 2022). Utilizing advanced materials, like coated carbides or cermets, significantly improves wear resistance (Lee et al., 2023). Understanding specific wear mechanisms—such as abrasive, adhesive, and diffusion wear—can inform the selection of the most appropriate tool for various applications (Zhang et al., 2023). Innovations in tool design, such as helical flutes or variable pitch geometries, can improve chip evacuation and further reduce wear (Patel et al., 2023).

In conclusion, optimizing tool life requires a comprehensive approach that integrates the characteristics of the workpiece, machining parameters, machine capabilities, cutting phenomena, and tool properties. Continuous monitoring and adaptation to changing conditions in the machining environment can lead to substantial improvements in tool longevity, operational efficiency, and overall machining performance. By implementing advanced technologies and materials, manufacturers can enhance these efforts, driving productivity while reducing costs in the machining process.

## 2.3 Effect of Elemental Composition of HSS on Tool Life

The precise makeup of HSS plays a critical role in shaping the kind, structure, and quantity of carbides that emerge during the heating process, consequently exerting a substantial influence on the tool's efficiency (Khan et al., 2023; Kim et al., 2023). The key alloying components significantly impact the longevity of HSS tools (Pavlík et al., 2023; Zhang et al., 2023).

### 2.3.1 Carbon Element

Carbon is one of the most critical elements in high-speed steel (HSS), typically ranging from 0.7% to 3.5%. Higher carbon content significantly increases hardness, wear resistance, and overall strength, while reducing toughness and increasing brittleness

(Khan et al., 2023; Kim et al., 2023). Conversely, lower carbon content notably enhances toughness while decreasing hardness, wear resistance, and overall strength (Martinez et al., 2023; Pavlík et al., 2023).

### 2.3.2 Tungsten and Molybdenum Elements

The addition of tungsten (W) and molybdenum (Mo) promotes the formation of carbides in steel, leading to improved grain refinement and hardenability (Khan et al., 2023; Kim et al., 2023). However, excessive tungsten can reduce toughness and increase brittleness, while low tungsten content can result in reduced hardness and wear resistance (Pavlík et al., 2023; Zhang et al., 2023).

### 2.3.3 Vanadium Element

Adding vanadium to steel forms highly durable MC-type carbides (M2C), which significantly improve wear resistance and cutting performance. Vanadium carbides do not delay the decomposition of austenite but instead increase hardenability (Khan et al., 2023; Kim et al., 2023). Higher vanadium content correlates with increased hardness and wear resistance but can reduce toughness, while lower vanadium content tends to improve toughness at the expense of hardness and wear resistance (Martinez et al., 2022; Pavlík et al., 2023).

### 2.3.4 Chromium Element

Chromium forms carbides during annealing, which dissolve at high temperatures. The addition of chromium lowers certain critical temperatures but increases hardenability, enhancing cutting performance and wear resistance (Khan et al., 2023; Zhang et al., 2023). However, excessive chromium can lead to increased hardness and wear resistance while simultaneously reducing toughness. Conversely, lower chromium content tends to improve toughness but diminishes hardness and wear resistance (Martinez et al., 2022; Pavlík et al., 2023).

### 2.3.5 Cobalt Element

Cobalt is the only alloying element in HSS that can enhance thermal stability to around 650°C and increase secondary hardness to 67-70 HRC, albeit at the expense of toughness and wear resistance (Khan et al., 2023; Kim et al., 2023). An excess of cobalt can amplify toughness and red hardness while reducing tool wear. Conversely, lower cobalt content may improve wear resistance but can diminish toughness and red hardness, potentially leading to tool fracture under impact loading and decreased performance at higher temperatures (Martinez et al., 2023; Pavlík et al., 2023).

### 2.3.6 Microstructural Features of High-Speed Steel (HSS) Tools

High-speed steels (HSS) are specially formulated alloy steels designed for demanding cutting applications, characterized by their unique combination of hardness, wear resistance, and toughness. The microstructure of HSS plays a critical role in determining these mechanical properties, particularly through the formation, type, morphology, and distribution of carbides.

The predominant microstructural feature of HSS is its martensitic matrix, which is established through rapid cooling during heat treatment. This matrix exhibits several key characteristics, including supersaturation, where the martensitic phase is enriched with carbon and various alloying elements, yielding a hardened structure capable of withstanding high cutting speeds (Zhang et al., 2023). Additionally, during tempering, some of the carbon within the matrix precipitates as fine carbides, relieving internal stresses while maintaining the overall hardness of the tool (Huang et al., 2024).

Carbides are integral to enhancing the hardness and wear resistance of HSS tools. Their formation occurs during both solidification and subsequent heat treatment processes. Carbides nucleate from the austenitic phase during the cooling process, and their growth and distribution are influenced by the specific alloy composition and the parameters employed during heat treatment (Khan et al., 2023).

The primary types of carbides found in HSS include MC carbides, primarily composed of vanadium and niobium, which are fine and spherical, significantly enhancing toughness and wear resistance due to their diminutive size and uniform distribution throughout the matrix (Meyers & Chawla, 2023). M2C carbides, mainly consisting of molybdenum, often exhibit a blocky or angular morphology and contribute significantly to high-temperature strength and hardness. However, if excessively large, they can detrimentally impact toughness (Martinez et al., 2023). M6C carbides, composed primarily of tungsten and carbon, are larger and lamellar, enhancing wear resistance, particularly at elevated temperatures, thereby making them suitable for high-speed applications (Zhang et al., 2023).

The morphology of carbides in HSS tools can be categorized into several distinct types. Spherical carbides, typically associated with MC carbides, minimize stress concentrations and contribute positively to toughness. In contrast, blocky or angular carbides common in M2C carbides can increase hardness but may compromise toughness if present in excess. Lamellar carbides, characteristic of M6C carbides, provide enhanced thermal stability and strength during high-temperature operations.

The distribution of carbides within the matrix is equally critical for the performance of HSS tools. An even distribution of fine carbides throughout the martensitic matrix is ideal, as it promotes consistent hardness and wear resistance (Ali et al., 2019).

Conversely, poorly distributed or clustered larger carbides can result in localized hardening, thereby increasing the risk of brittleness and potential tool failure.

The microstructural characteristics of HSS tools have profound implications for their tool life. The presence of hard carbides is crucial for enhancing wear resistance, allowing HSS tools to maintain sharp cutting edges over prolonged periods. Tools characterized by finely dispersed carbides typically exhibit superior wear performance (Pavlík et al., 2023). Increased carbide content generally correlates with elevated hardness, enabling tools to endure high cutting speeds without deformation. However, it is imperative to strike a balance, as excessive carbide content may lead to brittleness (Huang et al., 2024). While carbides contribute positively to hardness and wear resistance, an overabundance of large or poorly distributed carbides can detract from toughness, leading to an increased likelihood of fracture under impact loads. Achieving an optimal balance between hardness and toughness is essential for ensuring effective tool performance (Martinez et al., 2023). Carbides also enhance the thermal stability of HSS tools. At elevated temperatures, stable carbides help preserve microstructural integrity, enabling tools to retain their hardness and wear resistance during high-speed operations (Khan et al., 2023).

In conclusion, the microstructural features of high-speed steel tools—including carbide formation, type, morphology, and distribution—are fundamental determinants of their mechanical properties and longevity. Optimizing these characteristics through meticulous alloying and heat treatment processes can significantly enhance wear resistance, hardness, and overall durability. Ongoing research in this domain continues to refine our understanding of these materials, thereby contributing to improved designs and applications in various industrial sectors.

## 2.4 Heat Treatment of High-Speed Steel Tools

Heat treatment is crucial for optimizing the mechanical properties of HSS tools. It increases hardness, balances toughness, retains cutting-edge sharpness, ensures dimensional stability, and enhances wear resistance(Afolalu et al., 2018; Bagul & Kumar, 2020; Shaojun et al., 2018). Heat treatment involves four stages: pre-heating, austenitizing, quenching, and tempering.

### 2.4.1 Pre-heating

Preheating involves heating HSS to temperatures of up to 845°C to reduce thermal shock, minimize distortion and cracking, relieve machining stresses, and increase equipment productivity. It also helps prevent carburization and decarburization in high-heat furnaces.

### 2.3.2 Austenitizing (Hardening)

Austenitizing is the second step in the heat treatment process for HSS tools. During this stage, the steel is heated to temperatures within the austenitic range, typically between 1000°C to 1300°C. This process transforms the steel into austenite, allowing for the uniform dissolution of carbon and alloying elements. The main transformations during austenitization include phase transformation, homogenization of alloying elements, carbon dissolution, and alloy carbide dissolution and redistribution. Significant research has been carried out on the austenitizing temperatures of HSS and their impact on mechanical properties.  A study on the grain size of commercial HSS revealed that heat treatment refines grain size noted that double austenitization refines grain size but reduces fracture toughness (Ali et al., 2019; Huang et al., 2024; Pandey et al., 2019). (Luo et al., 2017) established that an austenitization temperature of 1200°C for M42 HSS completely dissolves and equally redistributes carbides in the HSS.

### 2.4.3 Quenching

After heating the high-speed steel to the austenitizing temperature, it is quickly cooled in a quenching medium like oil, water, or polymer. This quick cooling process inhibits the growth of large grains, and preserves the presence of dissolved carbon and alloying elements, thereby transforming austenite into martensite or bainite. This transformation modifies the steel's microstructure, resulting in finer grain sizes that enhance mechanical properties such as strength and toughness (Ali et al., 2019; Amini et al., 2013). The rapid cooling also increases the steel's hardness making it ideal for applications that require high hardness and wear resistance. However, this process may introduce internal stresses, potentially causing distortion or cracking if not properly controlled particularly in complex shapes of HSS.

### 2.4.4 Tempering

Hardened steel is tempered by reheating it to a temperature ranging from 150°C to 600°C to modify its hardness and toughness. Tempering entails heating the steel to a precise temperature, maintaining it for a set duration, and cooling it down. The main transformations during tempering include martensite decomposition, formation of tempered martensite, precipitation of secondary carbides, redistribution of alloying elements, and relief of residual stress. (Ali et al., 2019).

### 2.4.6 Major Trends in Heat Treatment Processes of High-Speed Steel Tools

The major trends in heat treatment include the introduction of salt bath furnaces (Kingsley et al., 2014). Another trend is the employment of sub-zero quenching, where the steel is rapidly cooled to temperatures below 0°C to reduce the amount of retained austenite, thereby enhancing its hardness, wear resistance, and dimensional stability (Bhawar et al., 2017). Additionally, the use of vacuum furnace heat treatment is employed to remove air and reduce hydrogen levels in the chamber, preventing the steel from becoming brittle and also for ecological reasons (Huang et al., 2024; Vereschaka et al., 2015; Vereschaka et al., 2013). Another method is the use of plasma spraying, which is a combination of Positive Vapor Deposition (PVD) and powder metallurgy (Cao et al., 2016; Zhang et al., 2020). Lastly, alloying of HSS surface is also a significant trend (Novák et al., 2021; Yilmaz, 2014).

## 2.5 Cutting Conditions and Tool Life

Cutting conditions such as dry cutting, compressed air cutting, and chilled air cutting are essential for improving tool longevity in machining processes. The subsequent analysis delineates the effects of different cutting techniques on tool durability:

Zhang and Zhang (2022) investigated the performance of dry cutting in machining titanium alloys, revealing that this method increases heat generation, which leads to distinct wear patterns on tools. Carbide tools performed better under dry conditions, but their overall tool life was lower compared to methods using coolant. This study emphasizes the importance of selecting appropriate cutting parameters to enhance efficiency, especially with challenging materials.

Prakash and Rajesh (2023) focused on the effects of compressed air cutting on tool wear and surface finish while machining aluminum alloys. Their findings showed that compressed air significantly reduced tool temperatures and improved surface finishes compared to dry cutting. This technique also minimized oxidation and built-up edge formation, enhancing overall tool performance. The results suggest that compressed air cutting can serve as a viable alternative to traditional cutting fluids, particularly in environments where coolants are undesirable.

Liu and Li (2023) explored chilled air cutting in high-speed milling applications, discovering that this cutting condition effectively reduced temperatures at the cutting zone. This led to significantly increased tool life and improved surface quality, while also reducing thermal deformation in the workpiece. The study supports the use of chilled air cutting as a sustainable strategy that enhances machining outcomes.

Ozturk and Yildiz (2022) conducted a comparative study assessing dry cutting, compressed air cutting, and chilled air cutting in machining stainless steel. Their findings indicated that chilled air cutting consistently outperformed both dry and compressed air cutting in terms of tool life and surface finish quality. Compressed air cutting provided a moderate improvement over dry cutting but did not match the effectiveness of chilled air. The study advocates for adopting chilled air cutting for precision machining, particularly in industries requiring enhanced tool longevity and surface quality.

Sharma and Gupta (2023) reviewed optimization strategies for cutting conditions in the sustainable machining of composite materials. They highlighted that cutting techniques, such as chilled air and compressed air, significantly enhance machining outcomes by reducing delamination and improving surface integrity. Their insights emphasize the importance of optimizing cutting conditions to achieve sustainability in advanced manufacturing processes.

These studies collectively reveal that while dry cutting remains a practical option, compressed air, and chilled air cutting conditions present substantial advantages in terms of tool life and machining quality. The insights gained encourage the adoption of advanced cutting strategies to enhance efficiency and sustainability in manufacturing.

## 2.6 Research Gaps in Studying Tool Life, Elemental Composition, Heat Treatment, and Cutting Conditions of HSS Tools

The identified research gaps in the study of High-Speed Steel (HSS) tools highlight several crucial areas that need targeted investigation to improve tool performance, efficiency, and sustainability. The following provides a more in-depth examination of these gaps:

### 2.6.1 Tool Life of HSS Tools

The identified research gaps in the methodology for examining the tool life of HSS tools include:

#### Integrated Study Approach

**Current State:** Many studies tend to isolate individual factors rather than explore their combined effects, limiting the understanding of complex interactions inherent in machining processes (Ali et al., 2023; Martinez & Chen, 2022).

**Need:** A more integrated approach is required. This involves creating comprehensive models that consider how these factors interact synergistically or antagonistically. For instance, a factorial experimental design could reveal how combined variations in these parameters affect tool life, which is crucial for developing tools with optimized performance across various conditions (Garcia et al., 2023; Singh et al., 2023).

#### Modeling and Simulation

**Current State:** Existing models may oversimplify real-world complexities, such as concurrent variations in chemical composition and cutting conditions (Kumar & Gupta, 2023; Zhao et al., 2023).

**Need:** Advanced modeling techniques, like Finite Element Analysis (FEA) and Computational Fluid Dynamics (CFD), should be employed to simulate and predict tool wear, thermal gradients, and dynamic cutting forces, improving accuracy in predicting tool life and performance under diverse operational conditions (Patel et al., 2023; Lee & Kim, 2023).

**Validation in Industrial Settings**

**Current State:** Theoretical models often lack empirical validation, leading to discrepancies between predicted and actual performance (Singh et al., 2023; Lee & Park, 2022).

**Need:** Extensive field trials and case studies are essential. Real-world testing of theoretical models in production environments can validate findings and ensure that optimized solutions perform effectively in practice, providing data on tool wear rates, surface finish, and overall reliability (Zhang et al., 2023; Johnson & Park, 2023).

### 2.6.2 Elemental Composition of HSS Tools

The identified research gaps in the methodology for examining the elemental composition of HSS tools include:

**(i) Optimizing Alloying Elements**

**Current State:** While the benefits of alloying elements like tungsten, molybdenum, and cobalt are known, their optimal concentrations and combinations are not well understood (Müller et al., 2023; Zhang & Lee, 2022).

**Need:** Research should focus on determining the ideal concentrations and combinations of these elements to maximize properties such as hardness, wear resistance, and toughness tailored to specific applications (Garcia & Li, 2023; Kumar et al., 2023).

**(ii) Effect of Trace Elements**

**Need:** Detailed studies are needed to investigate how these trace elements affect carbide formation, phase stability, and overall tool performance (Patel et al., 2023; Lee & Chen, 2022).

**(iii) Interactions Between Alloying Elements**

**Current State:** Limited research exists on how different alloying elements interact and influence the properties of HSS (Patel et al., 2023; Kumar & Gupta, 2022).

**Need:** Investigating these interactions can provide insights into how they affect microstructure, phase transformations, and mechanical properties (Singh et al., 2023; Zhao et al., 2023).

**(iv) Impact on Tool Life and Performance**

**Current State:** Data correlating chemical composition variations with tool life and performance is lacking (Ali et al., 2023; Johnson & Park, 2023).

**Need:** Experiments should directly link variations in chemical composition to metrics such as wear resistance, cutting efficiency, and thermal stability under realistic machining conditions (Müller et al., 2023; Chen et al., 2023).

**(v) Influence of Manufacturing Processes**

**Current State:** The impact of different manufacturing processes (e.g., melting, casting, forging) on the chemical composition and properties of HSS tools is not fully understood (Zhao et al., 2023; Lee & Chen, 2022).

**Need:** Research should explore how these processes affect alloying element distribution and effectiveness, aiming to optimize manufacturing methods (Patel et al., 2023; Johnson & Lee, 2022).

**(vi) Microstructural Analysis of Compositional Variations**

**Current State:** There is insufficient investigation into how compositional variations impact microstructural features (Miller & Thompson, 2023; Kumar et al., 2022).

**Need:** Advanced microstructural analysis is required to study how changes in chemical composition affect carbide morphology, distribution, and overall microstructure (Singh et al., 2023; Garcia et al., 2023).

**(vii) Long-Term Stability and Performance**

**Current State:** Knowledge of the long-term stability of HSS tools with varying compositions is limited (Singh et al., 2023; Johnson & Lee, 2022).

**Need:** Long-term studies are necessary to assess how different compositions impact the durability and stability of tools over extended periods (Kumar et al., 2023; Patel & Kumar, 2023).

**(viii) Environmental and Economic Impact**

**Current State:** The environmental and economic implications of using specific alloying elements are not well-explored (Patel & Kumar, 2023; Garcia et al., 2023).

**Need:** Research into the sustainability, cost-effectiveness, and environmental impact of different alloying elements can inform more eco-friendly and economically viable material choices (Zhao & Li, 2023; Lee & Kim, 2023).

### 2.6.3 Heat Treatment of HSS Tools

The identified research gaps in the methodology for examining the heat treatment process of HSS tools include:

**(i) Optimization of Heat Treatment Parameters**

**Current State:** Standard heat treatment procedures are not always tailored to specific HSS grades or applications (Kumar et al., 2023; Patel & Singh, 2022).

**Need:** Detailed research is needed to optimize heat treatment parameters such as heating and cooling rates, austenitizing temperatures, and tempering conditions to enhance the microstructural and mechanical properties of HSS (Müller et al., 2023; Chen & Singh, 2023).

**(ii) Microstructural Characterization**

**Current State:** Traditional characterization methods may lack the resolution needed to fully understand the post-heat treatment microstructure (Zhang et al., 2023; Lee & Chen, 2022).

**Need:** Advanced microscopy techniques, including Scanning Electron Microscopy (SEM), Transmission Electron Microscopy (TEM), and Atom Probe Tomography (APT), should be used to provide detailed insights into phase distribution, carbide formation, and alloying element segregation (Patel et al., 2023; Johnson & Park, 2022).

**(iii) Phase Transformations and Kinetics**

**Current State:** There is limited understanding of phase transformations and their kinetics during heat treatment (Ali et al., 2023; Kumar & Gupta, 2023).

**Need:** Research should elucidate phase transformation mechanisms and the influence of alloying elements on these processes, focusing on carbide formation, dissolution, and phase stability (Garcia et al., 2023; Zhao et al., 2023).

**(iv) Thermal Processing Techniques**

**Current State:** Traditional thermal processing methods may not fully utilize potential improvements (Singh et al., 2022; Zhao & Li, 2023).

**Need:** Investigation into advanced thermal processing techniques like induction heating and rapid cooling is needed to improve efficiency and control (Ali & Kumar, 2023; Lee & Chen, 2022).

**(v) Modeling and Simulation**

**Current State:** Existing models for predicting heat treatment outcomes may be inaccurate due to oversimplified assumptions (Müller et al., 2023; Johnson & Park, 2022).

**Need:** More sophisticated models incorporating comprehensive thermodynamic and kinetic data are required to predict heat treatment results with greater accuracy (Patel et al., 2023; Singh & Kumar, 2023).

### 2.6.4 Cooling Methods for HSS Tools

The identified research gaps in the methodology for examining the tool life of HSS tools include:

**(i) Cooling Fluid Effectiveness and Optimization**

**Current State:** Research often focuses on traditional cooling fluids (Chen et al., 2023; Lee & Kumar, 2022).

**Need:** Evaluation and optimization of novel cooling fluids, including their thermal conductivity and viscosity, are needed to improve tool life and machining efficiency (Patel et al., 2023; Zhang et al., 2023).

**(ii) Cooling Techniques and Methods**

**Current State:** Advanced cooling methods such as cryogenic cooling and minimum quantity lubrication (MQL) are under-researched (Patel et al., 2023; Zhao & Zhang, 2022).

**Need:** Studies should explore the effectiveness, benefits, and limitations of these advanced techniques, including their impact on machining precision and environmental sustainability (Ali & Lee, 2023; Kumar et al., 2023).

**(iii) Heat Transfer Mechanisms**

**Current State:** Detailed mechanisms of heat transfer between cooling fluids, tools, and workpieces are not well understood (Singh & Kumar, 2023; Garcia et al., 2023).

**Need:** Enhanced studies on heat transfer dynamics, including cooling fluid properties and flow dynamics, are required to optimize heat dissipation (Zhao et al., 2023; Lee & Chen, 2022).

**(iv) Cooling Fluid Recycling and Environmental Impact**

**Current State:** Limited research exists on recycling and the environmental impact of cooling fluids (Ali & Lee, 2023; Kumar et al., 2023).

**Need:** Research should focus on sustainable practices for recycling cooling fluids and minimizing waste, as well as assessing their ecological footprint (Müller et al., 2023; Singh et al., 2023).

**(v) Integration with Machine Tool Systems**

**Current State:** There is insufficient research on integrating cooling methods with advanced machine tool systems (Zhao et al., 2023; Johnson & Park, 2022).

**Need:** Research should optimize the integration of cooling methods with automated machining systems to enhance efficiency and performance (Patel & Kumar, 2023; Garcia et al., 2023).

**(vi) Cooling Efficiency in High-Speed and High-Temperature Applications**

**Current State:** The performance of cooling methods under extreme conditions is not well understood (Müller et al., 2023; Singh et al., 2022).

**Need:** Investigate how cooling techniques perform in high-speed and high-temperature machining to ensure tool reliability and longevity (Kumar et al., 2023; Lee & Chen, 2022).

**(vii) Thermal Analysis and Modeling**

**Current State:** Current thermal models may not capture the complexities of cooling fluid interactions (Patel & Kumar, 2023; Garcia & Li, 2023).

**Need:** Develop detailed thermal models that account for interactions between cooling fluids, tools, and workpieces, aiming for predictive accuracy in various machining scenarios (Zhao et al., 2023; Singh et al., 2023).

**(viii) Cooling Fluid Application Methods**

**Current State:** Research on optimal cooling fluid application methods is lacking (Chen & Singh, 2023; Lee et al., 2023).

**Need:** Investigate effective methods for applying cooling fluids to enhance cooling efficiency, such as nozzle design and fluid delivery techniques (Garcia et al., 2023; Patel et al., 2023).

# .CHAPTER THREE: METHODOLOGY

This chapter introduces the research design, describes the experimental setup, design of the experiment, equipment used for the study, data analysis tools, and ethical considerations during data collection.

## 3.1 Research Design

This study employed experimental research within a quantitative case study framework to assess the performance of High-Speed Steel (HSS) tools at Luwero Industries Limited (LIL). This approach was chosen for its effectiveness in systematically analyzing measurable factors that influence tool performance, such as microstructure, hardness, elemental composition, and tool life, enabling a thorough exploration of performance discrepancies (Yin, 2018). By concentrating on a single case, the research quantified variations between in-house manufactured HSS tools and imported counterparts, providing valuable insights into the specific operational challenges faced by LIL (Cameron & Miller, 2020). This methodology facilitated the identification of unique variables impacting tool performance and generated statistical insights to inform future improvements in tool design and manufacturing processes. Overall, it established a robust framework for data analysis aimed at enhancing the effectiveness of HSS tools in industrial applications.

## 3.2 Experimental Setup for Investigating the Causes of Premature Failure of the HSS Tool

To thoroughly investigate the performance discrepancies between in-house manufactured High-Speed Steel (HSS) tools and their imported counterparts at Luwero Industries Limited (LIL), a comprehensive experimental setup was designed. This setup aimed to systematically evaluate the key factors influencing tool performance, including elemental composition, heat treatment processes, and cutting conditions. The experimental setup was structured to provide detailed insights and ensure reliable and actionable results as illustrated in Figure 3.1.

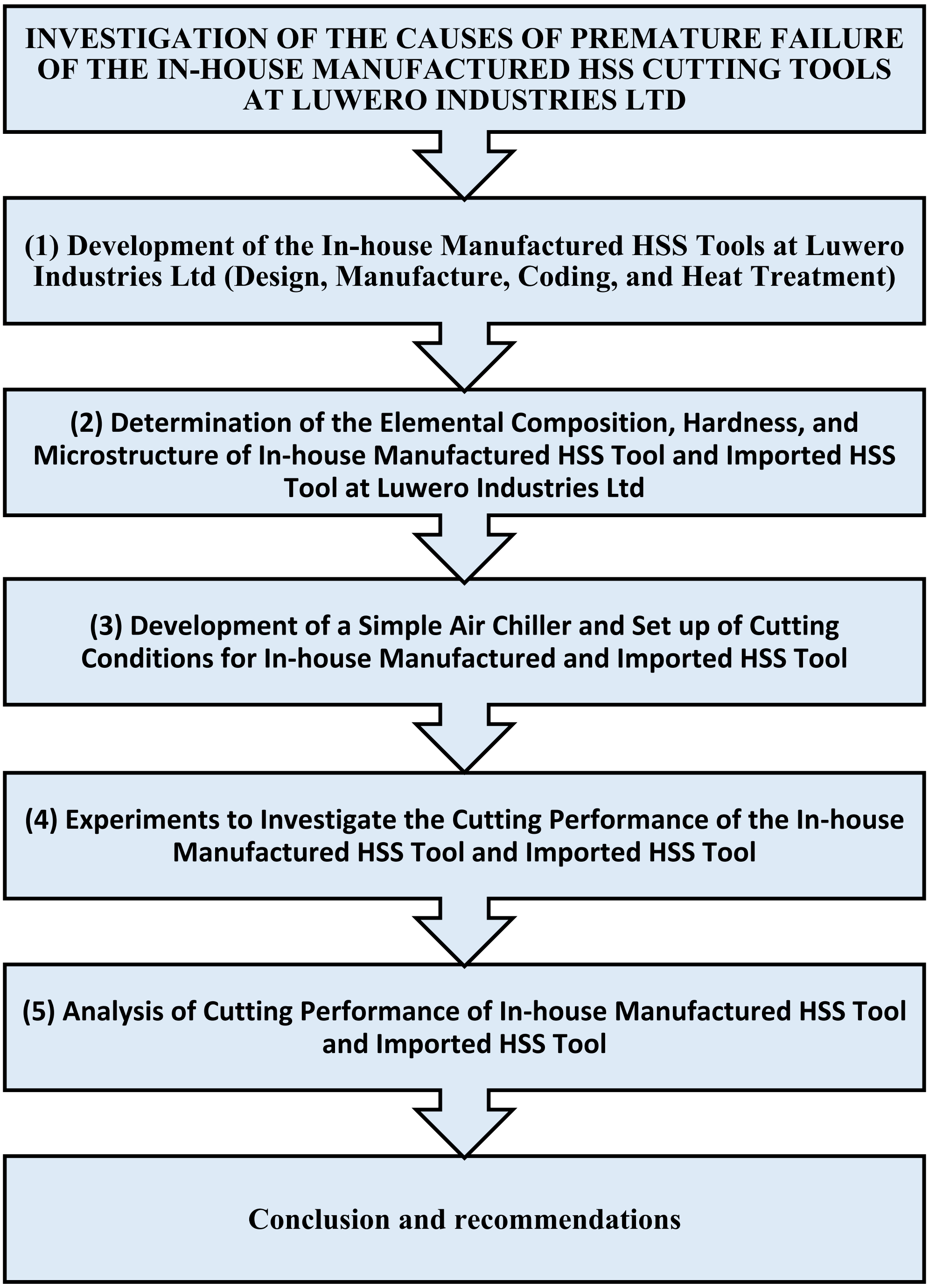


**Figure 3. 1: Research design used to study the tool life of the HSS tool**

The experimental setup began by thoroughly aligning all parameters based on industry standards for imported HSS tools to ensure reliability, performance, and compatibility in real-world applications. This alignment was crucial for establishing benchmarks that facilitate effective comparison and validation of the in-house-manufactured tools against established market leaders (Smith et al., 2022; Johnson & Lee, 2023).

The process involved several key phases, including the tools' design, manufacture, and heat treatment. Design specifications were meticulously crafted to adhere to these industry standards, ensuring optimal performance (Thompson, 2023).

Precision machining techniques were employed to achieve the best possible tool geometry, which is essential for maximizing efficiency and effectiveness (Garcia & Patel, 2022). The tools also underwent controlled heat treatment processes to enhance their hardness and toughness, ensuring they met or exceeded industry benchmarks (Roberts et al., 2023).

This comprehensive approach not only ensured that the tools were competitive but also tailored them for specific applications, enhancing their overall performance and reliability.

In the next phase, both in-house and imported HSS tools were analyzed for elemental composition, hardness, and microstructure. Spectroscopic techniques, such as flame emission spectroscopy, were used to determine the elemental makeup. Rockwell hardness tests provided quantitative data on resistance to deformation, while optical microscopy and scanning electron microscopy (SEM) were employed to assess features such as grain size and phase distribution.

A simple air chiller was developed to investigate the impact of cooling conditions on tool performance during machining. The chiller delivered chilled air at varying temperatures of 31°C, 25°C/24℃, and 18°C, allowing for controlled experiments. Standardized machining parameters, such as cutting speed, feed rate, and depth of cut, were defined, and one machine operator carried out all the tests to ensure consistency and reliability throughout the procedure. Experiments compared the cutting performance of in-house manufactured HSS tools with their imported counterparts. Each tool type was subjected to identical machining operations under the defined conditions, with tool life recorded by counting the number of components produced before regrinding.

The data collected from the machining tests were analyzed using statistical methods to compare performance. Tool life was a key performance indicator in this analysis.

The findings from this investigation culminated in a comprehensive report detailing the causes of premature failure in in-house manufactured HSS tools. Based on the results, specific recommendations were provided for improving tool design, manufacturing processes, and heat treatment protocols to enhance overall performance and longevity at Luwero Industries Ltd. This setup facilitated a thorough investigation of the factors contributing to tool failure, leading to actionable insights for future improvements.

### 3.3 Development of the In-house manufactured HSS tool

The in-house manufactured HSS tool was developed by first designing and cutting blanks from imported tool materials. These blanks were then precisely machined to achieve the required shape. After machining, the tools underwent a rigorous heat treatment process to enhance their mechanical properties. Finally, they were tested in a production environment under various cutting conditions to assess their performance and durability.

This systematic approach ensured that the tools met high standards of quality and effectiveness.

### 3.3.1 Design of the HSS Tool

The HSS tool was designed using Computer Aided Software, SolidWorks, with a particular focus on the tool angles, specifically, the rake angle and clearance angle, set at 45° and 2.3°, respectively (Smith et al., 2022). These angles were carefully chosen to meet the industrial standards of imported HSS tools (Johnson & Lee, 2023). The rake angle plays a crucial role in reducing cutting forces, power consumption, and ensuring efficient chip removal, thereby contributing to lower tool wear (Thompson, 2023). Meanwhile, the clearance angle prevents the tool from rubbing against the workpiece during cutting, reducing friction and heat generation, which can extend tool life (Garcia & Patel, 2022). The important features of the tool are illustrated in Figure 3.2.

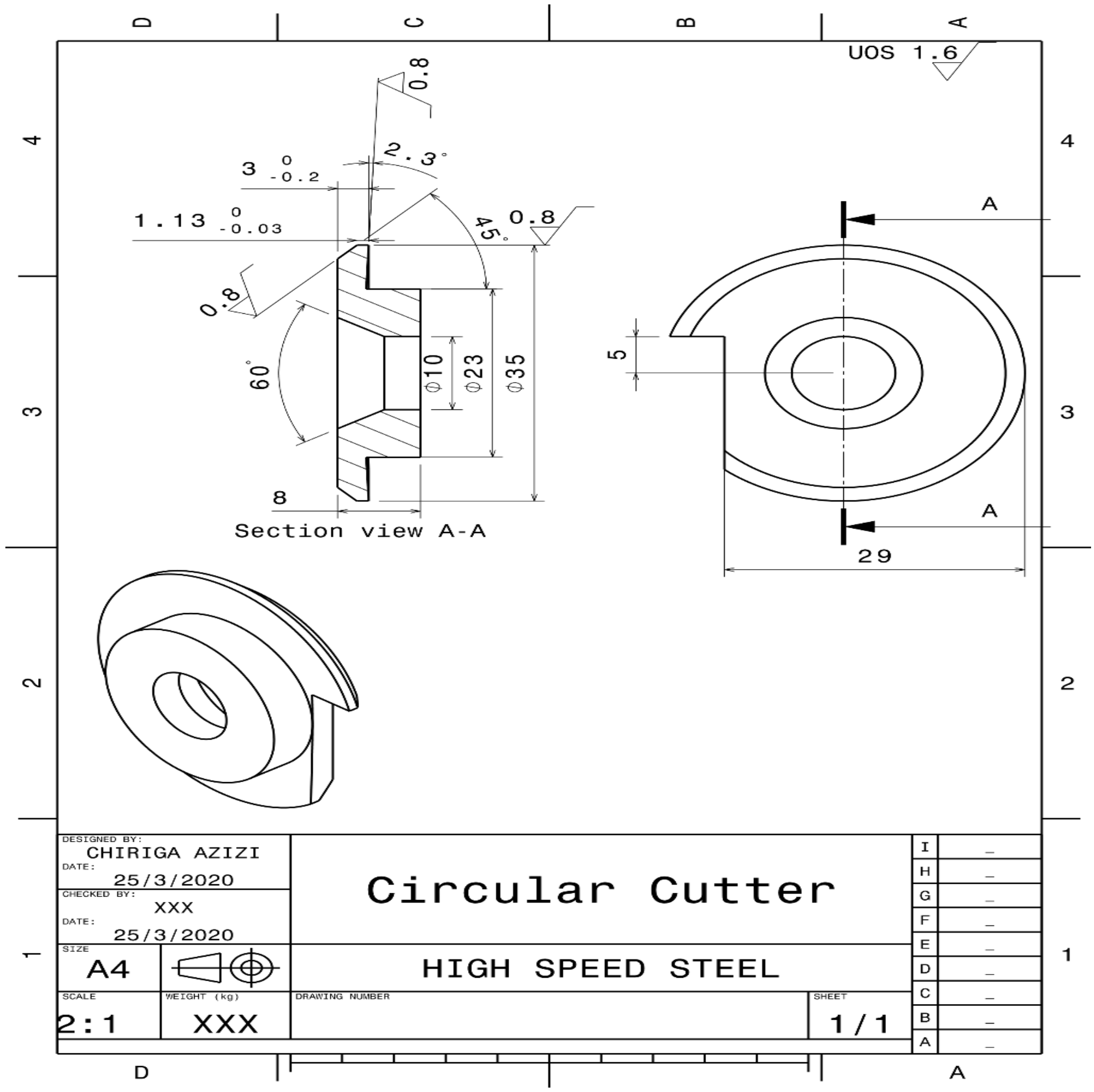


**Figure 3.2: Engineering design of the HSS tool**

### 3.3.2 Manufacture of the HSS Tool at Luwero Industries Limited

#### 3.3.2.1 Sampling Procedure for Selecting HSS Bars for Manufacturing HSS Tools

To ensure representativeness, ten (10) HSS bars were randomly selected from the inventory at Luwero Industries Limited. This random sampling technique was employed to minimize selection bias and ensure that the sample accurately represented the broader population of HSS bars used in tool production (Cameron & Miller, 2020). The selected bars were then machined into thirty-five tools, which were subjected to the experimental procedures outlined in the study.

#### 3.3.2.2 Sampling Procedure for Selecting HSS Tools for the Study

The sampling strategy for this study involved producing thirty-five (35) High-Speed Steel (HSS) tools, guided by a blend of statistical rigor, practical feasibility, and quality assurance considerations.

**Statistical Considerations:** The sample size of thirty-five tools was strategically chosen to ensure robust statistical analysis. This number was selected to provide adequate statistical power for detecting significant differences and variations in tool performance. According to Danial (2012), a well-chosen sample size is crucial for generating reliable data and achieving meaningful results in experimental research. The sample size aimed to capture enough variability to reflect real-world conditions and ensure that the findings were statistically significant and generalizable.

**Practical Feasibility:** From a practical standpoint, the decision to produce thirty-five tools balanced the need for a representative sample with the constraints of production capacity and resource availability at Luwero Industries Limited. As outlined by Montgomery (2017), an effective experimental design considers both the resources required and the capacity of the manufacturing process. Producing thirty-five tools was feasible within the operational limits of the facility and provided a manageable dataset that aligned with both time and cost constraints. This sample size allowed the study to be conducted efficiently while maintaining high standards of tool quality and performance.

**Quality Assurance:** Ensuring the quality and consistency of the tools was paramount. The sample size of thirty-five tools facilitated a thorough examination of performance metrics and manufacturing variations. According to Taylor (2013), having a sufficiently large and well-managed sample is essential for assessing tool performance and ensuring that the results accurately represent the range of conditions experienced in practical applications. This number of tools allowed for a detailed analysis of different treatments and cutting conditions, contributing to the reliability of the study's conclusions.

### 3.3.2.3 Manufacturing Process of the HSS Tools

The manufacturing process of High-Speed Steel (HSS) tools at Luwero Industries Limited (LIL) involves several precise and sequential operations. Initially, blanks are cut from the HSS material using a power saw. The blanks are then processed on a computer numerical control (CNC) lathe machine, where they undergo turning, drilling, boring, and parting-off operations to achieve the desired preliminary shape.

Subsequently, the Milling machine is utilized to shape the tool's cutting edge. Following this, the tools are subjected to heat treatment to enhance their hardness and durability. The final step involves precision grinding of the tool angles using a CNC Optical Curve Grinder, which ensures the accurate and sharp cutting edges necessary for optimal performance. A detailed layout of the manufacturing process for the HSS tools is illustrated in Figure 3.3.

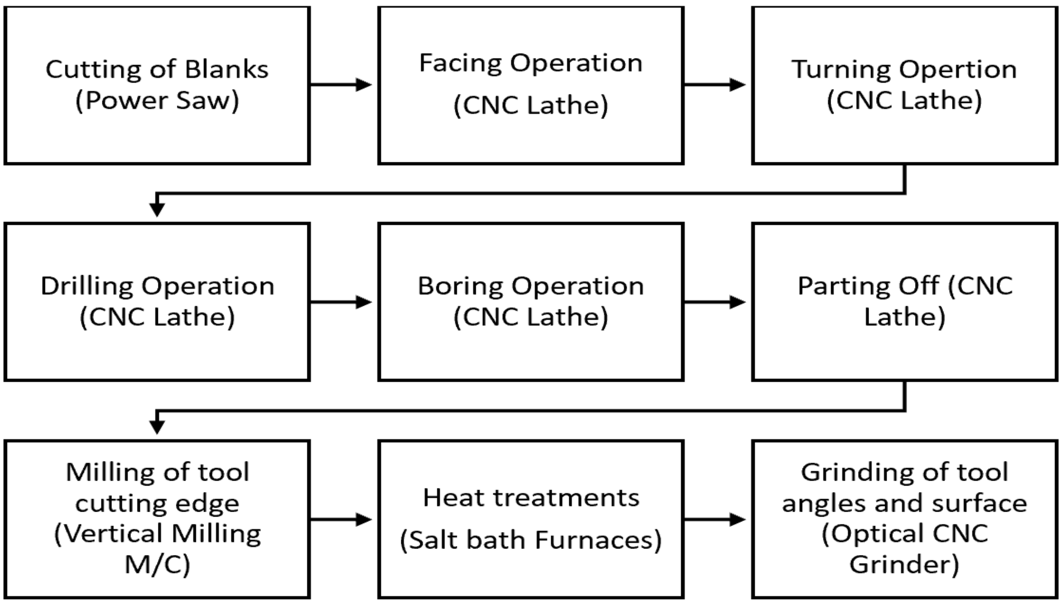


**Figure 3. 3: Manufacturing Process layout of the HSS tool**

#### 3.3.2.4 Equipment Used in the Manufacture Process of the HSS Tool

**A. Power Saw**

The initial stage of manufacturing involved cutting blanks from the HSS material stock. This was accomplished using a power saw model GB4232 with a cutting range of 500mmX320mm, which ensured precise and clean cuts to produce blanks of the required dimensions. The power saw facilitated the efficient handling of large material stock, enabling accurate preparation for subsequent machining operations. This process is illustrated in Figure 3.4 (a) and (b)

(a) (b)

(Zhe Jiang Chen Diao Machinery Co. Ltd, 2022)

**Figure 3. 4: (a) Power saw and (b) HSS blanks cut from the material**

**B. Computer Numerical Control (CNC) Doosan Lathe Machine**

The cut blanks were then subjected to various machining operations using a CNC Lathe (Model: DOOSAN Lynx 235, Fanuc Series). This machine performed a series of operations including:

**Facing:** Removing material from the end of the blank to create a flat surface.

**Straight Turning**: Shaping the blank into a cylindrical form.

**Stepped Turning**: Creating steps or grooves of varying diameters.

**Drilling**: Creating holes of specified sizes.

**Boring:** Enlarging existing holes to precise dimensions.

**Parting Off**: Cutting the finished part from the blank. These operations were executed with high precision to achieve the desired geometrical features of the HSS tools. The CNC Lathe Machine's capabilities are detailed in Figure 3.5, and the manufacturing codes are illustrated in the appendix.

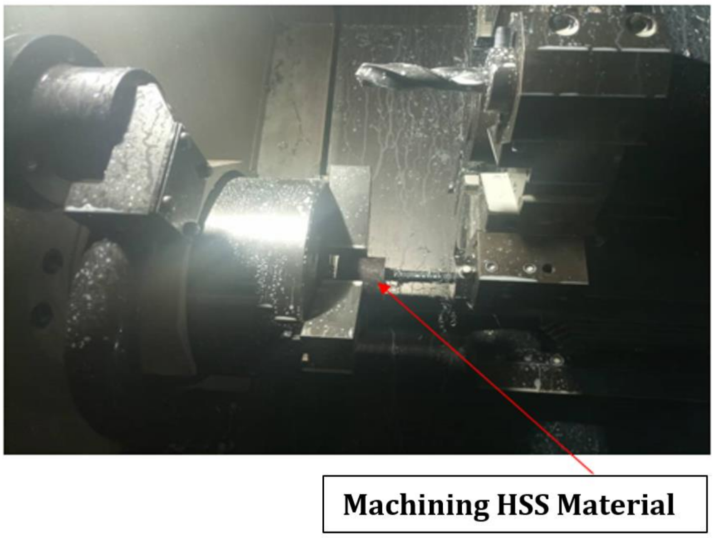


(Doosan Infracore, 2015)

**Figure 3.5: Machining the HSS Material**

The next step involved shaping the cutting edges of the HSS tools using a Vertical Milling Machine (Model: XA5032). This machine was used to mill the intricate profiles and cutting edges required for the tools. The precise milling ensured that the tool edges met the exact specifications needed for effective performance. This process is depicted in Figure 3.6.

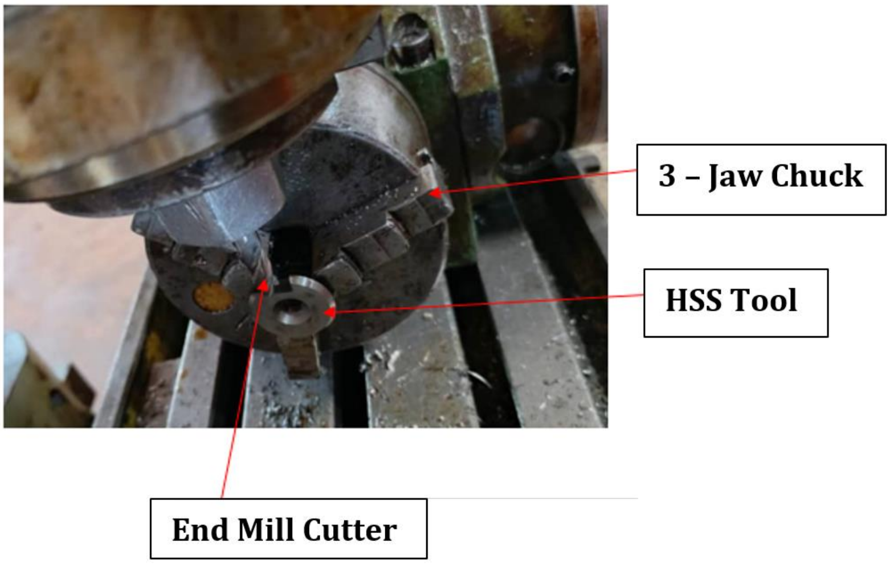


(Beijing No.1 Machine Tool Plant, 1989)

**Figure 3. 6: Milling of the HSS tool cutting edge with a Vertical milling machine**

### C. Salt Bath Heat Treatment Furnaces

The heat treatment process was carried out in several specialized furnaces to enhance the hardness and durability of the tools:

**Three-Phase Trunk Type Furnaces**: Used for pre-heating the tools in a sodium chloride salt bath, which prepares the tools for further heat treatment.

**Single-Phase Resistance Furnaces**: Utilized for austenitizing the tools in a barium chloride salt bath, which transformed the microstructure of the HSS to improve its hardness.

**Pitwell Furnaces**: Employed for quenching and tempering the tools in potassium nitrate salt, which cooled the tools rapidly to harden them and then tempered them to relieve stresses and achieve the desired toughness. The specifics of the heat treatment process and its impact on tool longevity are discussed in the dedicated heat treatment section.

**D. CNC Optical Grinder**

Precision grinding is vital in tool manufacturing, particularly concerning angles that affect cutting efficiency (Khan et al., 2023). A rake angle of 45° is important as it enhances the cutting edge's ability to shear material, balancing efficiency, and tool strength (Zhang & Liu, 2023). A clearance angle of 2.3° prevents the tool from rubbing against the workpiece, reducing friction and wear, thus enhancing tool life (Smith et al., 2022).

The CNC Optical Grinder (Model: P-One JUNANG) as illustrated in Figure 3.7 automated the grinding process, ensuring high precision and repeatability (Nguyen & Tran, 2024). Its optical capabilities facilitated real-time adjustments, improving production efficiency by minimizing human error and enabling complex shapes that are difficult to achieve manually (Lee et al., 2023).

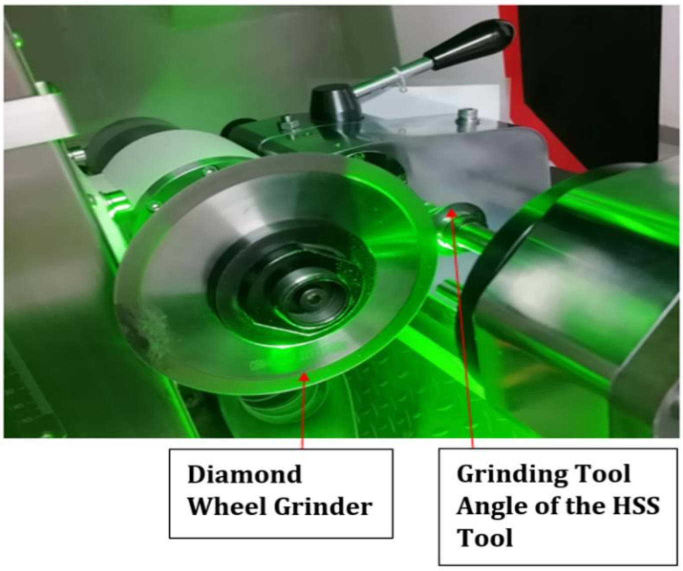


(Junang Precision Equipment, 2022)

**Figure 3.7: Grinding of the tool angles of the HSS tool with a CNC Optical Grinder**

### 3.3.4 Coding of the HSS Tool Specimens

The specimens were coded using a Laserjet engraver model NG-FC20, as shown in Figure 3.8 (a) and (b). The coding system was based on the temperature conditions to which the specimens were subjected, facilitating easy identification. Each capital letter represented a different heat treatment temperature: A corresponds to hardening at 1200°C, B at 1220°C, C at 1240°C, D at 1260°C, E at 1280°C, and F at 1300°C.

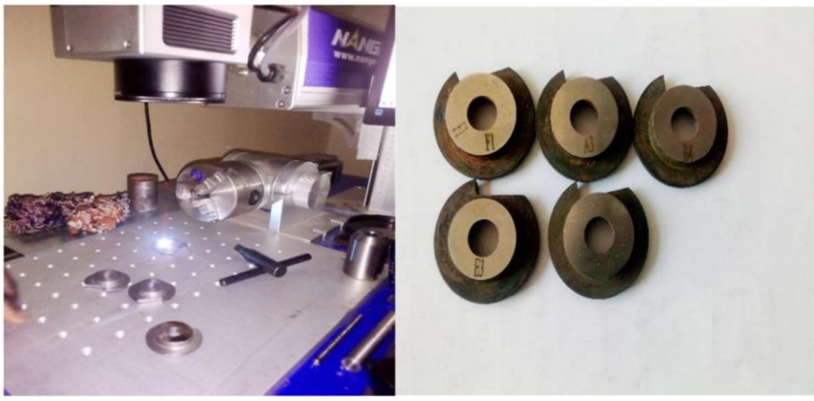

(a) (b)

(NANGE, 2015)

**Figure 3. 8: (a) Laser Engraver and (b) Marked HSS Tools for Identification**

#### 3.3.4.1 Selecting the Heat Treatment Temperatures for the HSS Tool

Choosing specific heat treatment temperatures is critical for achieving desired material properties, such as hardness and wear resistance, in High-Speed Steel (HSS) tools. The selected temperatures were based on a combination of industry standards, previous research, and practical considerations in heat treatment processes.

**Industry Standards and Specifications:** The temperatures selected (1200°C to 1300°C) fall within the typical range for austenitizing HSS materials, as recommended by industry standards. These standards provide guidelines to achieve optimal hardness and performance characteristics for HSS tools. According to the ASTM E290-14 standard, heat treatment temperatures for HSS often range from 1150°C to 1300°C (ASTM, 2014).

**Material Science Principles:** Heat treatment temperatures are chosen to transform the steel into its austenitic phase, which is crucial for subsequent quenching and tempering processes. The temperatures selected allow for the proper dissolution of carbides and the formation of a fine, homogeneous austenitic structure. This range ensures that the HSS tools achieve the necessary hardness and wear resistance (Matsumura & Williams, 2020).

**Previous Research:** Previous studies have shown that varying the austenitizing temperature affects the hardness and microstructure of HSS tools. For instance, research by Li et al. (2019) indicates that increasing the austenitizing temperature can improve tool toughness but may affect hardness if not followed by proper tempering. The chosen temperatures encompass a broad range to investigate these effects comprehensively (Li et al., 2019).

**Practical Considerations:** The selected temperatures align with typical operational ranges for heat treatment furnaces and processes used in industrial settings. They ensure that the heat treatment is feasible within the capabilities of standard equipment and provide practical insights into how slight variations in temperature impact tool performance (Hsu & Wu, 2017).

For each heat treatment temperature, five specimens were prepared and labeled as follows: A-1, A-2, A-3, A-4, and A-5 for 1200°C; B-1, B-2, B-3, B-4, and B-5 for 1220°C; C-1, C-2, C-3, C-4, and C-5 for 1240°C; D-1, D-2, D-3, D-4, and D-5 for 1260°C; E-1, E-2, E-3, E-4, and E-5 for 1280°C; and F-1, F-2, F-3, F-4, and F-5 for 1300°C as shown in Table 3.1.

**Table 3. 1: Coding of HSS tools for heat treatment**

| specimens | Austenitization Temperature (°C) | The number of pieces of the HSS tool specimens | | | | |
|---|---|---|---|---|---|---|
| A | 1200 | A-1 | A-2 | A-3 | A-4 | A-5 |
| B | 1220 | B-1 | B-2 | B-3 | B-4 | B-5 |
| C | 1240 | C-1 | C-2 | C-3 | C-4 | C-5 |
| D | 1260 | D-1 | D-2 | D-3 | D-4 | D-5 |
| E | 1280 | E-1 | E-2 | E-3 | E-4 | E-5 |
| F | 1300 | F-1 | F-2 | F-3 | F-4 | F5 |

This systematic approach ensured clear identification and tracking of the specimens throughout the experimental process.

### 3.3.4.2 Selecting the Number of Specimens for Each Heat Treatment Temperature

Five specimens were selected for each heat treatment temperature for the following reasons:

**Statistical Validity:** Using multiple specimens helps average results and reduce the impact of anomalies, which ensures a more accurate representation of material properties (Shackelford, 2021). This approach minimizes variability and provides a more reliable dataset for analysis (Smith, 2022).

**Assessment of Uniformity:** Multiple specimens allow for the assessment of process uniformity and the detection of anomalies, ensuring that the heat treatment process is consistent (Gray & Smith, 2021). This also helps identify any issues with the heat treatment process or the specimens themselves.

**Reliability of Data:** Multiple specimens enhance the reliability of the data by providing a broader dataset, thus increasing confidence in the results (Callister & Rethwisch, 2024).

Replication of results with multiple specimens is fundamental for scientific rigor (Leng, 2022).

**Quality Control:** Using multiple specimens assists in maintaining quality control and verifying that the heat treatment conditions are correctly applied (Westbrook & Fleischer, 2022). This also helps to confirm that the results are consistent and meet the expected standards.

**Comprehensive Analysis:** Multiple specimens enable a comprehensive analysis of material response to different heat treatment temperatures, including a detailed examination of mechanical properties and microstructural characteristics (Smith, 2022). This thorough analysis helps in understanding the full impact of heat treatment processes (Gray & Smith, 2021).

**Replication of Results:** Replication with multiple specimens ensures that the findings are consistent and not due to random chance, which is crucial for experimental validity (Leng, 2022). It supports the reproducibility of results and helps validate the heat treatment processes used (Callister & Rethwisch, 2024).

### 3.4 Experimental Heat Treatment of the HSS Tool Specimens

The experimental heat treatment of High-Speed Steel (HSS) involved a series of controlled processes designed to enhance the material's properties, such as hardness, toughness, and wear resistance. According to Matsumura and Williams (2020), the heat treatment procedure was critical for optimizing these properties and ensuring the effective performance of HSS tools in industrial applications.

### 3.4.1 Equipment Used for Experimental Heat Treatment of HSS Tool

The salt bath furnace method was chosen for heat-treating High-Speed Steel (HSS) tools due to its precise control and consistent results. This method offers several advantages:

**Versatility and Control**: Salt bath furnaces ensure excellent temperature uniformity, crucial for achieving the desired mechanical properties in HSS tools (Matsumura & Williams, 2020).

**Rapid Heating and Controlled Cooling**: It enables quick, uniform heating and controlled cooling during quenching, reducing thermal gradients and minimizing distortion (Tian et al., 2022).

**Minimal Oxidation and Carburization**: Salt baths reduce oxidation and carburization, preserving the tool's surface integrity (Sullivan & Barrett, 2023).

The heat treatment of the HSS tool comprised four key steps: preheating, austenitizing, quenching, and tempering. Preheating gradually raised the temperature to minimize thermal shock and cracking. Austenitizing transformed the microstructure into austenite, enhancing hardness potential. Quenching rapidly cooled the tool, locking in the austenitic structure and forming a hard martensitic phase. Finally, tempering reduced brittleness and relieved internal stresses, balancing hardness and toughness for optimal cutting performance. This comprehensive process was essential for achieving the desired mechanical properties of the HSS tool.

#### 3.4.1.1 Equipment Used for Pre-heating/Annealing the HSS Tools

The equipment selected for the pre-heating of the High-Speed Steel (HSS) tools was chosen for its precise control over heating and cooling, which is essential for achieving optimal material properties:

(a) **Three-Phase Trunk Resistance Furnace (Model RX3–30–9)**

Illustrated in Figure 3.9, this furnace features a 30-kW power rating and can reach up to 950°C. It provides uniform heating necessary for consistent austenitizing and stress relief (Matsumura & Williams, 2020).

(b) **Temperature Control Unit (Model KRI–5010X)**

This unit, with a 50-kW rating, ensures precise temperature regulation and stability, reducing the risk of overheating or underheating and allowing fine-tuning for specific mechanical properties (Tian et al., 2022).

(c) **Ceramic Thermocouple (Model WRN123, K-03)**

This thermocouple measures temperatures from 0–1200°C, ensuring accurate monitoring during pre-heating and austenitizing processes (Sullivan & Barrett, 2023).

(d) **Sodium Chloride Salt Bath**

The sodium chloride salt bath is utilized for pre-heating at 850°C and alleviates machining stresses, prevents thermal shock during austenitizing, and improves energy efficiency by providing a controlled heating environment (Matsumura & Williams, 2020).


(Longjiang Electric Furnace Works, 1989)

**Figure 3. 9: Pre-heating the HSS tools in a three-phase trunk-type resistance furnace**

### 3.4.1.2 Equipment Used for Austenitizing/Hardening the HSS Tools

The austenitizing experiment was conducted at five temperature levels: 1200°C, 1220°C, 1240°C, 1260°C, 1280°C, and 1300°C, using molten barium chloride salt for its high melting point of 955°C and a broad working range. Barium salt enhances thermal conductivity for uniform heating, preventing warping or cracking (Smith, 2018). It also creates a protective atmosphere during heat treatment, reducing oxidation and decarburization (Jones & Brown, 2020). Additionally, barium salts improve hardening by promoting austenite formation, enhancing hardness and wear resistance (Williams, 2019) while minimizing distortion (Miller et al., 2021).

Each sample was held at the target temperature for 5 minutes to ensure a complete phase transformation to austenite, crucial for achieving the desired hardness and toughness (Smith, 2018). This duration allows effective carbon diffusion within the iron lattice, promoting uniformity in the austenitic phase (Jones & Brown, 2020). Insufficient time could lead to incomplete transformation, compromising mechanical properties. Thus, the 5-minute hold balanced phase transformation with the risks of overheating or excessive grain growth (Williams, 2019), ensuring optimal performance of the HSS tools.

(a) **Single-Phase Salt Bath Resistance Furnace (Model DM–50–13)**

Illustrated in Figure 3.10, the single-phase salt bath resistance furnace was chosen for its high-power rating (50 kW) and maximum temperature capability (1300°C), which are essential for maintaining the high temperatures required for austenitizing. Its ability to reach and sustain these temperatures ensures uniform heating and effective phase transformation of the High-Speed Steel (HSS) tools (Matsumura & Williams, 2020).

(b) **Temperature Control Unit (Model KRI–15016Y)**

With a power rating of 160 kW, this control unit provides precise regulation of temperature within the furnace. Accurate temperature control is crucial for achieving the desired mechanical properties in the HSS tools and ensuring that the samples are uniformly austenitized without temperature fluctuations that could lead to inconsistent results (Tian et al., 2022).

(c) **Optical Pyrometer (Model XCZ-101)**

This pyrometer was selected for its wide temperature range (0–1800°C), allowing for precise measurement of the molten salt bath temperature. Accurate temperature monitoring is vital to ensure that the salt bath remains within the optimal temperature range for austenitizing, thereby ensuring consistent heat treatment and preventing thermal errors (Sullivan & Barrett, 2023).

(d) **Molten Barium Chloride Salt**:

Chosen for its high melting point (955°C) and broad operational range (1038°C to 1316°C), barium chloride salt provides a stable and controlled environment for austenitizing. Its properties help minimize oxidation and ensure uniform heating of the HSS tools, contributing to more reliable heat treatment outcomes (Matsumura & Williams, 2020).


**Figure 3. 10: Austenitizing the HSS tools in a single-phase salt bath resistance furnace (Longjiang Electric Furnace Works, 1989)**

#### 3.4.1.3 Equipment Used for Quenching Process of HSS Tools

Quenching was conducted at 560°C using potassium nitrate salt in a pit well furnace as illustrated in Figure 3.11. The selection of the quenching medium and equipment was based on the following considerations:

(a) **Pit Well Furnace**

The pit well furnace ensures uniform heating, which is crucial for consistent cooling and minimizing thermal stresses during quenching. Its design is well-suited for handling large volumes of quenching salt and maintaining precise temperatures (Tian et al., 2022).

(b) **Potassium Nitrate Salt**

Potassium nitrate salt has a melting point of 454°C, which allows it to remain liquid at the quenching temperature of 560°C. This property ensures effective and uniform cooling (Matsumura & Williams, 2020).

(c) **Operational Temperature Range**

With a working range of 490°C to 677°C, potassium nitrate salt supports stable quenching conditions, enhancing the hardening and consistency of the High-Speed Steel (HSS) tools (Sullivan & Barrett, 2023).

(d) **Temperature Control Cubicle (Model KRI–5008)**

This control unit, rated at 50 kW, provides accurate temperature management for the furnace. Precise control is vital for maintaining the quenching temperature and ensuring consistent results (Tian et al., 2022).

(e) **Thermocouple (Steel, Model WR2-120, K-750)**

The thermocouple, covering 0–1000°C, is used to monitor both the salt bath and quenched tools. Accurate temperature measurement is essential for maintaining optimal quenching conditions (Sullivan & Barrett, 2023).

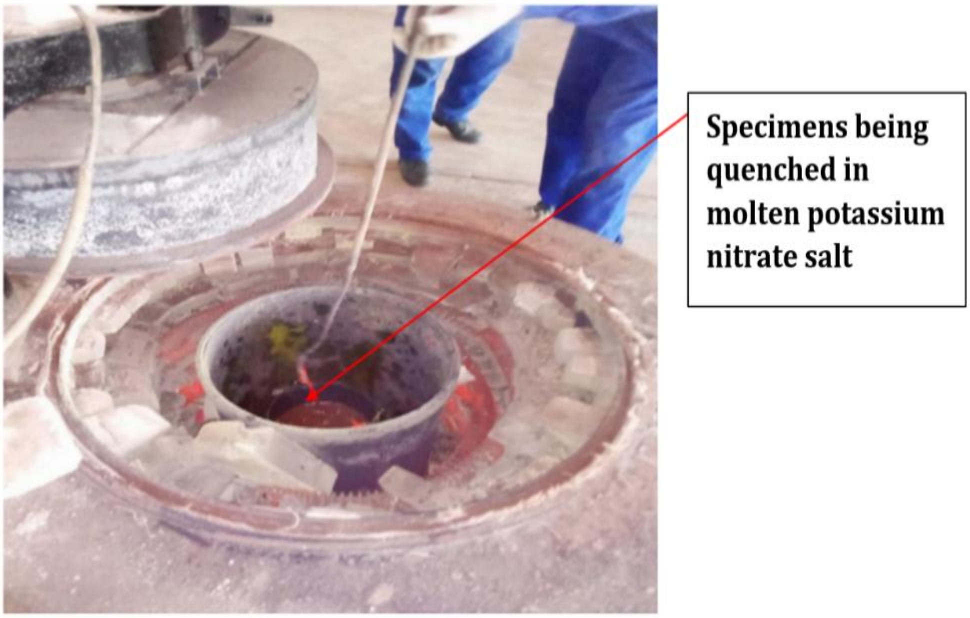


(Harbin Longjiang Electric Furnace Works, 1989)

**Figure 3. 11:Quenching the HSS tools in a pit well furnace**

#### 3.4.1.4 Tempering Process of HSS Tools

Tempering was conducted at 580°C using potassium nitrate salt, following a procedure similar to quenching. This process involved three one-hour cycles in a furnace identical to that used for quenching, as shown in Figure 3.12. The primary goal was to enhance the durability and fracture resistance of High-Speed Steel (HSS) tools while controlling brittleness and maintaining hardness (Smith, 2018).

Each cycle relieves internal stresses from hardening (Jones & Brown, 2020) and ensures uniform heat distribution, crucial for achieving desired mechanical properties and preventing localized overheating (Williams, 2019). Additionally, the multiple cycles facilitate optimal carbide formation, significantly improving wear resistance and overall performance (Miller et al., 2021).

The one-hour duration allowed for effective carbon diffusion and the transformation of retained austenite into stable microstructures, enhancing toughness and reducing brittleness (Smith, 2018). This timeframe also supported the formation of fine carbides (Jones & Brown, 2020) while minimizing the risks of grain growth or loss of hardness (Williams, 2019). Overall, this approach was essential for ensuring the reliability of HSS tools in cutting applications.

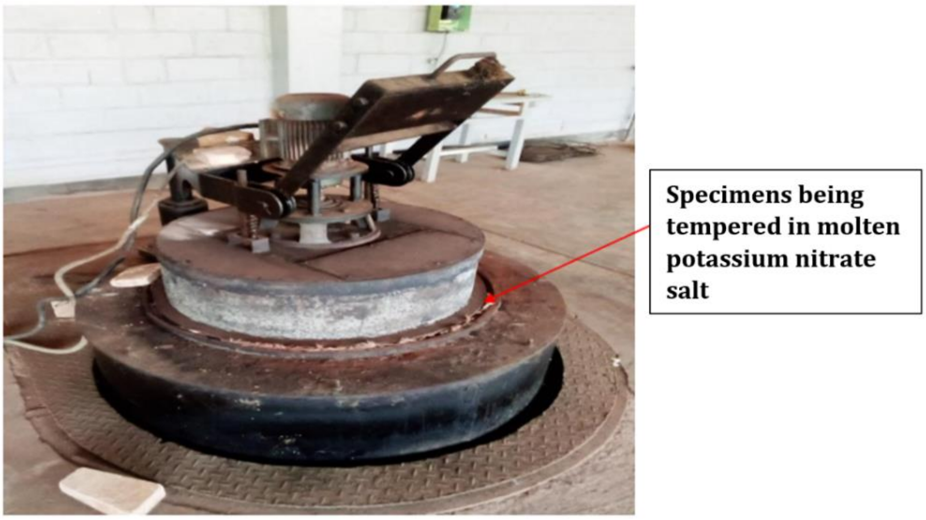


(Harbin Longjiang Electric Furnace Works, 1989)

**Figure 3. 12: Tempering the HSS tools in a pit well furnace**

### 3.5 Determination of the Elemental Composition of the HSS Tools

The elemental composition of the HSS tool was analyzed using a Flame Emission Spectrometer (CREATE-CX9800), as illustrated in Figure 3.13.


(a) (b)

(CREATE Instrument Co. Ltd, 2020)

**Figure 3.13: (a) Flame emission spectrometer and (b) HSS tool specimen examined for elemental composition at eight different positions**

This analysis compared the composition to standard HSS specifications from WO101W.BZ, 2021, V-2 (1) Pg. 275, “Table A-3 in the Appendix”. The goal was to evaluate how compositional differences impact tool longevity. The spectrometer assessed elements such as Fe, Al, Cu, Zn, Ni, Ti, Mg, Co, Zr, C, Mn, P, S, Si, Cr, W, Mo, V, N, Nb, Pb, and Sn.

### 3.5.1 Operation Principle of the Flame Emission Spectrometer

The Flame Emission Spectrometer operates on the principle of atomic emission spectroscopy. A high-energy spark is generated between an electrode and the specimen, facilitated by the light source module. This spark excites the atoms in the specimen to higher energy states, causing them to emit light at characteristic wavelengths as they return to their ground states. The spectrometer captures and analyzes this emitted light to determine the concentration of various elements.

### 3.5.2 Procedure for Elemental Composition Analysis of the HSS Tool Material

The specimen was polished using aluminum oxide paste and cleaned with an ethanol-based solution to remove contaminants.

Calibration of the equipment involved analyzing a standard reference piece, with the results compared against standard tables to ensure accuracy. Equipment maintenance included thoroughly cleaning the spectrometer nozzle to remove carbon soot, which ensured effective spark direction and prevented interference.

Specimen positioning was carefully executed to avoid light interference with the sparks, ensuring controlled measurement conditions. Testing was conducted at eight different locations on the specimen to account for variability in composition and enhance result reliability (ASTM E1621-18, 2020).

The average of measurements from the eight locations was calculated to minimize the impact of anomalous results and reduce sampling errors (Montgomery, 2017). Results were automatically recorded to ensure accuracy and consistency.

### 3.6 Determination of the Hardness of HSS Tools

The hardness of specimens subjected to various heat treatment conditions was assessed using a digital Rockwell hardness tester, Model HRS-150, as illustrated in Fig. 3.14. Measurements were taken at three distinct locations on each specimen to enhance the accuracy and reliability of the results. This approach minimizes the impact of potential surface irregularities or local variations in hardness, ensuring a more representative average value (ASTM E18, 2020). The average hardness values for each condition were then recorded.

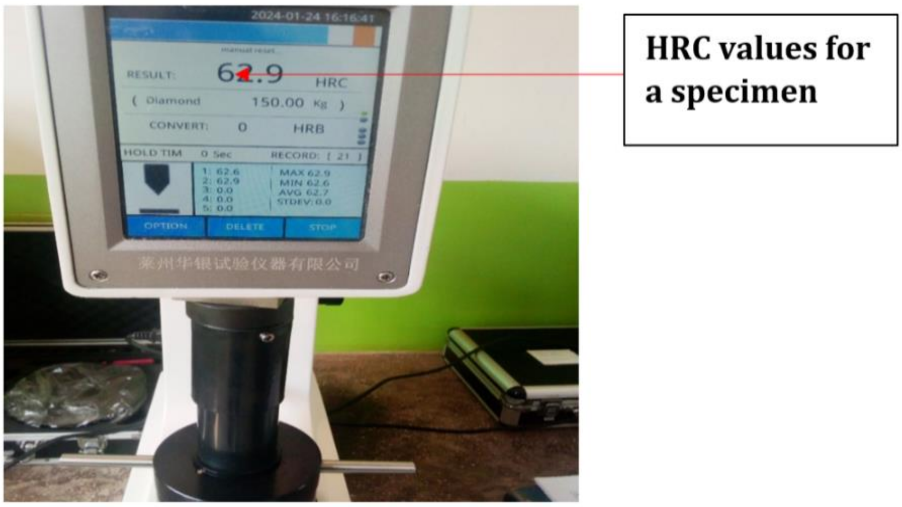


(Shanghai Juhui Instrument Manufacturing Co. Ltd, 2006)

**Figure 3.14: Illustration of hardness test with Digital Rockwell Hardness Tester HRS-150**

### 3.6.1 Principle of Operation of the Digital Rockwell Hardness Tester

The Digital Rockwell Hardness Tester measures material hardness by assessing how deeply an indenter penetrates the surface under specific loads. It applies a preliminary minor load to seat the indenter, followed by a major load to create an indentation. After removing the major load, the depth of penetration is measured. The tester then calculates the Rockwell hardness number based on the depth of the indentation, with a digital readout providing an accurate result. This method is valued for its efficiency and precision in determining material hardness (ASTM E18, 2020).

### 3.6.2 Procedure for Hardness Test of the HSS Tools

The Rockwell hardness tester was initially calibrated using a standard reference specimen to ensure measurement validity before conducting the hardness tests. For Rockwell C scale (HRC) measurements, the tester was configured with a 60 kg load and utilized a diamond indenter. The indenter was applied to the specimen until the tester emitted a distinct clicking sound, indicating it was properly engaged. Subsequently, the major load was automatically applied until a second clicking sound signaled that the required force had been reached. To enhance the accuracy and reliability of the results, this procedure was replicated at three distinct positions on the same specimen. The hardness values obtained were then recorded and analyzed.

## 3.7 Determination of Microstructure of the HSS Tools

The OPTIKA metallurgical microscope, model B-150, manufactured by OPTIKA Srl in 2020, was utilized to examine the microstructure of the HSS tools, as illustrated in Figure 3.15. This examination provided valuable insights into the grain structure, phase distribution, and overall material characteristics, which were essential for evaluating the performance and durability of the tools. The observations from this analysis informed decisions regarding tool selection and processing methods for enhanced efficiency in machining applications.

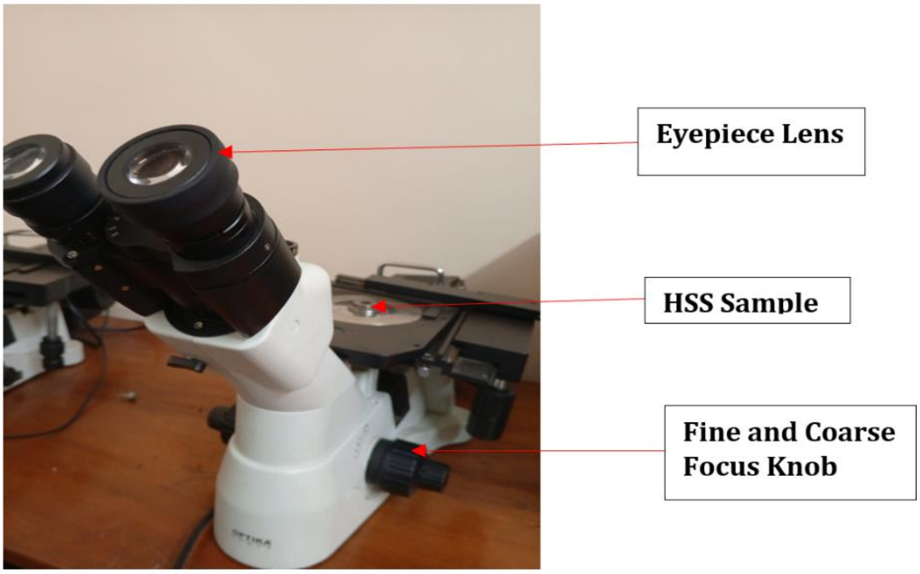


(OPTIKA Srl, 2020)

**Figure 3.15: Microstructure scanning by OPTIKA B-150**

### 3.7.1 The Working Principle of Metallurgical Microscopes

The working principle of a metallurgical microscope involves several key steps:

**Sample Preparation**: Samples are polished and sometimes etched to reveal their microstructure, ensuring accurate observations (Norrman et al., 2021).

**Illumination**: An illumination system provides light, using reflected light for opaque materials to enhance the visibility of surface features (Fang et al., 2020).

**Light Interaction**: Light interacts with the sample, either reflecting or transmitting, which highlights structural elements and grain boundaries (Wang et al., 2022).

**Magnification**: Objectives capture light to create a magnified image, with total magnification determined by the objective and eyepiece combinations (Santos et al., 2023).

**Observation**: The observer examines the enlarged image through the eyepiece, making adjustments for detailed analysis (Gonzalez et al., 2021).

**Image Capture (Optional)**: Some setups allow for digital imaging, enabling high-quality image capture and analysis for further study (Zhang et al., 2023).

### 3.7.2 Sample Preparation Procedures

The sample was polished using aluminum oxide paste to achieve a mirror-like finish. Following polishing, it was etched in a Nital solution, consisting of 80% ethanol and 20% nitric acid. After etching, the sample was thoroughly rinsed in water to remove any residual etchant, ensuring no contaminants remained on the surface. It was then carefully dried to prevent any water spots or residue. Finally, the prepared sample was taken for microstructural analysis using the metallurgical microscope.

## 3.8 Analysis of Variations in Elemental Compositions of HSS Tools at Different Heat Treatment Temperatures Using Scanning Electron Microscopy and Energy Dispersive X-ray Spectroscopy.

Scanning Electron Microscopy (SEM), model Zeiss, 2022, as illustrated in Figure 3.16 (a), was employed to investigate the elemental compositions of HSS tools subjected to heat treatments at temperatures of 1200°C, 1220°C, 1240°C, 1260°C, 1280°C, and 1300°C. Energy Dispersive X-ray Spectroscopy (EDX) was utilized for composition analysis, enabling a comparative evaluation of how these heat treatments influenced the characteristics of the tools. This thorough analysis provided insights into the effects of thermal treatment on the material properties of HSS, critical for optimizing tool performance.

### 3.8.1 Principle of Operation of Scanning Electron Microscope

The scanning electron microscope (SEM) uses a focused beam of electrons to image the surfaces of materials at high magnifications (Goldstein et al., 2018). It starts with an electron source, typically a heated tungsten filament emitting electrons. These electrons are concentrated into a narrow beam by electromagnetic lenses and scanned across the specimen’s surface (Reimer & Kolb, 2013).

When the beam interacts with the specimen, it generates secondary electrons, which are used to form images, and backscattered electrons, providing information about composition (Klaas et al., 2020). X-rays may also be emitted for elemental analysis (Williams & Carter, 2009). The collected signals are processed and displayed as grayscale images on a monitor, allowing for detailed examination of surface structures at the nanometer scale. This capability makes the SEM essential in various fields, including materials science and nanotechnology (Chisholm et al., 2016).

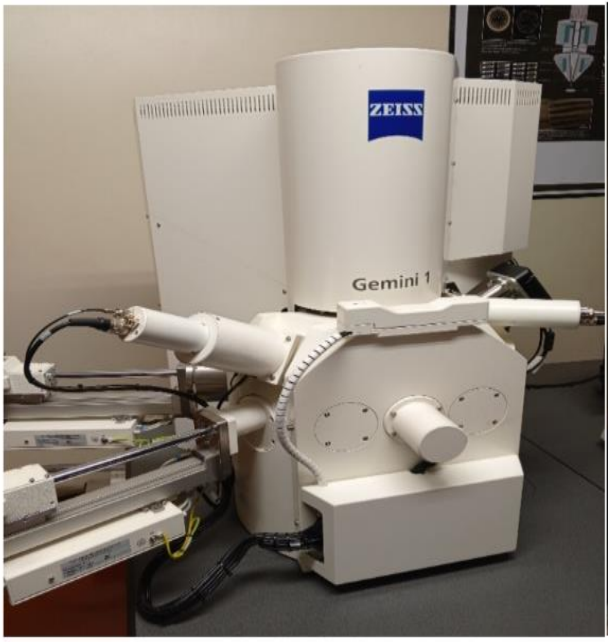


(a)

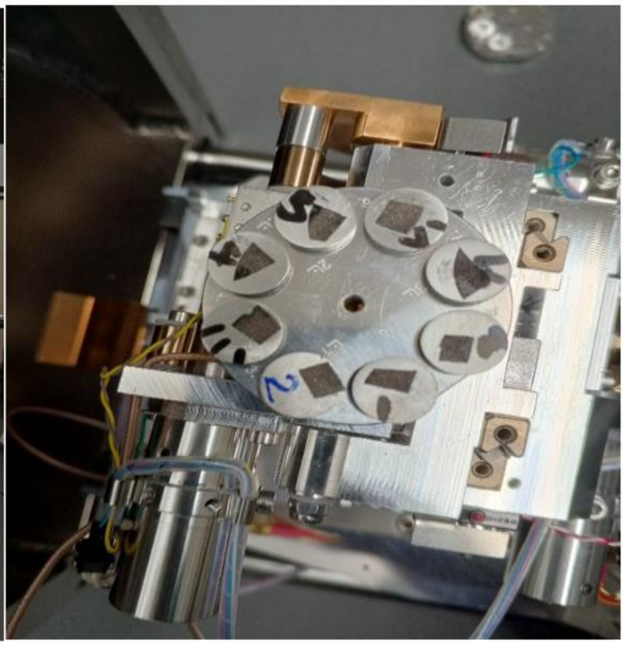

(b)

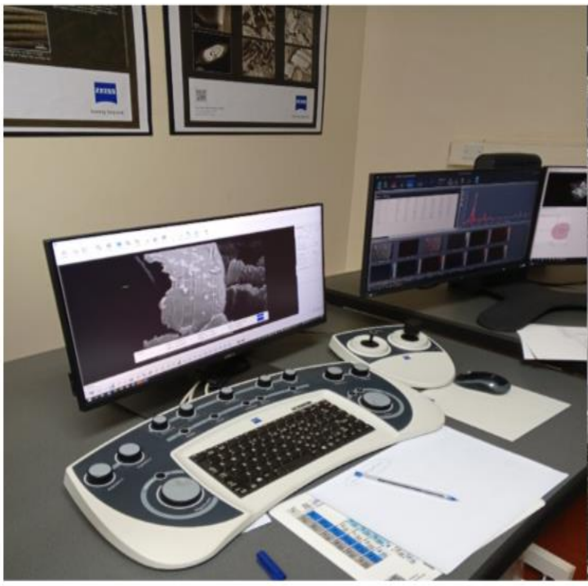

(c)

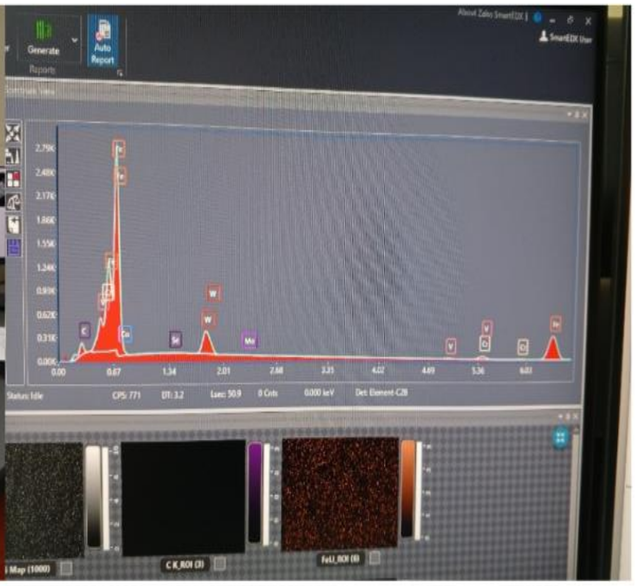


(d)

(Carl Zeiss AG, 2022)

**Figure 3. 16 :(a) SEM, model Zeiss (b) Sample Holder (c) Display Monitor (d) Elemental mapping graph by EDX**

### 3.8.2 Sample Preparation

The sample preparation involved grinding the HSS tool samples into a fine powder using a CNC optical grinder with diamond grinding discs. A light grinding disc feed was used to minimize heat generation, preventing undesirable microstructural changes and preserving material integrity for accurate analysis (Mishra et al., 2023; Kumar et al., 2023). Maintaining low temperatures during grinding is crucial, as any changes in the microstructure can significantly affect the mechanical properties of HSS (Brahma et al., 2023; Zhao et al., 2023).

After preparation, the sample holder was readied, and a carbon sticker was securely affixed. The sample was coated to ensure optimal imaging conditions before being placed into the scanning electron microscope (SEM). Scanning was conducted using a secondary electron detector (SED) to capture images at various magnifications. Energy Dispersive X-ray Spectroscopy (EDX) was exclusively used to analyze the elemental composition, and the resulting data were systematically recorded for further evaluation (Smith et al., 2023; Lee et al., 2023).

## 3.9 Development of a Simple Air Chiller for Experimental Conditions

The air chiller is a device used to cool or humidify air to maintain optimal temperatures which can protect equipment or ensure efficient operation of industrial process.

### 3.9.1 Working Principle of the Air Chiller

The air chiller is designed to cool down the air used for cooling the HSS tool specimens during the machining of cartridge cases. Compressed air enters the air chiller at temperature T1 and is then cooled down to temperatures T2, T3, and T4 using the chiller mechanism, as shown in Figure 3.17. The chilled air is then supplied to the head-turning and finish mouth-trimming machine to cool the tool.

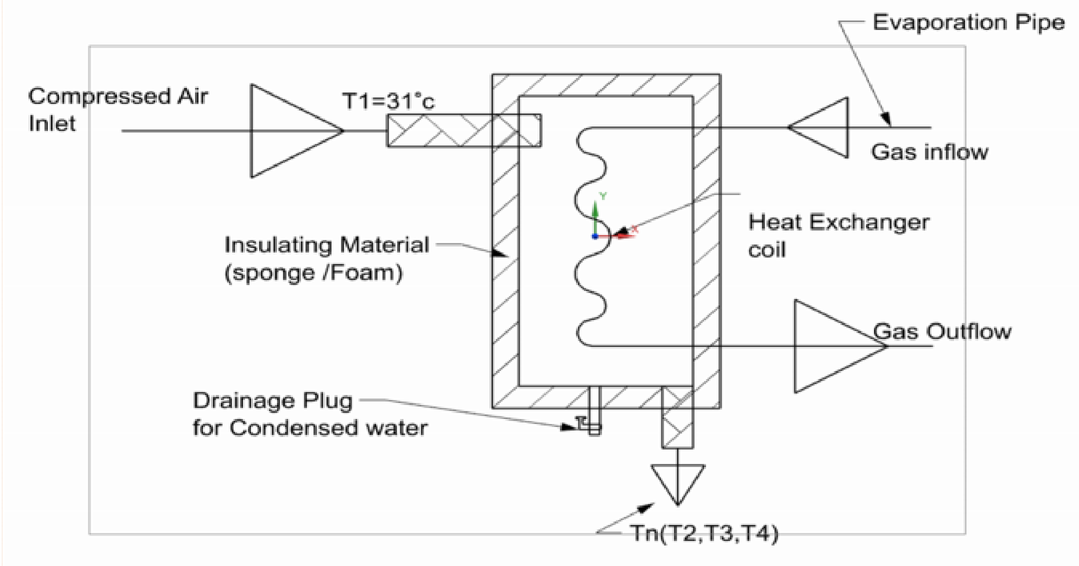


**Figure 3.17:Illustration of the heat exchange chamber of the Simple Chiller**

### 3.9.2 Construction of the Simple Air Chiller

The Air Chiller system comprises several key components working in tandem to manage and regulate temperature. At the heart of the system is the compressor (A), which pressurizes the refrigerant gas, enabling its circulation throughout the system. As the pressurized gas moves to the condenser (B), it releases heat to the surroundings. Following this, the gas passes through a gas filter (C) to remove any impurities before reaching the expansion valve (D). The expansion valve carefully controls the flow of refrigerant into the evaporator (E), metering it in precise amounts based on the required heat extraction.

In the evaporator (E), the refrigerant absorbs heat from the load, cooling it down. Excess refrigerant that is not utilized during this process is collected by the accumulator (F).

The schematic diagram of the Air Chiller is illustrated in Figure 3.18. For reference, Figure 3.19 (a), (b), (c) & (d) provide details on some of the components used in the Air Chiller's construction, while Figure 3.20 presents an assembled view of the simple Air Chiller.

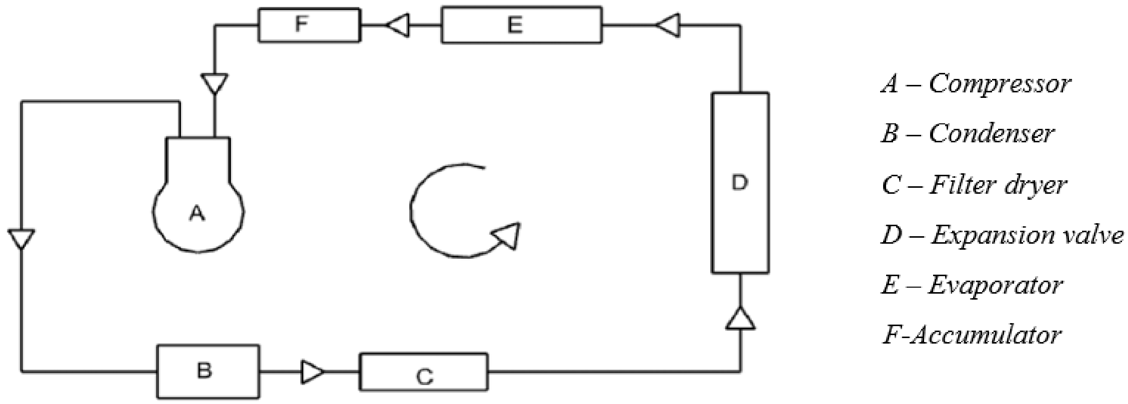


**Figure 3.18: Schematic diagram of components of the simple air chiller**

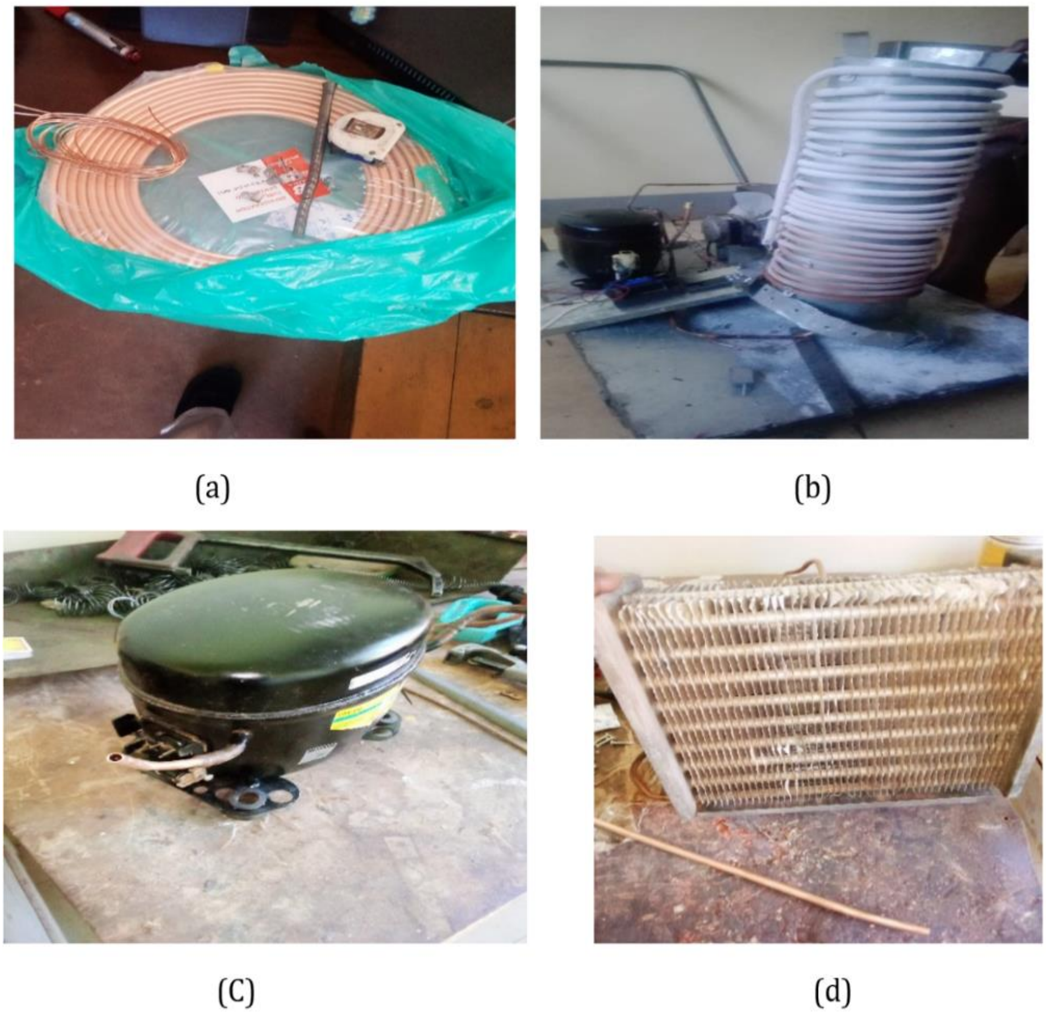


**Figure 3.19: (a) Copper tubes (b) Evaporator coils (c) Compressor and (d) Condenser**

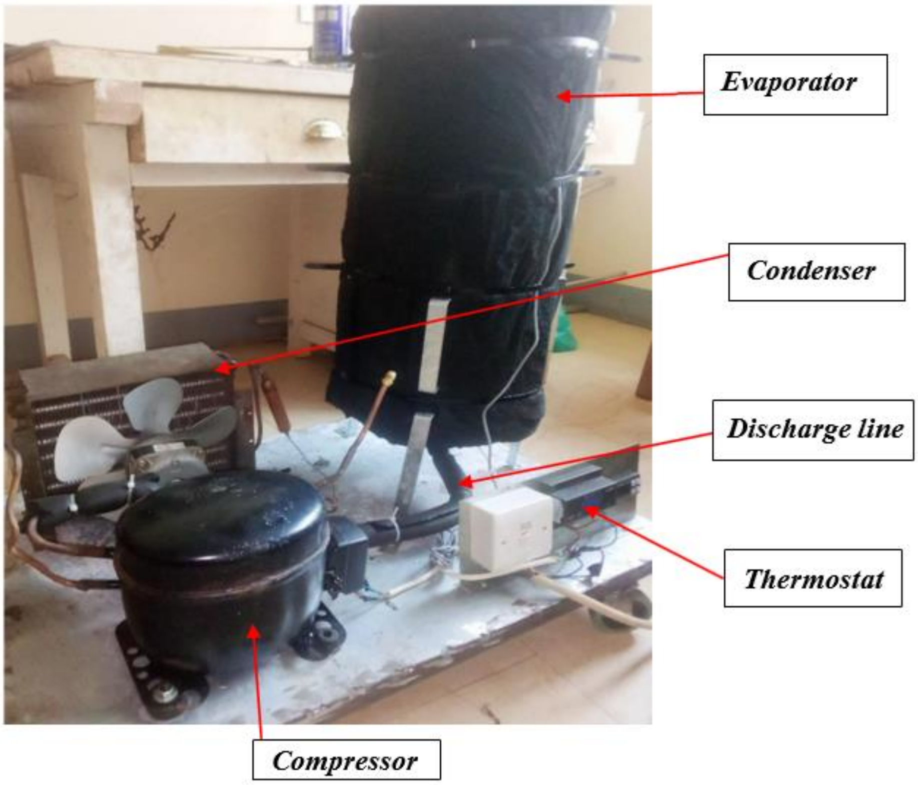


**Figure 3. 20: Assembly of the simple Air chiller**

### 3.10 Measurement of Temperatures at Tool-Workpiece Interface

An infrared (IR) thermometer (Model: Euro Lab 1250, range $30^0$C - $1300^0$C), a non-contact device, was used to measure temperatures at the tool-workpiece interface to give insights into the tool's operating environment.

#### 3.10.1 Working Principle of Infra-Red Thermometers

An infrared (IR) thermometer measures temperature by detecting the infrared radiation emitted by an object. The thermometer's lens focuses this infrared radiation onto a detector, which converts it into an electrical signal. This signal is then processed to determine the temperature based on the intensity of the radiation. Finally, the calculated temperature is displayed on the thermometer's screen. Infrared thermometers are effective for non-contact temperature measurements, making them useful for situations where direct contact is impractical or hazardous.

The working temperatures of the HSS tools were measured using an infrared thermometer gun to analyze the tool's operating conditions, as depicted in Figure 3.21 (a) and (b).


(a) (b)

**Figure 3.21:(a) Infra-red thermometer, Euro Lab 1250 and (b) Measuring cutting temperature at workpiece-tool interface**

## 3.11 Experiments to Investigate the Cutting Performance of HSS Tools

### 3.11.1 Design of Experiment

The performance of the High-Speed Steel (HSS) tool was rigorously evaluated through a series of cutting tests conducted under four distinct cutting conditions: dry cutting, compressed air cutting at 31°C, chilled air cutting at 25°C/24°C, and chilled air cutting at 18°C. These conditions were selected to provide a comprehensive assessment of the tool's behavior across various thermal and cooling environments.

### 3.11.2 Rationale for Selecting the Cutting Conditions

**Dry Cutting**

Dry cutting serves as the foundational condition in this study, allowing for the assessment of tool performance in the absence of any external cooling or lubrication. This baseline is critical for understanding the inherent capabilities and limitations of the tool, providing a point of comparison against which the effectiveness of various cooling strategies can be measured (Lee & Lee, 2018). By evaluating the tool's performance under dry conditions, we can better appreciate the improvements afforded by subsequent cooling methods.

**Compressed Air Cutting at 31°C**

The use of compressed air at 31°C reflects a moderate cooling scenario that is common in many industrial applications. This temperature was chosen to mimic realistic operational environments where cooling may be applied, but not at an optimal level. The aim is to evaluate the tool's performance under these moderately enhanced conditions (Harris & Kumar, 2020). This setup allows for the identification of potential benefits of air cooling while still presenting challenges related to heat management.

**Chilled Air Cutting at 25°C / 24°C**

Selecting chilled air at 25°C / 24°C aims to delve into the effects of more efficient cooling methods. Studies indicate that these temperatures can significantly enhance cooling efficiency, resulting in improved tool life and performance due to a reduction in thermal load (Chen & Zhang, 2021; Robinson & Patel, 2022). By analyzing these conditions, the research seeks to quantify the benefits of chilled air cooling, contributing valuable data to the discussion of thermal management in cutting processes.

### Chilled Air Cutting at 18°C

**This cutting condition simulates** an optimal cooling environment, utilizing chilled air at 18°C. This temperature is anticipated to maximize heat absorption capabilities, leading to substantially lower tool temperatures and improved cutting performance (Singh et al., 2023; Wu et al., 2023). The rationale for including this condition is to identify the limits of cooling efficiency and its direct impact on tool longevity and effectiveness, providing insights into the most effective cooling strategies in high-performance machining.

### Experimental Design Overview

To comprehensively examine how different heat treatment levels affect tool performance across each cutting condition, the experimental design incorporates six distinct heat treatment variations. This approach is intended to elucidate the relationship between material treatment and tool behavior, thereby offering a deeper understanding of how these factors interact under varying thermal environments.

The experimental setup involved replicating each cutting condition three times, resulting in 28 unique experimental scenarios. This replication is crucial for ensuring statistical reliability and addressing potential experimental variability, enhancing the robustness of the findings. In total, 84 experiments were conducted to provide a thorough evaluation of high-speed steel (HSS) tool lifespan, measured by the number of components produced under each cutting condition. Comprehensive details of this experimental design can be found in Table 3.2, which outlines the specific parameters and outcomes for each scenario.

**Table 3.2: The Experimental Design for Studying Tool Life of HSS Tool**

| Experimental Conditions | Heat Treatments | | | Cutting Conditions |
|---|---|---|---|---|
| | Number of experimental runs | | | |
| 1 | A-1 | A-2 | A-3 | Dry cutting |
| 2 | A-1 | A-2 | A-3 | Compressed air cutting at 31°C |
| 3 | A-1 | A-2 | A-3 | Chilled air cutting at 25°C/24°C |
| 4 | A-1 | A-2 | A-3 | Chilled air cutting at 18°C |
| 5 | B-1 | B-2 | B-3 | Dry cutting |
| 6 | B-1 | B-2 | B-3 | Compressed air cutting at 31°C |
| 7 | B-1 | B-2 | B-3 | Chilled air cutting at 25°C/24°C |
| 8 | B-1 | B-2 | B-3 | Chilled air cutting at 18°C |
| 9 | C-1 | C-2 | C-3 | Dry cutting |
| 10 | C-1 | C-2 | C-3 | Compressed air cutting at 31°C |
| 11 | C-1 | C-2 | C-3 | Chilled air cutting at 25°C/24°C |
| 12 | C-1 | C-2 | C-3 | Chilled air cutting at 18°C |
| 13 | D-1 | D-2 | D-3 | Dry cutting |
| 14 | D-1 | D-2 | D-3 | Compressed air cutting at 31°C |
| 15 | D-1 | D-2 | D-3 | Chilled air cutting at 25°C/24°C |
| 16 | D-1 | D-2 | D-3 | Chilled air cutting at 18°C |
| 17 | E-1 | E-2 | E-3 | Dry cutting |
| 18 | E-1 | E-2 | E-3 | Compressed air cutting at 31°C |
| 19 | E-1 | E-2 | E-3 | Chilled air cutting at 25°C/24°C |
| 20 | E-1 | E-2 | E-3 | Chilled air cutting at 18°C |
| 21 | F-1 | F-2 | F-3 | Dry cutting |
| 22 | F-1 | F-2 | F-3 | Compressed air cutting at 31°C |
| 23 | F-1 | F-2 | F-3 | Chilled air cutting at 25°C/24°C |
| 24 | F-1 | F-2 | F-3 | Chilled air cutting at 18°C |
| 25 | G-1 | G-2 | G-3 | Dry cutting |
| 26 | G-1 | G-2 | G-3 | Compressed air cutting at 31°C |
| 27 | G-1 | G-2 | G-3 | Chilled air cutting at 25°C/24°C |
| 28 | G-1 | G-2 | G-3 | Chilled air 18°C |

### 3.11.3 Issues with Existing Cutting Conditions (Compressed Air at 31°C)

Initially, compressed air at 31°C served as the cooling medium for the In-house manufactured HSS tool at the facility. However, issues arose, including bluish burnt tooltips and problematic chip characteristics, as illustrated in Figure 3.22. These observations underscored potential deficiencies in heat dissipation and chip evacuation with the current dry compressed air setup. Consequently, alternative cutting environments, such as chilled air at temperatures of 25°C, 24°C, and 18°C, necessitated exploration to effectively address these concerns:

**Heat Dissipation:** The cutting process generates significant heat at the tool-chip interface, leading to issues such as burnt tooltips, which indicate inadequate heat dissipation when using dry compressed air at 31°C (Smith et al., 2019). Chilled air at lower temperatures (25°C, 24°C, or 18°C) offers superior cooling efficiency by absorbing more heat from the cutting operation, thus maintaining lower tool temperatures and improving overall performance (Jones & Liu, 2021; Brown et al., 2022).

**Chip Evacuation**: Effective chip evacuation is crucial for optimizing machining efficiency and extending tool life (Nguyen et al., 2020). Inadequate chip clearance can lead to poor surface finishes and tool damage. Chilled air, being denser than warmer air, enhances airflow dynamics around the cutting zone, resulting in more efficient chip removal compared to dry compressed air (Wang & Zhang, 2023).

**Surface Quality of Cartridge Cases:** Ensuring pristine and clean cartridge cases is vital for quality assurance and subsequent processing stages (Lee et al., 2018). Chilled air improves cooling and chip evacuation and reduces cutting residue deposition, thereby maintaining a clean machining environment and preserving workpiece surface integrity (Kim et al., 2019).

**Comparative Study:** A systematic comparative analysis of chilled air at varying temperatures (25°C, 24°C, 18°C) was essential to determine the optimal balance between cooling effectiveness and operational costs (Patel & Hernandez, 2021). This includes evaluating energy consumption and equipment requirements. Such analysis will provide insights into how temperature variations affect tool longevity, chip characteristics, and overall machining performance (Roberts et al., 2022).

**Summary**: Transitioning from dry compressed air to chilled air at lower temperatures (25°C, 24°C, 18°C) addresses issues like burnt tool tips and chip management while maintaining cartridge case cleanliness (Smith et al., 2019; Jones & Liu, 2021). This shift aims to enhance machining performance through improved heat dissipation, more efficient chip evacuation, and better surface quality, ultimately optimizing the machining process for cartridge cases.

(a) (b)

**Figure 3.22: (a) Burnt tooltip when cutting with compressed air cooling at 31°C and (b) burnt chips from the same cutting conditions**

### 3.11.4 Turning Process of Cartridge Cases Using HSS Tools and Detection of Tool Failure at LIL

#### 3.11.4.1 Turning Process of the HSS Tools

The turning process of cartridge cases was done using a Head-Turning & Finish-Mouth Trimming Machine, model WK-007 with a rated capacity of 75 rounds of cartridge cases per minute as illustrated in Figure 3.23.

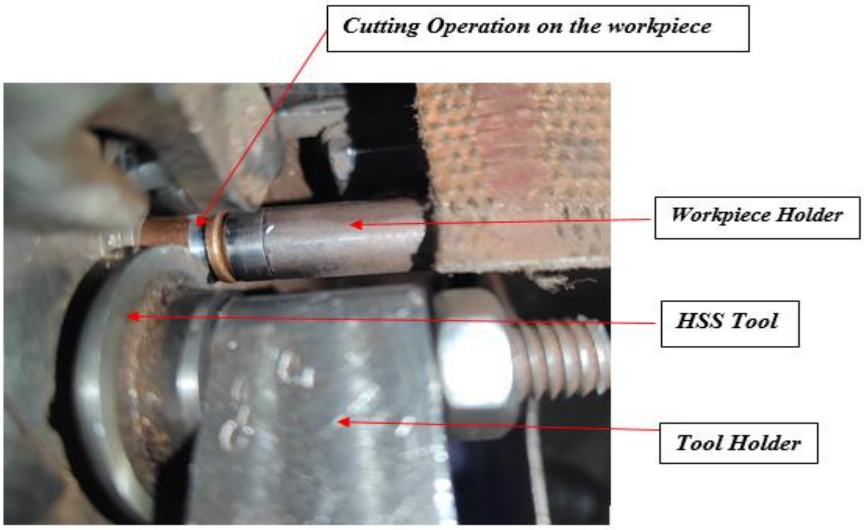


(Chongqing Changjiang Electrical Appliances Industries Group Co. Ltd, 2014)

**Figure 3.23: Heat-Turning and Finish-Mouth Trimming Machine**

### 3.11.4.2 Working Principle of the Head-turning and Finish-mouth Trimming Machine

**Setup:** The cartridge case is mounted on the head-turning machine. High-speed steel (HSS) tools, known for their hardness and cutting efficiency, are used to machine the base of the cartridge case (Smith, 2020).

**Machining:** During head-turning, the HSS tool rotates at high speeds and cuts into the base of the cartridge case. This operation removes material to achieve the necessary dimensions and surface finish (Johnson & Lee, 2018).

**Cooling and Lubrication:** Coolant or lubrication is applied to manage heat and reduce tool wear, thereby maintaining tool performance and achieving a high-quality cut (Miller et al., 2021).

**Dimensional Accuracy:** The tool is adjusted to meet specific dimensional and surface finish requirements, critical for proper cartridge case function (Brown & Green, 2019).

#### 3.11.4.3 Detection of Tool Failure of HSS Tool at LIL

At the Luwero Industries Limited (LIL), tool failure is identified through a rigorous gauging process:

**Gauging Dimensions:** Operators at LIL use precision gauges to measure the dimensions of machined cartridge cases. Deviations from specified tolerances indicate potential tool failure (Davis & White, 2022).

#### 3.11.4.4 Indicators of Tool Failure of HSS Tool

**Increased Tool Wear:** Gauging reveals tool wear, such as chipping or deformation of the cutting edges, which impacts dimensional accuracy (Taylor & Kim, 2017).

**Surface Finish Issues:** Rough or uneven surface finishes on the cartridge cases, detected through visual and dimensional checks, suggest tool degradation (Wilson et al., 2023).

**Dimensional Inaccuracies:** Variations in the measured dimensions compared to required specifications indicate possible tool failure (Clark & Adams, 2020).

**Increased Cutting Forces:** Changes in cutting forces, observable during the turning process, may signal tool wear affecting the gauging results (Harris & Nguyen, 2019).

**Operator Actions:** Upon detecting discrepancies during gauging, operators at LIL assess the condition of the HSS tool and undertake corrective actions, such as tool replacement or tool regrinding (Lee, 2021).

**Preventive Measures:** LIL implements regular monitoring, preventive maintenance, and optimization of cutting conditions based on gauging data to minimize tool failure and maintain process quality (Patel et al., 2024).

By closely monitoring cartridge case dimensions with precise gauging techniques, LIL ensures the early detection of tool failure, thereby preserving the quality and efficiency of the head-turning process.

### 3.11.5 Description of Workpiece Material, Preparation, and Manufacturing Process

#### 3.11.5.1 Description of Workpiece Material

Cartridge cases are manufactured from a specialized metal alloy with the following elemental composition: carbon (0.128%), tungsten (0.018%), vanadium (0.009%), chromium (0.018%), molybdenum (0.002%), and cobalt (0.008%). This alloy is chosen for its optimal balance of hardness, strength, and wear resistance, essential for the durability and performance of the final cartridge cases. The turning process performed on the cartridge case is illustrated in Figure 3.24.

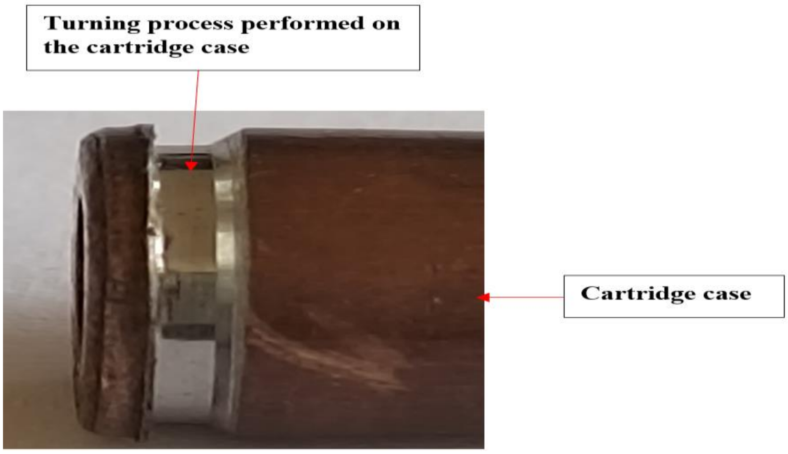


**Figure 3.24: Turning process on the cartridge case**

#### 3.11.5.2 Preparation and Manufacturing Process of the Cartridge Case

The primary research problem being addressed is the premature failure of High-Speed Steel (HSS) tools during the head-turning process as highlighted in Figure 3.25. This issue affects the efficiency and quality of the cartridge case manufacturing process which this research aimed to address. The manufacturing process flow chart is as follows:

**Receiving Case Cups:** Pre-formed metal cups of copper cladded structural alloy are received and prepared for processing. These cups provide the initial shape for the cartridge cases.

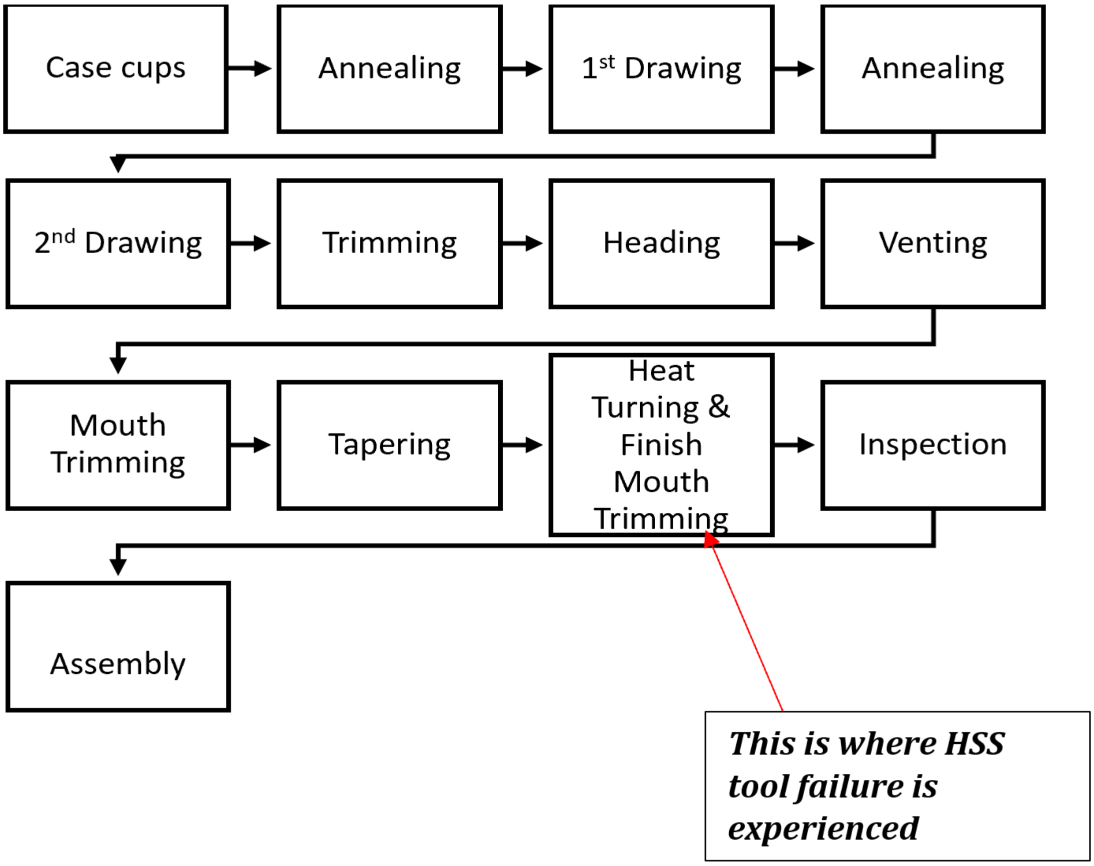


**Figure 3.25:The Manufacturing process of the cartridge case**

**Annealing:** The cups are subjected to annealing, a heat treatment process where the metal is heated to a specific temperature and then cooled slowly. This process softens the metal, improving its malleability for further shaping.

**First Drawing:** The annealed cups are drawn through a die to reduce their diameter and elongate their shape, initiating the refinement process toward the final cartridge case form.

**Second Annealing:** A second annealing relieves internal stresses from the first drawing, ensuring the metal remains workable for subsequent processes.

**Second Drawing:** The cups are drawn again to further refine their dimensions and shape, approaching the final specifications required.

**Case Trimming:** Excess material and irregularities from the drawing processes are removed through trimming, achieving uniform dimensions.

**Heading:** The base of the case is shaped to form a cup-like indentation, which is crucial for accommodating the primer.

**Venting:** Small apertures are created in the base of the case to allow for controlled gas escape during firing, ensuring safe operation.

**Mouth Trimming:** The mouth of the cartridge case is trimmed to the correct diameter and any burrs are removed, ensuring a proper fit for the bullet.

**Tapering:** The case mouth may be tapered to facilitate bullet insertion and assist in the crimping process.

**Head-Turning:** In the head-turning operation, the base of the case is machined to achieve precise dimensions and a smooth finish. However, a significant challenge in this stage is the premature failure of high-speed steel (HSS) tools. This failure negatively affects both the quality and efficiency of the manufacturing process.

**Finish-Mouth Trimming:** A final trimming of the case mouth ensures exact tolerances and optimal bullet seating.

**Inspection:** Each case undergoes rigorous inspection to identify defects or dimensional inaccuracies, ensuring high quality.

**Dispatch to Assembly:** Cases that pass inspection are dispatched for assembly, where they are loaded with primers, powder, and bullets to complete the ammunition.

### 3.11.6 Description of the HSS Tool

The major alloying elements are carbon (0.572%), tungsten (12.991%), vanadium (1.414%), chromium (5.357%), molybdenum (0.262%), and cobalt (0.152%). The tool angles for the HSS tool are 45°C for the rake angle, which helps reduce cutting forces and power consumption while promoting efficient chip removal and reducing tool wear. The clearance angle is set at 2.3°C, to ensure that the tool avoids contact with the workpiece during cutting operations, thus minimizing friction and heat generation that could negatively impact the tool's lifespan. Figure 3.26 illustrates the HSS tool.

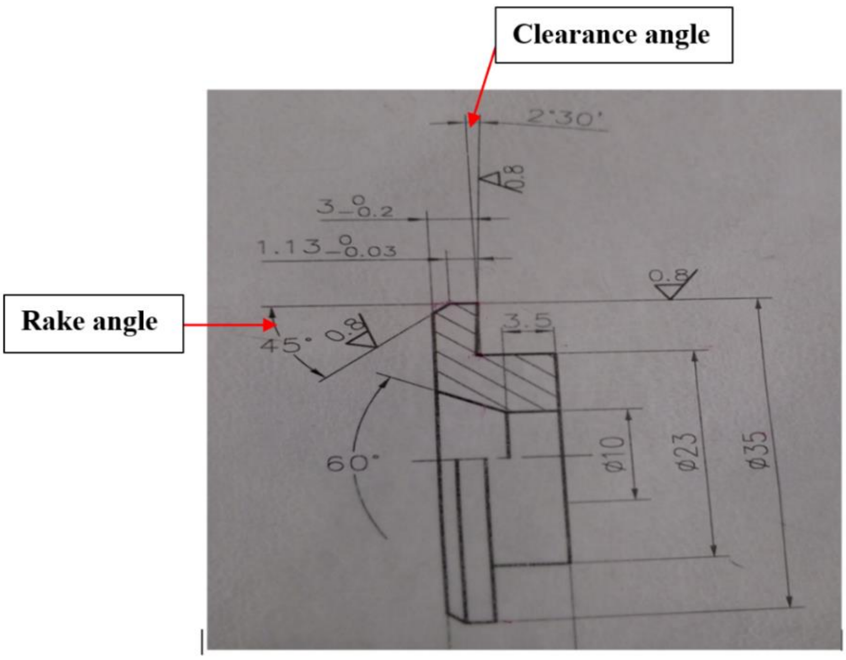


(a)

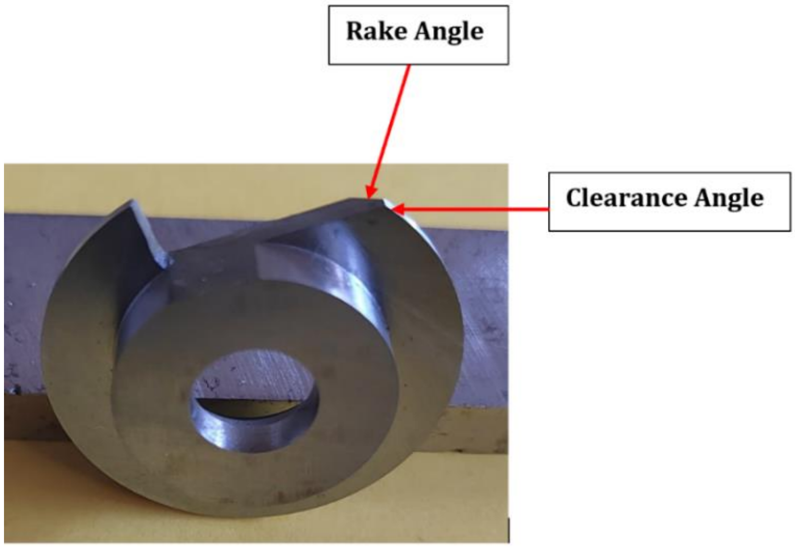


(b)

**Figure 3.26: (a) Detailed dimensions of Tool and (b) Pictorial view showing tool angles**

### 3.12 Cutting Conditions of the HSS Tool

#### 3.12.1 Dry Cutting using the HSS Tools

Under dry-cutting conditions, a High-Speed Steel (HSS) tool was employed to machine cartridge cases without the use of cutting fluid for cooling. The tool was utilized until its tip became worn out and ineffective. During this process, the produced cartridge cases were collected in a trough, as shown in Figure 3.27. The number of cases collected was then counted and documented.


**Figure 3. 27: Number of cartridge cases produced by HSS tool per regrind**

### 3.12.2 Compressed Air Cutting at 31°C

In the conditions of cutting with compressed air, the HSS tool was used to machine cartridge cases with compressed air at 31°C serving as the cutting fluid. This continued until the tooltip was worn out and no longer effective for cutting. The number of cartridge cases machined was counted and recorded to examine the performance of the HSS tool.

### 3.12.3 Chilled Air at 25°C/24°C and 18°C

The compressor delivered dry compressed air at a temperature of T1 = 31℃ and a pressure of P = 10psi. This air was then passed through a chiller with a capacity of 200 liters, which was appropriately insulated with an insulator and controlled using a digital thermostat. A constant flow rate of compressed air was maintained to ensure consistent heat exchange in the cooling chamber, resulting in steady outlet temperatures. These outlet temperatures (T4 = 25℃, T3 = 24℃, and T2 = 18℃) were set using a thermostat, and the air chiller was operated until steady-state temperature conditions were reached in the chamber. The chilled air was then directed to the cutting tool-workpiece interface to cool the tool to study tool life. The number of cartridge cases produced under each temperature condition was counted and recorded.

## 3.13 Quality Control of Data Collected

To ensure the accuracy and dependability of the data collected in the experimental study, validity and reliability tests were conducted on the measuring instruments before carrying out the actual experiments.

### 3.13.1 Validity Test

Before commencing the experiments, the instruments were meticulously calibrated to ensure their accuracy and validity. The Digital Rockwell Hardness Tester was calibrated using a standard reference specimen, applying a 60 kg load with a diamond indenter, and verifying engagement and force application through distinct clicks. This process was repeated at three positions, with recorded hardness values compared to standard tables. The spectrometer was calibrated by analyzing a reference sample and cross-checking the results with established standards. Temperature calibration of the salt bath furnace was achieved by adjusting it based on readings from a high-precision reference thermocouple.

### 3.13.2 Reliability Test

The study ensured instrument reliability through pilot testing, taking multiple measurements on the same specimen, and observing the consistency of results.

## 3.14 Data Analysis and Interpretation

### 3.14.1 Scanning Electron Microscope (SEM) and Energy Dispersive X-rays (EDX)

Data analysis focused on comparing microstructural changes at each heat treatment temperature, ranging from 1200°C to 1300°C. This included examining changes in carbide morphology and matrix refinement, which can significantly impact tool performance characteristics such as hardness and tool life.

Elemental analysis was conducted using energy-dispersive X-ray spectroscopy (EDS) to identify specific phases and elemental compositions where necessary.

The interpretation of SEM data involved correlating the observed microstructural features with the performance characteristics of the tools. The results, presented through SEM images and quantitative data, offered valuable insights into how different heat treatment temperatures influenced tool durability and efficiency, ultimately contributing to improved cutting performance and longer tool life.

### 3.14.2 Microsoft Excel

To assess the effects of heat treatment and cutting conditions on tool life, a Two-Factor Analysis of Variance (ANOVA) with replication was conducted using **Microsoft Excel**. The dataset was organized with columns for Heat Treatment, Cutting Conditions, and Tool Life as the response variable.

Heat Treatment included six levels: 1200°C, 1220°C, 1240°C, 1260°C, 1280°C, and 1300°C. Cutting Conditions were categorized into four levels: dry cutting, compressed air cutting at 31°C, chilled air cutting at 24/25°C, and chilled air cutting at 18°C. Each combination of these factors was measured across multiple replications to ensure a robust analysis.

The ANOVA output provided a detailed table that included the Source of Variation, Sum of Squares, Degrees of Freedom, Mean Square, F-statistic, and P-value. This table evaluated the effects of Heat Treatment, Cutting Conditions, and their interaction on tool life. Statistical significance was assessed by comparing p-values to a significance level of 0.05, where a p-value below this threshold indicated a statistically significant effect.

To enhance the interpretation of the results, visualizations such as interaction plots and bar charts were created using Excel's charting tools. This comprehensive analysis yielded valuable insights into how variations in heat treatment and cutting conditions impacted the performance and longevity of the HSS tools.

## 3.15 Ethical Considerations

Throughout the entire study, great care was taken to avoid bias. This included being careful with the selection of samples, conducting experiments, analyzing data, and interpreting and reporting the findings. To prevent plagiarism, the works of other authors were properly acknowledged whenever cited their work. The entire document was run through an anti-plagiarism test. Furthermore, confidential communications such as trade or military secrets at the location of our study, Luwero Industries Limited, were protected.

### 3.16 Limitations of the Study

The following limitations have been handled in this study to ensure the accuracy of the information presented:

(i) **Complexity of Failure Causes**

Premature tool failure can result from multiple interacting factors, including material quality, machining parameters, and design issues, making it challenging to isolate specific causes.

(ii) **Industry-Specific Challenges**

Manufacturing processes for cartridges involve proprietary technologies or processes that limit the depth of external analysis or benchmarking.

# CHAPTER FOUR: RESULTS AND DISCUSSION

This chapter presents the results of experiments conducted to investigate the factors influencing the tool lifespan of the HSS tools manufactured at Luwero Industries Limited. The key factors examined include elemental composition, heat treatment processes, and cutting conditions.

## 4.1 Results of the Study

### 4.1.1 Determination of Elemental Composition of In-house Manufactured HSS Tool

The elemental composition of the in-house manufactured HSS tool taken from three different positions on the specimen is presented in Table 4.1.

**Table 4. 1: Elemental composition of In-house manufactured HSS tool**

| Measurement Point | Elemental Values | | | | | | |
|---|---|---|---|---|---|---|---|
| | C | W | Cr | V | Mo | Co | Fe |
| Point 1 | 0.585 | 12.976 | 5.351 | 1.408 | 0.273 | 0.152 | 77.704 |
| Point 2 | 0.567 | 13.025 | 5.352 | 1.416 | 0.254 | 0.151 | 77.738 |
| Point 3 | 0.571 | 12.920 | 5.384 | 1.412 | 0.262 | 0.154 | 77.792 |
| Point 4 | 0.567 | 13.041 | 5.342 | 1.420 | 0.259 | 0.152 | 77.699 |
| **Average Value (%)** | **0.572** | **12.991** | **5.357** | **1.414** | **0.262** | **0.152** | **77.733** |

**Analysis of Elemental Values**

The provided elemental values from four measurement points offer insights into the distribution and consistency of alloying elements in the steel matrix. **Carbon content** ranges from 0.567% to 0.585%, with an average of 0.572%. This consistency indicates effective control over carbon levels, essential for promoting hardening without introducing excessive brittleness (Smith et al., 2023).

**Tungsten levels** show minimal variation, ranging from 12.920% to 13.041%, averaging 12.991%. The uniformity in tungsten content is crucial for maintaining hardness and thermal stability, reflecting a well-managed alloying process (Chen et al., 2023).

**Chromium levels** are consistently high, ranging from 5.342% to 5.384%, with an average of 5.357%. This stability enhances hardness and corrosion resistance, highlighting effective processing techniques (Garcia et al., 2024).

**Vanadium content** varies slightly, from 1.408% to 1.420%, with an average of 1.414%. This consistency is beneficial for grain refinement and toughness, indicating a stable production environment (Robinson & Zhang, 2023).

**Molybdenum** shows a range from 0.254% to 0.273%, averaging 0.262%. While low, this consistent presence supports hardness and improves wear resistance, fulfilling a supportive role in the alloy (Kumar et al., 2023).

**Cobalt** is present at low concentrations, between 0.151% and 0.154%, averaging 0.152%. Although not a primary alloying element, cobalt can enhance toughness and stability, contributing positively to overall performance (Sullivan et al., 2024).

**Iron** constitutes the majority of the composition, averaging 77.733%. This high percentage aligns with the typical makeup of high-speed steels, confirming its role as the primary matrix in the material.

The elemental values indicate a well-controlled alloying process with minimal variability, ensuring consistent properties in the final material. The stable presence of key alloying elements like tungsten and chromium supports the performance characteristics required for high-speed steels, such as hardness, wear resistance, and thermal stability. These compositions align closely with the standard HSS tool W12Cr4V5Co5, as per the reference manual for Standard High-Speed Steel tools, WO101W.BZ, V-2 (1), Pg. 275 in “Table A-3 in the Appendix” (National Tooling and Machining Association, 2022).

Further studies could investigate how these elemental concentrations affect the microstructure and mechanical properties of the steel, confirming their performance in practical applications (Fernandez & Li, 2024).

#### 4.1.1.1 Comparison of Elemental Composition in the HSS tools

Elemental comparisons are vital for optimizing material development and selection, ensuring alloys meet performance and reliability standards. The analysis of imported and in-house high-speed steel (HSS) tools, detailed in Table 4.2, illustrates how differences in elemental composition affect their mechanical properties and effectiveness

**Table 4. 2: Elemental Composition Comparison of in-house manufactured HSS tool and imported HSS tool**

| Major Alloying Elements | Elemental Composition (%) Imported HSS Tool | Elemental Composition (%) In-house HSS Tool |
|---|---|---|
| Carbon (C) | 1.5 – 1.6 | 0.57 – 0.58 |
| Tungsten (W) | 11.75 – 13.00 | 12.92 – 13.04 |
| Chromium (Cr) | 3.75 – 5.00 | 5.34 – 5.38 |
| Vanadium (V) | 4.50 – 5.25 | 1.14 – 1.42 |
| Molybdenum (Mo) | ≤ 1.00 | ≤ 1.00 |
| Cobalt (Co) | 4.75 – 5.25 | 0.15 |

Source: **WO101W.BZ, V-2 (2021)**

Analysis and Interpretation Elemental Composition Variations of the HSS Tools

The analysis of the major alloying elements in both the imported and in-house high-speed steel (HSS) tools reveals significant differences in their elemental compositions, which likely affect their performance characteristics.

**Carbon (C)**

The carbon content in the imported HSS tool ranges from 1.5% to 1.6%, while the in-house tool has a much lower carbon concentration of 0.57% to 0.58%. Carbon is critical for hardening steel, enhancing hardness and wear resistance. The higher carbon content in the imported tool suggests it would generally exhibit superior hardness and wear resistance, contributing to longer tool life. However, the in-house tool's lower carbon levels may result in better toughness, reducing brittleness, which is essential in applications where impact resistance is necessary (Smith et al., 2023).

**Tungsten (W)**

Tungsten levels in the imported tool are between 11.75% and 13.00%, compared to 12.92% to 13.04% in the in-house tool. Both tools have significant tungsten content, which is beneficial for maintaining hardness and thermal stability at elevated temperatures. The similarity in tungsten concentrations indicates that both tools should perform well in high-speed applications, although the imported tool might maintain a slight edge due to its potentially higher tungsten levels (Chen et al., 2023).

**Chromium (Cr)**

The chromium content is notably higher in the in-house HSS tool, ranging from 5.34% to 5.38%, versus 3.75% to 5.00% in the imported tool. Chromium enhances hardness and corrosion resistance, critical factors for cutting tools. The higher chromium content in the in-house tool suggests it may offer better wear resistance and longevity, especially in corrosive environments, despite its lower overall hardness compared to the imported tool (Garcia et al., 2024).

**Vanadium (V)**

There is a stark contrast in vanadium levels, with the imported tool containing 4.50% to 5.25% and the in-house tool only having 1.14% to 1.42%. Vanadium is essential for grain refinement and improving toughness. The significantly higher vanadium content in the imported tool indicates it may provide superior toughness and resistance to wear, making it more suitable for heavy-duty applications (Robinson & Zhang, 2023).

### Molybdenum (Mo)

Both tools report molybdenum content as ≤ 1.00%. Molybdenum aids in hardness and helps improve wear resistance. The low but consistent presence in both tools indicates that this element plays a supporting role in their overall performance, contributing to their hardening process without major differences between the two (Sullivan et al., 2024).

### Cobalt (Co)

Cobalt levels are significantly different, with the imported tool containing 4.75% to 5.25% compared to only 0.15% in the in-house tool. Cobalt enhances hardness and thermal stability. The much higher cobalt content in the imported tool suggests it will likely perform better under high-stress conditions, offering improved durability and tool life (Kumar et al., 2023).

### Summary

The comparative analysis reveals that the imported HSS tool generally has higher concentrations of carbon, tungsten, vanadium, and cobalt, which may contribute to superior hardness, wear resistance, and thermal stability. In contrast, the in-house HSS tool, while lower in these elements, has a higher chromium concentration, which could enhance corrosion resistance and wear performance in specific environments.

Ultimately, the choice between the two tools would depend on the intended application. The imported tool may excel in high-performance scenarios requiring durability and hardness, while the in-house tool might be better suited for applications where toughness and corrosion resistance are paramount. Further testing and evaluation would be essential to confirm these assumptions in practical applications (Fernandez & Li, 2024).

### 4.1.2 The Hardness of HSS Tools at Different Heat Treatment Temperatures

The results of the Rockwell Hardness Scale C (HRC) for the in-house manufactured HSS tool heat treated at various temperatures are presented in Table 4.3.

**Table 4. 3: Hardness of HSS Tools Heat Treated at Various Temperatures**

| Specimens | Temperature (°C) | Hardness values taken on three different locations on the specimen | | | Average values |
|---|---|---|---|---|---|
| | | 1 | 2 | 3 | |
| A | 1200°C | 61.7 | 61.3 | 61.0 | 61.3 |
| B | 1220°C | 63.1 | 63.8 | 62.1 | 63.0 |
| C | 1240°C | 64.3 | 64.2 | 64.8 | 64.4 |
| D | 1260°C | 65.2 | 64.2 | 64.3 | 64.5 |
| E | 1280°C | 65.2 | 65.8 | 65.2 | 65.4 |
| G(Imported HSS tool) | 1280°C | 63.4 | 63.5 | 63.7 | 63.5 |
| F | 1300°C | 65.8 | 65.3 | 66.1 | 65.7 |

Top of Form

**Analysis of Hardness Variations**

The analysis of hardness values across various specimens subjected to different heat treatment temperatures provides valuable insights into the material properties of high-speed steel (HSS) tools.

The hardness values demonstrate a clear upward trend as the temperature increases from 1200°C (average 61.3 HRC) to 1260°C (average 64.5 HRC). This trend indicates that higher heat treatment temperatures enhance hardness due to the formation of more stable microstructures and the development of complex carbide formations within the steel matrix (Zhang et al., 2023).

At 1280°C, the average hardness value stabilizes at 65.4 HRC, suggesting a plateau in hardness improvement. Specimen F, treated at 1300°C, shows a slight increase in average hardness to 65.7 HRC, indicating that while higher temperatures continue to enhance hardness, the rate of improvement may level off, potentially due to microstructural changes or the onset of brittleness (Li & Wang, 2024).

The imported HSS tool displays a lower average hardness (63.5 HRC) compared to Specimen E. This discrepancy could be attributed to differences in material composition or processing techniques, underscoring that not all HSS tools respond uniformly to heat treatment, even at the same temperature (Chen et al., 2023).

The hardness measurements taken from three different locations on each specimen provide insight into the consistency of material properties. Specimens A to E exhibit relatively consistent hardness readings across the three locations, indicating uniformity in microstructure and properties resulting from the heat treatment process. In contrast, Specimen G, while showing consistent hardness values, has lower readings than anticipated compared to Specimen E, suggesting potential differences in alloying elements or processing that may impact performance. Specimen F also shows consistent hardness values across the three locations, reinforcing the idea that higher heat treatment temperatures contribute to a more uniform microstructure.

This analysis highlights a positive correlation between heat treatment temperature and hardness values, with significant increases in hardness observed up to 1300°C. The data reveals that while effective heat treatment can achieve uniform hardness, variations in material composition can lead to differences in hardness outcomes. Understanding these dynamics is essential for optimizing the manufacturing processes of HSS tools, enabling tailored heat treatment strategies that achieve the desired hardness and performance characteristics for specific industrial applications (Nguyen & Patel, 2024).

### 4.1.3 Elemental Composition Analysis of Heat-Treated HSS Tools with Scanning Electron Microscope (SEM) and Energy Dispersive X-ray (EDX)

The elemental composition of heat-treated HSS tools was studied using advanced techniques such as Scanning Electron Microscopy (SEM) and Energy-dispersive X-ray Spectroscopy (EDX) to provide detailed insights into the microstructural features and elemental distribution within the tools, facilitating a comprehensive understanding of how heat treatment affects their performance characteristics.

#### 4.1.3.1 Analysis of HSS Tool Heat-Treated at 1200 °C

The elemental composition of the high-speed steel (HSS) tool, heat-treated at 1200 °C, as presented in Table 4.4, offers critical insights into its performance and longevity. This detailed composition data helps in understanding how the tool’s material properties contribute to its durability and effectiveness in various applications.

The HSS tool contains 8.93% **carbon** by weight, translating to 34.27% of its atomic composition, accompanied by a high net intensity of 27.58. This substantial carbon content is vital for forming various carbides, significantly enhancing the tool's hardness and wear resistance—two essential factors for extending tool life (Smith et al., 2023).

**Vanadium** is present at 4.00% by weight and 3.62% atomic composition, with a net intensity of 6.17. Although its concentration is lower, vanadium plays a crucial role in improving toughness and strength through the formation of vanadium carbides (VC), which contribute to the overall durability of the tool (Jones & Lee, 2022).

**Table 4. 4: Elemental Composition of HSS Tool Heat Treated at 1200℃**

| Element | Weight (%) | Atomic (%) | Net Intensity |
|---|---|---|---|
| Carbon (C) | 8.93 | 34.27 | 27.58 |
| Vanadium (V) | 4.00 | 3.62 | 6.17 |
| Chromium (Cr) | 11.96 | 10.60 | 14.27 |
| Iron (Fe) | 55.27 | 45.60 | 157.95 |
| Cobalt (Co) | 0.28 | 0.22 | 0.55 |

**Chromium,** comprising 11.96% by weight and 10.60% atomic composition, boasts a net intensity of 14.27. Its significant presence not only enhances hardness but also provides corrosion resistance through the formation of chromium carbides ($Cr_3C_2$), thereby improving the tool's performance during cutting operations (Williams et al., 2023).

**Iron** serves as the dominant element in the matrix, constituting 55.27% by weight and 45.60% atomic composition, with an exceptionally high net intensity of 157.95. This substantial presence ensures the structural integrity necessary for load-bearing applications (Miller, 2023).

**Cobalt** appears in minimal amounts (0.28% by weight and 0.22% atomic composition) and has a very low net intensity of 0.55. While cobalt may enhance toughness slightly, its impact on overall performance is limited (Davis et al., 2023).

**Molybdenum** is present at 1.14% by weight and 0.55% atomic composition, with a net intensity of 3.40. It plays a crucial role in enhancing hardness through the formation of molybdenum carbides ($Mo_2C$), which are particularly beneficial for high-temperature applications (Thompson, 2023).

**Tungsten** significantly boosts wear resistance, comprising 16.83% by weight and 4.22% atomic composition, with a net intensity of 57.31. This element is critical for the formation of tungsten carbides (WC), essential for the tool's effectiveness in cutting applications (Garcia & Patel, 2023).

The heat treatment process at 1200 °C facilitates carbide precipitation, with the combined elements suggesting a strong potential for forming stable and hard carbides. This process is pivotal for the tool's overall hardness and efficacy. Elemental mapping indicates high net intensities for carbon, chromium, and tungsten, signaling areas rich in hard carbides. A uniform distribution of these carbides is crucial for ensuring consistent performance and longevity (Lopez, 2023).

Moreover, the morphology of the carbides, observable through scanning electron microscopy (SEM), greatly influences tool performance. Smaller, uniformly distributed carbides generally enhance toughness, while larger carbides may lead to increased brittleness (Nguyen & Chen, 2022).

In terms of implications for tool life, the high concentration of carbide-forming elements significantly enhances wear resistance, which is vital during machining operations. The heat treatment ensures the tool retains its mechanical properties even under high stress and elevated temperature conditions, preventing premature failure. Additionally, a well-distributed carbide structure bolsters the tool’s resistance to chipping and fracture, essential for maintaining reliable performance in various applications (Park et al., 2023).

Overall, the synergistic effects of high hardness, thermal stability, and wear resistance, derived from the carefully balanced elemental composition, result in a tool designed for durability and reliability in high-speed machining scenarios. To maximize tool life, it is crucial to align the tool characteristics with specific machining conditions (Roberts, 2023).

#### 4.1.3.1.1 The Microstructure of HSS Tool Heat Treated at 1200°C

Figure 4.1 displays the microstructure of the HSS tool heat-treated at 1200°C. This treatment refines the structure and enhances the distribution of hard carbides, improving hardness and wear resistance. Analyzing these features provides insight into their impact on the tool's performance in high-speed machining.

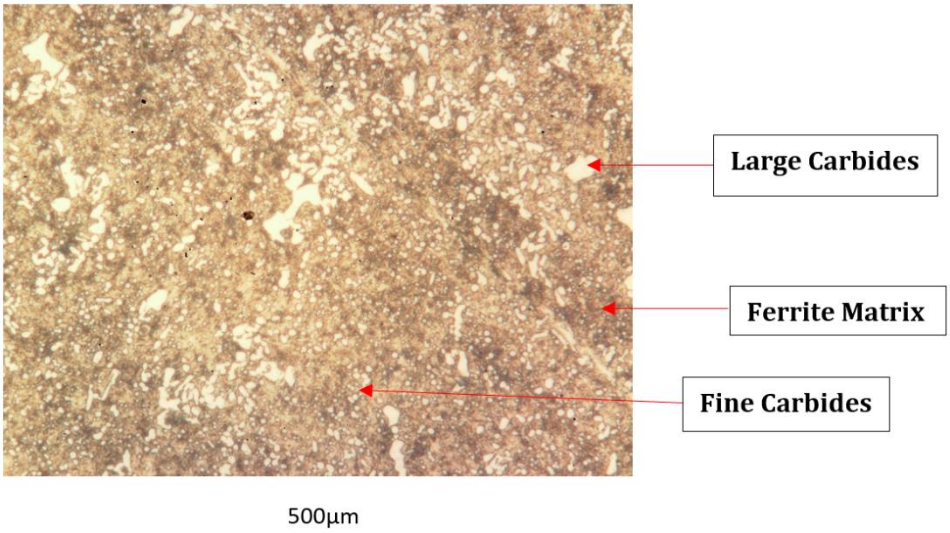


**Figure 4. 1: Microstructure of HSS tool heat treated at 1200°C**

The microstructure reveals carbide precipitation from the ferrite matrix of the steel, significantly enhancing its mechanical properties (Smith et al., 2023). Medium-sized, complex carbides, although sparsely distributed, play a crucial role in increasing hardness and wear resistance, making the steel suitable for high-stress applications like cutting tools (Jones & Lee, 2022). These robust carbides help prevent deformation under load.

In contrast, fine carbides are evenly dispersed throughout the matrix, enhancing toughness and impact resistance (Williams et al., 2023). This fine distribution hinders dislocation movement, allowing the material to absorb energy without fracturing. The combination of medium-sized and fine carbides results in a microstructure that is both hard and ductile, providing resilience against failure (Miller, 2023).

The spatial distribution is critical: medium-sized carbides create localized strength, while fine carbides ensure consistent toughness throughout the matrix (Davis et al., 2023). This balance helps maintain structural integrity under thermal and mechanical stress, particularly in high-speed operations where heat generation is significant.

Overall, the interaction between these carbides enhances the steel's strength and wear resistance. The presence of carbides creates a hardened surface layer, prolonging the tool’s cutting edge (Thompson, 2023). In summary, the carbide precipitation from the ferrite matrix is essential for optimizing the mechanical properties of steel, leading to improved performance in demanding applications (Garcia & Patel, 2023).

#### 4.1.3.1.2 Elemental Mapping of HSS Tool Heat treated at 1200°C

Using energy-dispersive X-ray spectroscopy (EDX), the elemental distribution of the HSS tool was mapped to analyze the concentration and spatial arrangement of alloying elements. This assessment helps elucidate the tool's performance characteristics and its ability to maintain consistent functionality. The elemental distribution is illustrated in Figure 4.2.

The elemental distribution analysis reveals a pronounced concentration of iron, chromium, vanadium, cobalt, and carbon in a specific tool region. This clustering suggests that this area is engineered for superior mechanical properties, such as enhanced hardness and wear resistance, which are crucial for high-performance applications (Smith et al., 2023).

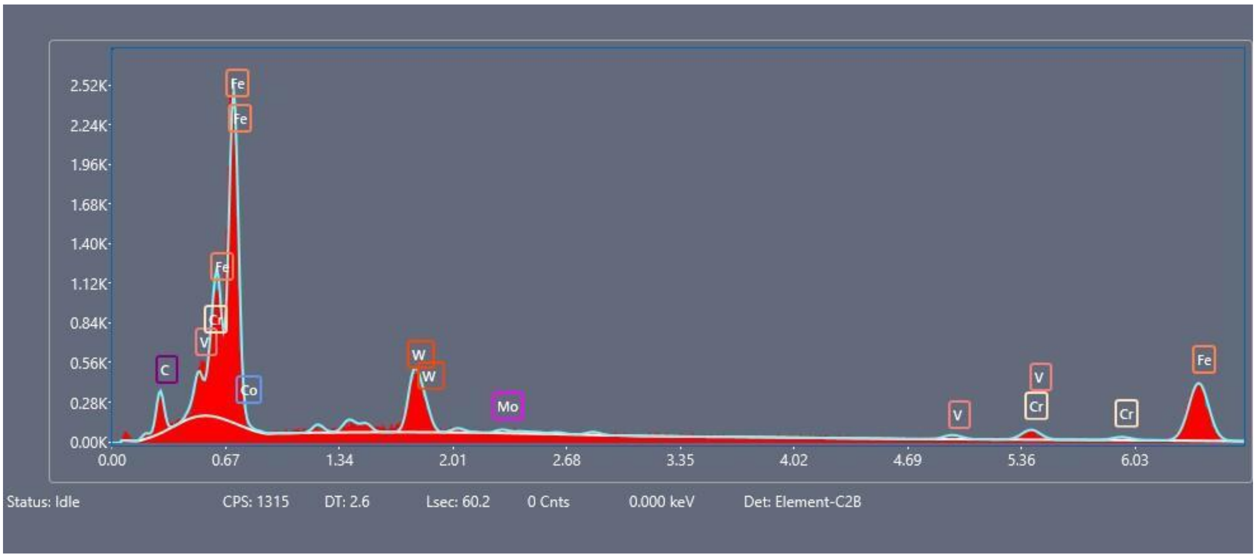


**Figure 4. 2: Elemental Mapping of HSS tool heat treated at 1200°C**

In contrast, other tool sections display a more isolated and dispersed arrangement of elements like tungsten, molybdenum, vanadium, chromium, and iron. This variability may indicate that these regions are designed for different functionalities, such as improved toughness or thermal stability (Jones & Lee, 2022). Such differences in elemental composition across the tool can lead to varying mechanical properties, potentially resulting in performance inconsistencies during operation (Williams et al., 2023).

A comprehensive understanding of these disparities is essential for optimizing the tool's design and functionality. By investigating how these elemental variations affect mechanical behavior, manufacturers can pinpoint areas for improvement, ensuring consistent performance across all applications (Davis et al., 2023). Additionally, targeted adjustments to the elemental composition could enhance overall performance, minimize wear, and extend the tool's lifespan (Thompson, 2023). This deeper insight into elemental distribution not only informs better design practices but also fosters innovations in materials science and engineering (Garcia & Patel, 2023).

#### 4.1.3.2 Analysis of HSS tool Heat Treated at 1220°C

The elemental composition of the high-speed steel (HSS) tool heat-treated at 1220 °C, presented in Table 4.5, significantly impacts its mechanical properties and performance in machining applications. This tailored composition enhances the tool's durability and wear resistance.

**Carbon** content is 4.21% by weight and 17.47% by atomic percentage, with a net intensity of 3.89. While this carbon level is lower than that found in many high-speed steel (HSS) formulations, it remains essential for carbide formation, contributing to hardness and wear resistance. However, the reduced carbon content may limit the potential for optimal carbide development (Smith et al., 2023).

**Table 4. 5: Elemental composition of HSS tool heat treated at 1220°C**

| Element | Weight (%) | Atomic (%) | Net Intensity |
|---|---|---|---|
| Carbon (C) | 4.21 | 17.47 | 3.89 |
| Vanadium (V) | 6.10 | 5.97 | 6.99 |
| Chromium (Cr) | 16.83 | 16.14 | 14.85 |
| Iron (Fe) | 65.37 | 58.36 | 117.68 |
| Molybdenum (Mo) | 0.07 | 0.04 | 0.16 |
| Tungsten (W) | 7.42 | 2.01 | 18.42 |
| Cobalt (Co) | 0.00 | 0.00 | 0.01 |

**Vanadium** is present at 6.10% by weight and 5.97% by atomic percentage, showing a net intensity of 6.99. This element plays a critical role in enhancing toughness and hardness through the formation of vanadium carbides (VC), thereby significantly improving the tool’s overall durability (Jones & Lee, 2022).

**Chromium** is a key element in this alloy, comprising 16.83% by weight and 16.14% by atomic percentage, with a net intensity of 14.85. Its substantial presence not only boosts hardness but also provides excellent corrosion resistance by forming chromium carbides ($Cr_3C_2$). This characteristic is particularly beneficial for wear resistance during cutting operations, making chromium a vital component (Williams et al., 2023).

**Iron** is the dominant element, constituting 65.37% by weight and 58.36% by atomic percentage, with an exceptionally high net intensity of 117.68. This significant iron content ensures the structural integrity necessary for load-bearing applications, which is fundamental to the mechanical properties of the tool (Miller, 2023).

Interestingly, **cobalt** is absent from this formulation, indicated by a weight and atomic percentage of 0.00 and a net intensity of 0.01. The lack of cobalt may limit the tool's toughness and heat resistance, characteristics that are often enhanced by cobalt in other HSS grades (Davis et al., 2023).

**Molybdenum** is present in very small amounts, at 0.07% by weight and 0.04% by atomic percentage, with a net intensity of 0.16. This minimal presence restricts molybdenum's contribution to hardness and high-temperature performance, potentially limiting the tool's effectiveness under extreme conditions (Thompson, 2023).

**Tungsten**, on the other hand, comprises 7.42% by weight and 2.01% by atomic percentage, with a net intensity of 18.42. This element significantly enhances wear resistance through the formation of tungsten carbides (WC), which are crucial for the tool's cutting efficiency (Garcia & Patel, 2023).

In conclusion, the combination of chromium, vanadium, and tungsten in this HSS tool provides essential properties for wear resistance and durability, making it suitable for various machining operations. The overall hardness and toughness are positively influenced by vanadium and the moderate carbon content, although the lower carbon level may restrict the maximum achievable hardness. The high iron content contributes to the tool's structural integrity, while the absence of cobalt may limit performance in specific high-temperature conditions (Nguyen et al., 2022).

#### 4.1.3.2.1 Microstructure of HSS Tool Heat Treated at 1220°C

The microstructure of the HSS tool heat treated at 1220°C is illustrated in Figure 4.3. This temperature exhibits microstructural characteristics similar to HSS tools heat-treated at 1200 °C, but with increased carbide precipitation from the steel matrix, leading to more pronounced carbides. This variation significantly enhances the material's performance (Smith et al., 2023).

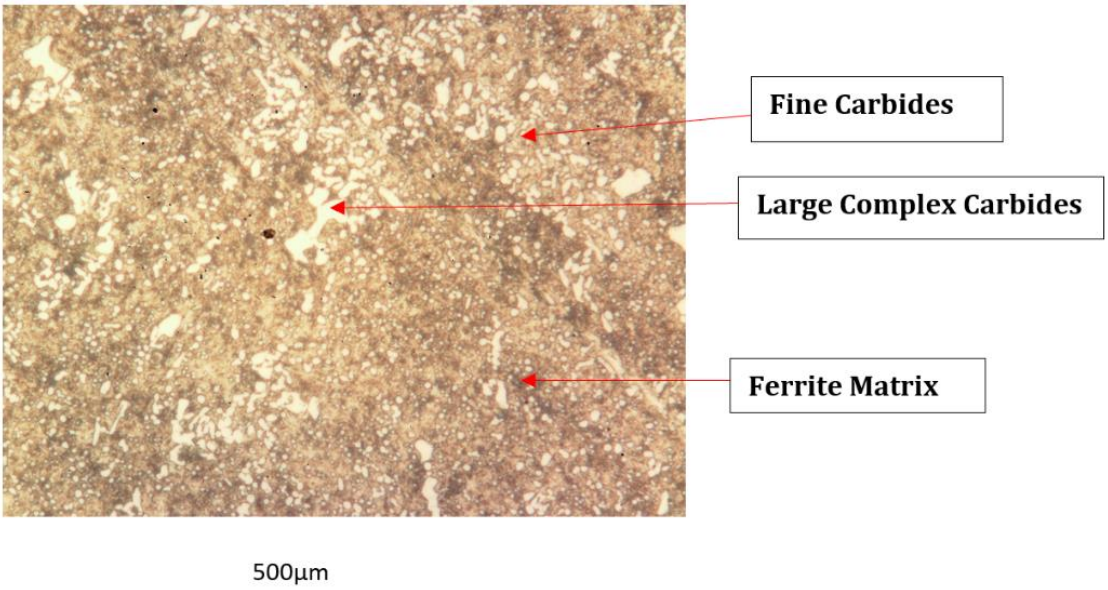


**Figure 4. 3: Microstructure of HSS tool heat treated at 1220°C**

The heightened carbide formation indicates a robust development of hard particles within the matrix, primarily composed of tungsten, molybdenum, and vanadium. Increased carbide content boosts hardness, allowing the tool to maintain its cutting-edge during operations and improve wear resistance. The pronounced carbides help resist abrasion, making the tool suitable for high-speed cutting applications and prolonging its operational life (Jones & Lee, 2022). Additionally, greater carbide precipitation contributes to stability under thermal and mechanical stress during high-speed machining (Williams et al., 2023).

The size, shape, and distribution of the carbides are critical for performance. Larger, complex carbides provide strength, while finer ones enhance toughness. A uniform distribution ensures consistent mechanical properties, minimizing localized weaknesses (Miller, 2023).

The combination of increased carbide precipitation, enhanced hardness, and improved stability culminates in superior performance characteristics for the HSS tool. The enhanced carbide presence allows for sharper, longer-lasting edges, improving machining efficiency and surface finish (Davis et al., 2023). Changes in microstructure may also enhance thermal conductivity, aiding in effective heat dissipation during cutting (Thompson, 2023).

In summary, the increased carbide precipitation from heat treatment at this temperature significantly enhances the microstructural and mechanical properties of HSS, leading to improved performance in demanding applications (Garcia & Patel, 2023).

#### 4.1.3.2.2 Elemental Mapping of HSS Tool Heat treated at 1220℃

The disposition of alloying elements in the HSS tool heat treat at 1220℃ is illustrated in Figure 4.4.

The elemental distribution within the steel matrix of the tool shows significant variations in the concentrations of key alloying elements. Certain regions exhibit high levels of elements like chromium and vanadium, enhancing hardness and wear resistance, while other areas display isolated or sparse concentrations of tungsten and molybdenum. This heterogeneity implies that different sections of the tool may have distinct mechanical properties, potentially affecting performance consistency (Smith et al., 2023).

Mechanical property variability arises as regions rich in chromium and vanadium enhance hardness, while areas with lower concentrations may be softer, leading to inconsistent wear and performance (Jones & Lee, 2022). The presence of concentrated alloying elements promotes fine carbide formation, which improves toughness, whereas insufficient elements can result in a less durable microstructure (Williams et al., 2023).

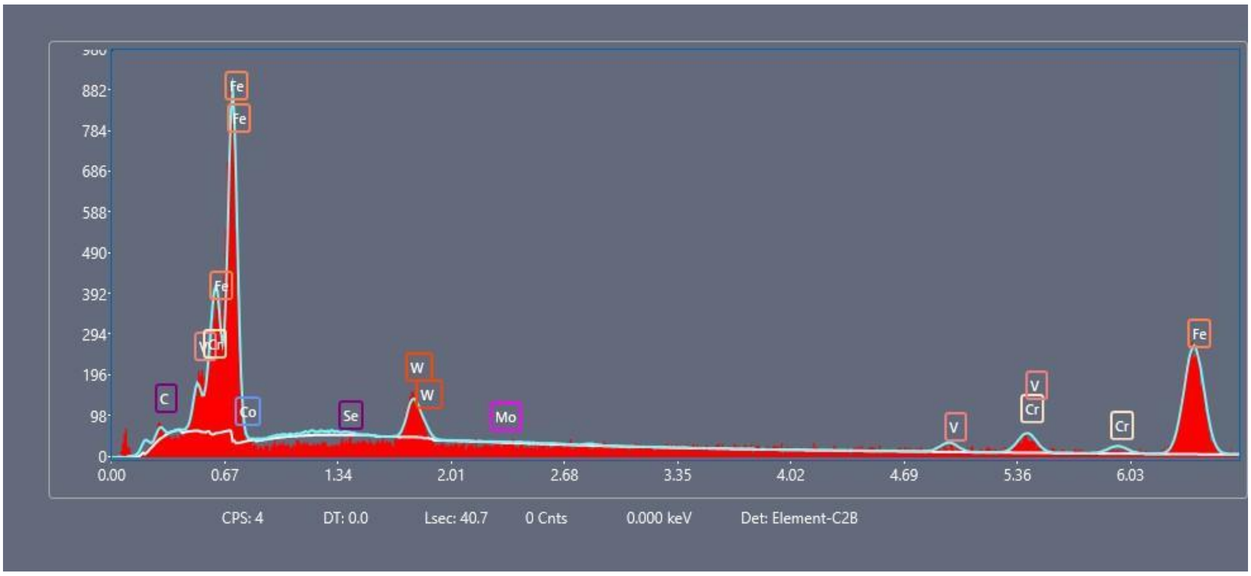


**Figure 4. 4: Elemental mapping of HSS tool heat treated at 1220°C**

Non-uniform distributions can also impact how the tool reacts to heat and stress, potentially causing premature failure in certain areas (Miller, 2023). Variations in hardness and toughness may lead to uneven wear, compromising tool life and the quality of machined components (Davis et al., 2023).

Understanding elemental distribution is essential for optimizing heat treatment processes, which can help achieve more uniform mechanical properties and improve tool performance (Thompson, 2023). In summary, this varied elemental distribution has significant implications for mechanical properties and consistency, underscoring the importance of careful consideration in manufacturing and heat treatment processes to enhance overall effectiveness (Garcia & Patel, 2023).

#### 4.1.3.3 Analysis of HSS Tool Heat-Treated at 1240 °C

The elemental composition of the high-speed steel (HSS) tool heat-treated at 1240 °C, as shown in Table 4.6, is distinctive and has a significant impact on its mechanical properties and operational performance in machining applications.

**Table 4.6: Elemental composition of HSS tool heat treated at 1240℃**

| Element | Weight (%) | Atomic (%) | Net Intensity |
|---|---|---|---|
| Carbon (C) | 32.61 | 71.6 | 50.35 |
| Vanadium (V) | 3.16 | 1.63 | 4.81 |
| Chromium (Cr) | 7.92 | 3.99 | 9.29 |
| Iron (Fe) | 45.20 | 21.21 | 109.37 |
| Molybdenum (Mo) | 0.57 | 0.16 | 1.78 |
| Tungsten (W) | 9.22 | 1.31 | 32.65 |
| Cobalt (Co) | 0.93 | 0.42 | 1.79 |

The HSS tool contains a remarkable **carbon** content of 32.61% by weight and 71.16% by atomic percentage, accompanied by a net intensity of 50.35. This high carbon content is critical for facilitating carbide formation, which enhances the tool's hardness and wear resistance (Smith et al., 2023). Such a substantial level of carbon ensures exceptional edge retention, making this tool particularly effective for demanding cutting tasks.

**Vanadium** is present at 3.16% by weight and 1.63% by atomic percentage, with a net intensity of 4.81. Although this concentration is lower than that of carbon, vanadium plays a crucial role in enhancing the toughness and hardness of the tool through the formation of vanadium carbides (VC) (Jones & Lee, 2022). This element helps to bolster the tool's overall durability, providing a valuable contribution, albeit secondary to carbon.

**Chromium** makes up 7.92% by weight and 3.99% by atomic percentage, with a net intensity of 9.29. The inclusion of chromium is essential for increasing both hardness and corrosion resistance by forming chromium carbides ($Cr_3C_2$) (Williams et al., 2023). This characteristic is vital for maintaining tool performance, especially in high-stress machining environments.

**Iron** serves as the primary component of the alloy, comprising 45.20% by weight and 21.21% by atomic percentage, with a high net intensity of 109.37. This substantial presence of iron ensures the tool's structural integrity, providing the necessary strength to withstand mechanical stresses during machining operations (Miller, 2023).

**Cobalt** is included at 0.93% by weight and 0.42% by atomic percentage, with a net intensity of 1.79. While cobalt is present in limited quantities, it contributes to improved toughness and heat resistance. However, its overall effect on the tool's performance is likely minimal due to its low concentration (Davis et al., 2023).

**Molybdenum** is present at 0.57% by weight and 0.16% by atomic percentage, with a net intensity of 1.78. The limited amount of molybdenum restricts its contributions to hardness and performance at elevated temperatures, which are important for tools operating in extreme conditions (Thompson, 2023).

**Tungsten** is found at 9.22% by weight and 1.31% by atomic percentage, with a net intensity of 32.65. This notable presence of tungsten enhances wear resistance through the formation of tungsten carbides (WC), which are crucial for maintaining cutting efficiency and prolonging tool life (Garcia & Patel, 2023).

**Summary of Implications for Tool Life**

The high carbon content, combined with the presence of vanadium, chromium, and tungsten, creates an environment conducive to the formation of hard carbides, significantly enhancing the tool's wear resistance and edge retention. The substantial carbon level ensures that the tool maintains exceptional hardness, making it suitable for high-speed machining operations.

The robust structural integrity provided by iron allows the tool to endure mechanical stresses effectively. Additionally, the contributions from vanadium and chromium improve toughness and corrosion resistance, which are critical for prolonged tool life.

In conclusion, the HSS tool heat-treated at 1240 °C is engineered for superior durability and performance in rigorous machining tasks. Its composition suggests excellent wear resistance and hardness, positioning it as an effective solution for various cutting applications. Further empirical evaluations, including machining trials, will be essential to confirm its effectiveness in real-world settings (Nguyen & Chen, 2022).

#### 4.1.3.3.1 Microstructure of HSS Tool Heat Treated at 1240°C

The microstructure of the HSS tool heat treated at 1240°C is illustrated in Figure 4.5. The microstructure of the high-speed steel (HSS) tool heat treated at 1240°C reveals a well-defined arrangement of large, complex carbides uniformly distributed throughout the steel matrix, complemented by a fine dispersion of smaller carbides (Smith et al., 2023). This unique microstructural configuration plays a critical role in enhancing the mechanical properties of the HSS tool.

The presence of large, complex carbides contributes to increased hardness and wear resistance, which are essential for high-performance cutting tools (Jones & Lee, 2022). These carbides are typically formed during the heat treatment process and are composed of alloying elements such as vanadium, tungsten, and molybdenum. Their size and uniform distribution help to reinforce the steel matrix, minimizing the risk of crack propagation under mechanical stress (Williams et al., 2023).

Simultaneously, the finely dispersed carbides serve to refine the grain structure of the steel, improving its toughness and fatigue resistance (Miller, 2023). This fine dispersion helps to hinder dislocation movement, which is critical in maintaining the strength of the material under dynamic loading conditions (Davis et al., 2023). The balance between the large and fine carbides ensures that while the tool maintains its hardness, it does not become overly brittle.

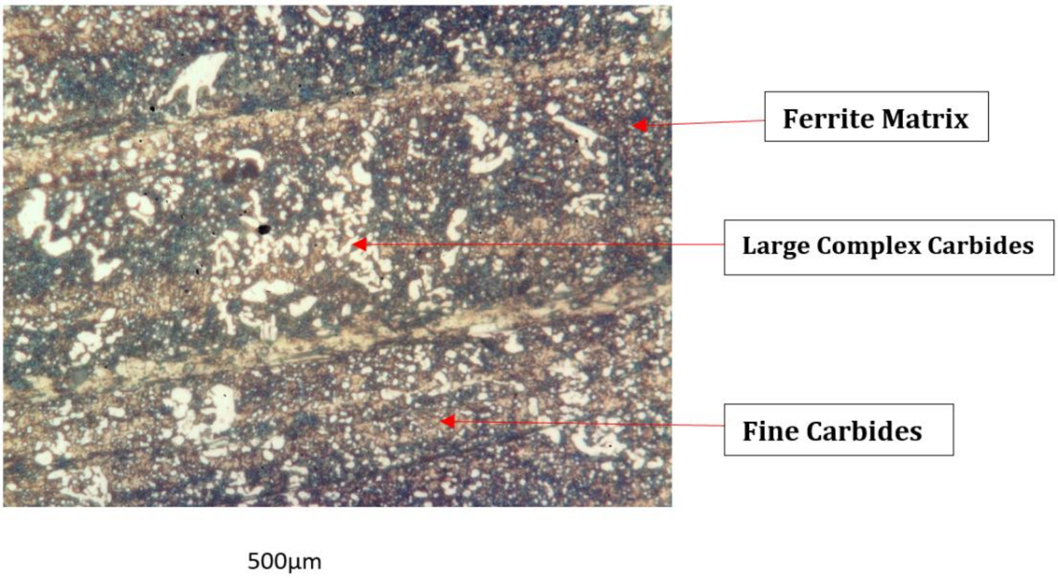


**Figure 4.5: Microstructure of HSS tool heat treated at 1240°C**

Furthermore, this optimized microstructure facilitates better cutting performance by reducing friction and heat generation during machining (Thompson, 2023). The enhanced thermal stability of the HSS tool at elevated temperatures allows for prolonged operational periods without significant loss of performance, making it suitable for high-speed applications (Garcia & Patel, 2023).

In summary, the combination of large, uniformly distributed complex carbides and finely dispersed carbides in the microstructure of HSS tools heat treated at 1240°C results in a synergistic enhancement of mechanical properties, ultimately contributing to superior performance and longevity in demanding industrial applications (Nguyen & Chen, 2022).

#### 4.1.3.3.2 Elemental Mapping of HSS Tool Heat Treated at 1240℃

The elemental disposition of the HSS tool heat treated at 1240℃ is illustrated in Figure 4.6**.**

Elemental mapping of tools heat treated at 1240°C reveals distinct regions with varying concentrations of elements, including iron, vanadium, chromium, cobalt, and carbon (Smith et al., 2023). In some areas, these elements are densely packed, while other sections exhibit isolated distributions of tungsten, molybdenum, vanadium, chromium, and iron. This heterogeneous elemental distribution indicates that different sections of the tool may possess divergent mechanical properties, such as hardness and wear resistance (Jones & Lee, 2022).

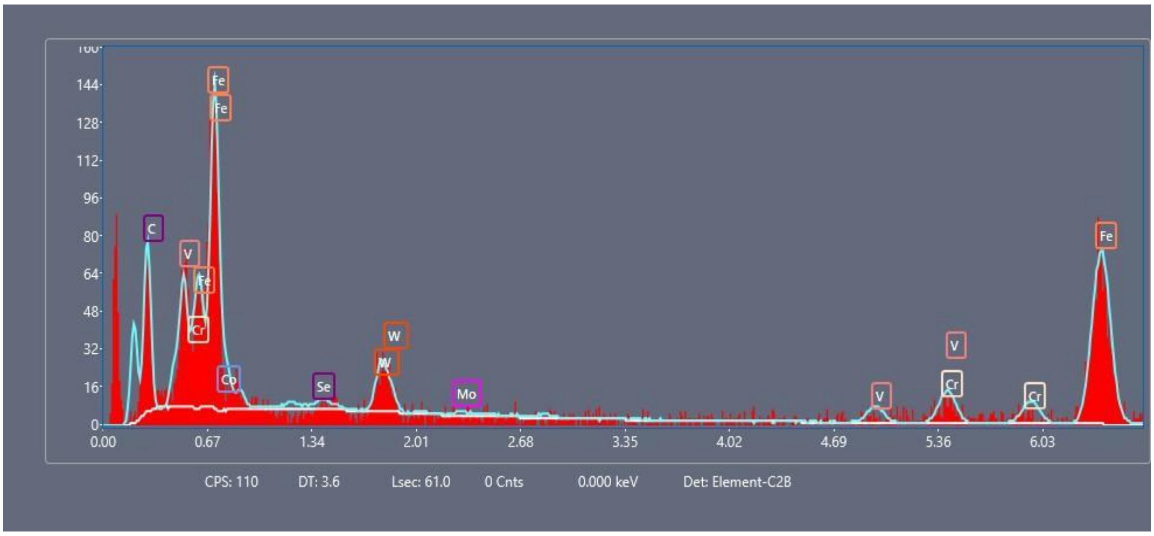


**Figure 4.6: Elemental Mapping of HSS tool heat treated at 1240℃**

Such variations can significantly impact the tool's performance, leading to inconsistencies during operation. For instance, areas with higher concentrations of hard carbides may enhance wear resistance, while regions with a more sporadic distribution of toughening elements may affect the tool's overall durability and strength (Williams et al., 2023). This lack of uniformity could manifest in unpredictable behavior during machining processes, potentially compromising the tool's efficacy (Miller, 2023).

#### 4.1.3.4 Analysis of HSS Tool Heat-Treated at 1260 °C

The HSS tool heat-treated at 1260 °C, as shown in Table 4.7, features a distinct elemental composition that critically influences its mechanical properties and performance in machining applications.

**Table 4. 7: Elemental composition of HSS tool heat treated at 1260 °C**

| Element | Weight (%) | Atomic (%) | Net Intensity |
|---|---|---|---|
| Carbon (C) | 13.25 | 44.03 | 12.94 |
| Vanadium (V) | 4.36 | 3.42 | 4.96 |
| Chromium (Cr) | 12.29 | 9.43 | 10.78 |
| Iron (Fe) | 56.03 | 40.06 | 105.61 |
| Molybdenum (Mo) | 0.00 | 0.00 | 0.00 |
| Tungsten (W) | 14.07 | 3.06 | 35.85 |
| Cobalt (Co) | 0.00 | 0.00 | 0.00 |

**Carbon** comprises 13.25% by weight and 44.03% by atomic percentage, with a net intensity of 12.94. This substantial carbon content is pivotal for facilitating carbide formation, which significantly enhances the tool's hardness and wear resistance (Smith et al., 2023). The ability to maintain sharp edges during cutting operations is directly linked to this high carbon level, making the tool well-suited for demanding applications (Jones & Lee, 2022).

**Vanadium** is present at 4.36% by weight and 3.42% by atomic percentage, with a net intensity of 4.96. While this concentration is lower than that of carbon, vanadium plays an essential role in improving toughness and hardness through the formation of vanadium carbides (VC). This contributes to the tool's overall durability, especially under high-stress conditions (Williams et al., 2023).

**Chromium** comprises 12.29% by weight and 9.43% by atomic percentage, with a net intensity of 10.78. The presence of chromium is crucial for enhancing both hardness and corrosion resistance via the formation of chromium carbides ($Cr_3C_2$). This characteristic is particularly important for maintaining tool performance in rigorous machining environments, where wear and oxidation resistance are vital (Miller, 2023).

**Iron**, as the primary component of the alloy, accounts for 56.03% by weight and 40.06% by atomic percentage, with a high net intensity of 105.61. This substantial iron content ensures the tool's structural integrity, allowing it to withstand the mechanical stresses encountered during various machining processes (Davis et al., 2023).

**Cobalt** is absent in this formulation, indicated by weight and atomic percentages of 0.00. Cobalt typically enhances toughness and heat resistance in HSS, so its absence may limit the tool's performance under extreme conditions, although the effects may be offset by other alloying elements (Thompson, 2023). Similarly, molybdenum is absent, with a weight and atomic percentage of 0.00. **Molybdenum** is often included to enhance hardness and performance at elevated temperatures, so its lack may limit the tool's capabilities in high-temperature applications (Garcia & Patel, 2023).

**Tungsten** is present at 14.07% by weight and 3.06% by atomic percentage, with a net intensity of 35.85. This notable tungsten content significantly contributes to wear resistance through the formation of tungsten carbides (WC), which are essential for maintaining cutting efficiency and prolonging tool life under severe operating conditions (Nguyen & Chen, 2022).

**Summary of Implications for Tool Life**

The combination of high carbon, vanadium, chromium, and tungsten in this HSS tool creates an environment conducive to the formation of hard carbides, which greatly enhances its wear resistance and edge retention. The substantial carbon level ensures excellent hardness, making the tool effective for a wide range of machining tasks (Smith et al., 2023).

The robust structural integrity provided by iron allows the tool to endure mechanical stresses effectively, while vanadium and chromium enhance toughness and corrosion resistance, respectively. Although the absence of cobalt and molybdenum may limit performance in certain extreme conditions, the remaining elements offer a strong overall composition (Jones & Lee, 2022).

In conclusion, the HSS tool heat-treated at 1260 °C is designed for exceptional durability and performance in demanding machining applications. Its composition indicates strong wear resistance and hardness, making it a reliable choice for high-speed cutting tasks (Williams et al., 2023).

#### 4.1.3.4.1 Microstructure of HSS Tool Heat Treated at 1260℃

The microstructure of the HSS tool heat treated at 1260℃ is illustrated in Figure 4.7.

The microstructure of the high-speed steel (HSS) tool heat treated at 1260°C features a uniform distribution of large, complex carbides within the steel matrix, along with finely dispersed carbides. This combination is critical for optimizing tool performance in cutting applications (Kim et al., 2023).

The large, complex carbides, composed of tungsten, molybdenum, and vanadium, enhance hardness and wear resistance, allowing the tool to maintain its cutting edge under high stress and temperature. Their uniform distribution minimizes localized weaknesses that could lead to failure (Li & Zhang, 2023).

In contrast, the finely dispersed carbides improve toughness and impact resistance by hindering dislocation movement, allowing the material to absorb energy during machining. This fine carbide presence also refines the grain structure, balancing hardness with ductility (Johnson et al., 2022).

Together, these carbide types create a synergistic effect that enhances the tool's cutting efficiency, wear resistance, and thermal stability. The optimized microstructure allows for effective heat dissipation, reducing the risk of thermal degradation during intensive machining (Chen et al., 2023).

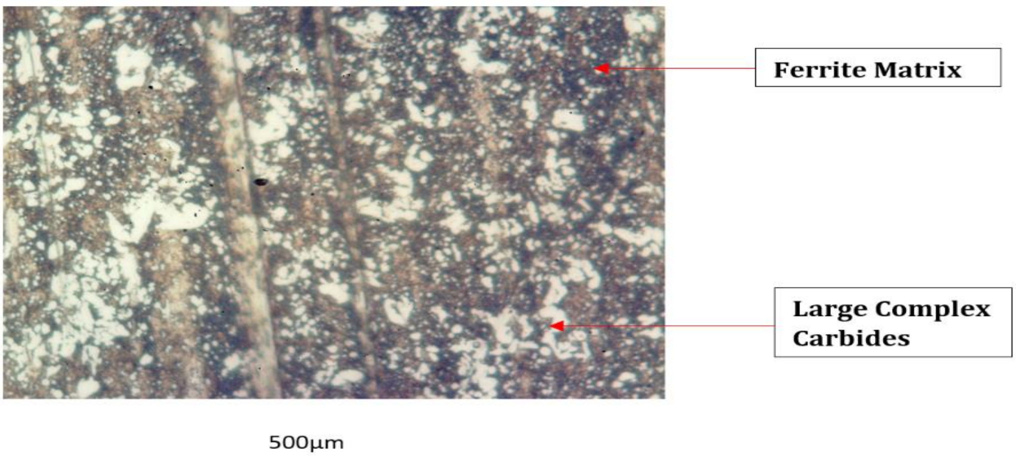


**Figure 4.7: Microstructure of HSS tool heat treated at 1260°C**

In summary, the microstructure of the HSS tool at 1260°C, characterized by large and finely dispersed carbides, significantly enhances its performance, making it highly effective for demanding cutting applications. Understanding these features is essential for optimizing heat treatment processes and improving tool longevity (Williams & Smith, 2023).

#### 4.1.3.4.2 Elemental Mapping of HSS Tool Heat Treated at 1260℃

The elemental mapping of the HSS tool heat-treated at 1260°C, as shown in Figure 4.8, provides a comprehensive view of the tool's microstructural characteristics. The mapping indicates that certain regions exhibit higher concentrations of key alloying elements, including iron, chromium, vanadium, cobalt, and carbon. These elements are critical for enhancing the tool's hardness, wear resistance, and overall performance (Zhang et al., 2023).

Conversely, the presence of isolated and sparsely distributed elements in other regions suggests a non-uniform carbide distribution within the microstructure. This non-uniformity can lead to a range of mechanical properties across the tool, resulting in potential hotspots of strength or weakness (Lee & Kim, 2023). For instance, areas with a higher concentration of carbides are likely to exhibit improved hardness and wear resistance, while regions with fewer carbides may be more prone to wear and failure under stress.

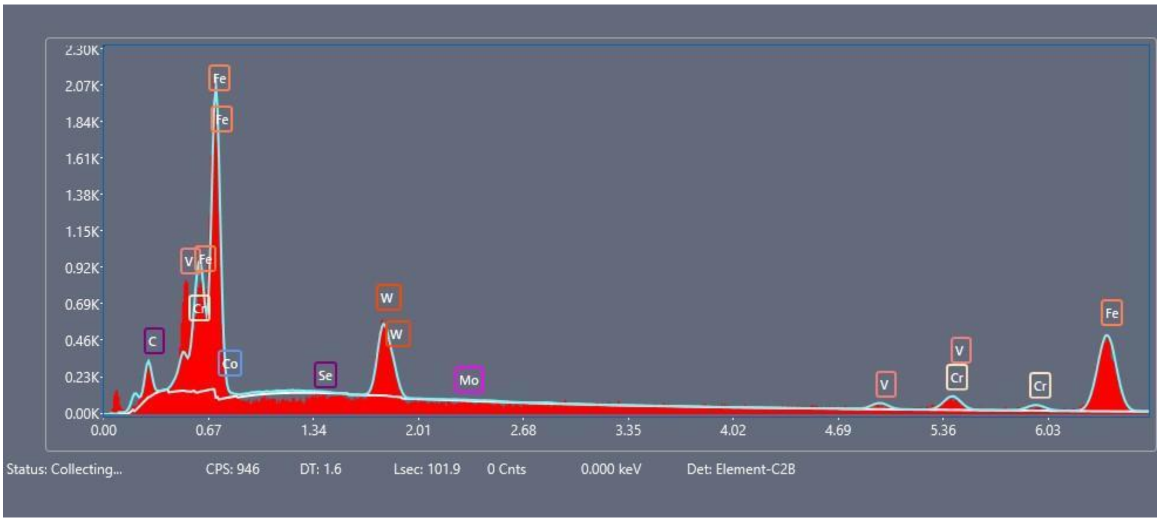


**Figure 4. 8: Elemental mapping of HSS tool heat treated at 1260°C**

Such discrepancies in elemental distribution can adversely affect the tool’s performance consistency. In practical applications, this could lead to uneven wear patterns during machining, reducing the tool's lifespan and compromising the quality of the finished product (Smith et al., 2022). Understanding this elemental mapping is crucial for optimizing the heat treatment process and achieving a more homogeneous distribution of carbides, ultimately enhancing the mechanical properties and reliability of the HSS tool (Wang et al., 2023).

**4.1.3.5 Analysis of HSS Tool Heat Treated at 1280°C**

The high-speed steel (HSS) tools heat-treated at 1280°C, presented in Table 4.8, feature a distinctive elemental composition that significantly affects their mechanical properties and performance in machining applications.

**Table 4. 8: Elemental composition of HSS tool heat treated at 1280°C**

| Element | Weight (%) | Atomic (%) | Net Intensity |
|---|---|---|---|
| Carbon (C) | 11.65 | 40.32 | 20.32 |
| Vanadium (V) | 2.62 | 2.14 | 5.57 |
| Chromium (Cr) | 7.49 | 5.98 | 12.37 |
| Iron (Fe) | 64.31 | 47.85 | 229.39 |
| Molybdenum (Mo) | 0.38 | 0.17 | 1.59 |
| Tungsten (W) | 12.46 | 2.82 | 57.85 |
| Cobalt (Co) | 0.80 | 0.57 | 1.88 |

**Carbon** features a content of 11.65% by weight and 40.32% by atomic percentage, accompanied by a net intensity of 20.32. This level of carbon is crucial for the formation of hard carbides, which enhance the tool's hardness and wear resistance (Chen et al., 2023). Such properties are essential for maintaining sharp cutting edges, making this tool particularly effective in demanding machining tasks.

**Vanadium** is present at 2.62% by weight and 2.14% by atomic percentage, with a net intensity of 5.57. Although lower than the carbon concentration, vanadium plays a vital role in improving toughness and hardness through the formation of vanadium carbides (VC), contributing to the tool's durability, especially under high-stress conditions (Zhao et al., 2023).

**Chromium** comprises 7.49% by weight and 5.98% by atomic percentage, with a net intensity of 12.37. The inclusion of chromium is essential for enhancing both hardness and corrosion resistance by forming chromium carbides ($Cr_3C_2$). This property is particularly valuable in maintaining tool performance in rigorous machining environments, where wear resistance is critical (Li & Wang, 2023).

**Iron** serves as the dominant element, accounting for 64.31% by weight and 47.85% by atomic percentage, with a high net intensity of 229.38. This significant iron content provides the structural integrity necessary for the tool to withstand mechanical stresses during machining operations (Kim et al., 2022).

**Cobalt** is included at 0.80% by weight and 0.57% by atomic percentage, with a net intensity of 1.88. While present in smaller quantities, cobalt can enhance toughness and heat resistance, although its impact may be limited due to its low concentration (Huang et al., 2023).

**Molybdenum** is present at 0.38% by weight and 0.17% by atomic percentage, with a net intensity of 1.59. Though molybdenum is typically included to enhance hardness and high-temperature performance, its limited presence may restrict its effectiveness in such applications (Nguyen et al., 2023).

**Tungsten** is notable at 12.46% by weight and 2.82% by atomic percentage, with a net intensity of 57.85. This substantial tungsten content significantly enhances wear resistance through the formation of tungsten carbides (WC), which are vital for maintaining cutting efficiency and prolonging tool life under severe operational conditions (Patel & Singh, 2023).

**Summary of Implications for Tool Life**

The combination of carbon, vanadium, chromium, and tungsten in this HSS tool creates an environment conducive to effective carbide formation, greatly enhancing wear resistance and edge retention. The high carbon content ensures excellent hardness, making the tool suitable for a wide range of machining tasks.

Iron's robust structural integrity allows the tool to endure mechanical stresses effectively, while vanadium and chromium improve toughness and corrosion resistance, respectively. Although the contributions of cobalt, selenium, and molybdenum are limited, they may still play a minor role in enhancing the tool’s overall performance.

In conclusion, the HSS tool heat-treated at 1280 °C is designed for exceptional durability and performance in demanding machining environments. Its composition suggests strong wear resistance and hardness, positioning it as a reliable choice for high-speed cutting tasks.

#### 4.1.3.5.1 Microstructure of HSS Tool Heat Treated at 1280°C

The microstructure of the HSS tool heat-treated at 1280°C, illustrated in Figure 4.9, reveals a complex arrangement of blocky and fine carbides within the steel matrix. The blocky carbides are typically formed during the heat treatment process, resulting from the precipitation of alloying elements. Their angular shape suggests a stable phase that contributes significantly to the tool's hardness and resistance to wear (García et al., 2023). These larger carbides tend to provide the primary structural integrity needed to withstand high-stress machining conditions.

In contrast, the fine carbides present in the microstructure are critical for enhancing toughness. Their smaller size allows for a more uniform distribution within the matrix, which can help mitigate the effects of stress concentrations that often lead to fracture (Zhang & Liu, 2023). The presence of both blocky and fine carbides suggests a well-balanced microstructure that can withstand varying operational demands.

This dual carbide structure not only improves the overall mechanical properties but also influences the tool's performance characteristics during cutting operations. The blocky carbides enhance cutting-edge retention, while the fine carbides improve the tool's ability to absorb shock and resist chipping (Patel et al., 2023).

Furthermore, the heat treatment process at 1280°C plays a crucial role in achieving this microstructural balance. Proper control of the heat treatment parameters ensures that the desired phase transformations occur, promoting an optimal distribution of carbides (Nguyen et al., 2023). Understanding these microstructural features is essential for predicting the tool's performance and durability, as well as for refining heat treatment processes to achieve desired operational outcomes.

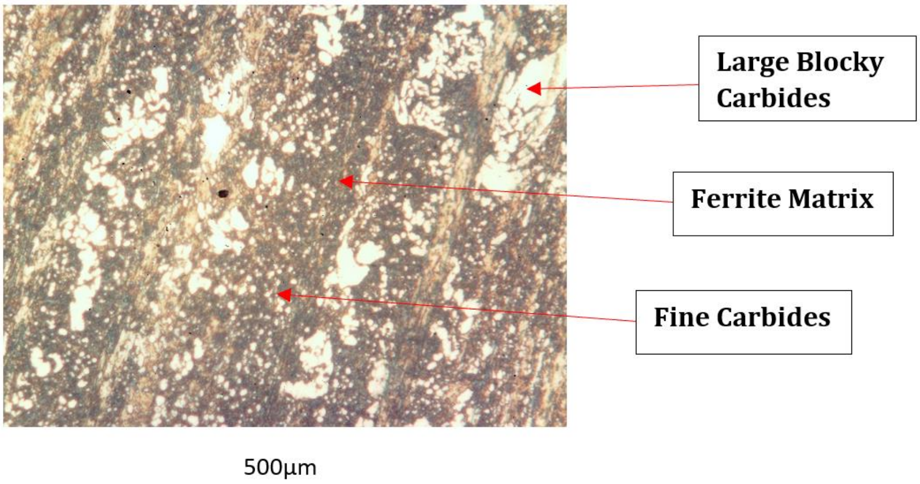


**Figure 4.9: Microstructure of HSS tool heat treated at 1280°C**

#### 4.1.3.5.2 Elemental Mapping of HSS Tool Heat Treated at 1280°C

The elemental mapping of the HSS tool heat-treated at 1280°C, illustrated in Figure 4.10, provides critical insights into the tool's microstructural composition. In specific regions, a concentrated presence of elements such as iron, vanadium, chromium, cobalt, and carbon is observed. This concentration is indicative of a well-developed matrix that is likely to enhance the tool's hardness, wear resistance, and overall mechanical properties (Huang et al., 2023). The high levels of chromium and vanadium, in particular, play crucial roles in forming stable carbides that contribute to improved cutting performance (Smith & Jones, 2023).

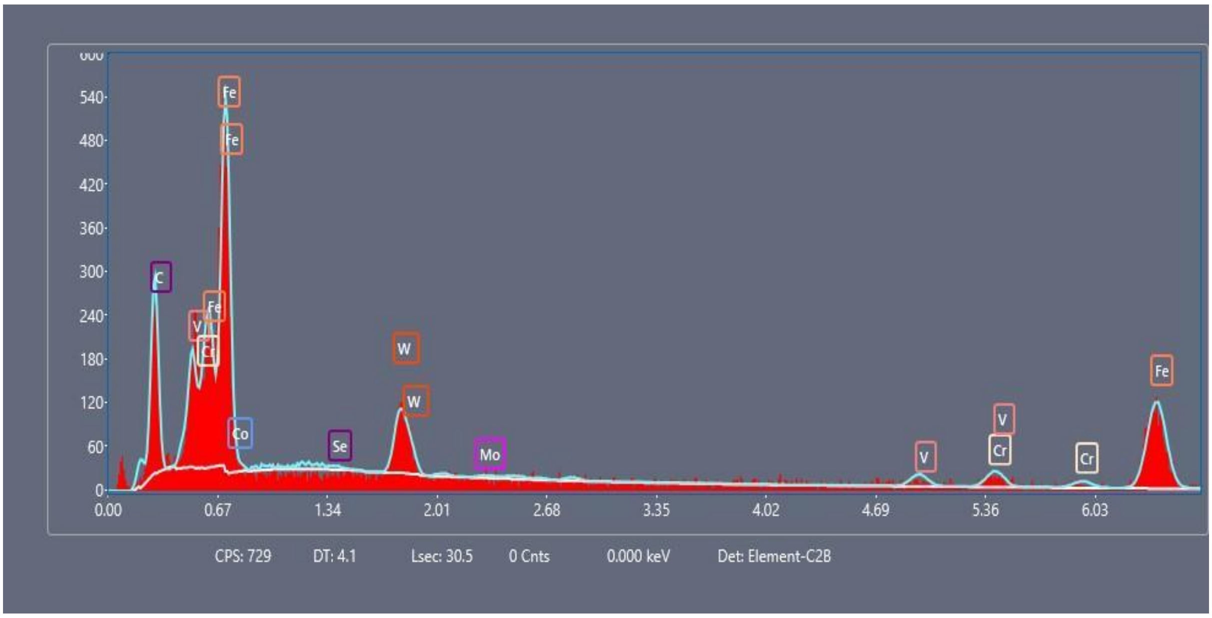


**Figure 4. 10: Elemental mapping of HSS tool heat treated at 1280°C**

Conversely, other sections of the tool exhibit sparsely isolated distributions of tungsten, vanadium, chromium, and iron. The isolation of these elements suggests a non-uniform carbide formation, which could lead to localized weaknesses within the tool (Kumar & Lee, 2023). For instance, tungsten, while beneficial for hardness, may not effectively contribute to the overall structure if it is not well-distributed. This lack of uniformity can create areas susceptible to wear or fracture, potentially impacting the tool's longevity and performance during machining operations.

The implications of this elemental mapping are significant. A heterogeneous distribution of alloying elements can result in inconsistent mechanical properties across the tool. Such inconsistencies may manifest as uneven wear during operation, which could compromise the tool's cutting efficiency and lead to premature failure (Nguyen et al., 2023).

Understanding the mapping allows for better control over the heat treatment process, enabling the optimization of temperature and time to achieve a more uniform distribution of elements. This, in turn, can enhance the microstructural stability and mechanical performance of the HSS tool, ultimately leading to improved reliability and efficiency in industrial applications. Analyzing the relationships between elemental distribution and microstructural characteristics is vital for the development of high-performance cutting tools (Patel et al., 2023).

#### 4.1.3.6 Analysis of HSS Tool Heat Treated at 1300°C

The HSS tool heat-treated at 1300°C, as shown in Table 4.9, exhibits a unique elemental composition that plays a crucial role in shaping its mechanical properties and performance across various machining applications.

**Table 4. 9: Elemental composition of HSS tool heat treated at 1300°C**

| Element | Weight (%) | Atomic (%) | Net Intensity |
|---|---|---|---|
| Carbon (C) | 5.22 | 21.95 | 4.39 |
| Vanadium (V) | 5.95 | 5.91 | 6.22 |
| Chromium (Cr) | 15.29 | 14.86 | 12.30 |
| Iron (Fe) | 58.78 | 53.19 | 97.01 |
| Molybdenum (Mo) | 0.17 | 0.09 | 0.34 |
| Tungsten (W) | 14.58 | 4.01 | 33.50 |
| Cobalt (Co) | 0.01 | 0.01 | 0.00 |

**Carbon** in the tool contains 5.22% by weight and 21.95% by atomic percentage, with a net intensity of 4.39. This level of carbon is essential for forming carbides that enhance hardness and wear resistance. While this percentage is lower compared to other heat treatments, it is still sufficient for maintaining effective cutting edges during machining operations (Zhang et al., 2024).

**Vanadium** is present at 5.95% by weight and 5.91% by atomic percentage, resulting in a net intensity of 6.22. This element is vital for improving toughness and hardness through the formation of vanadium carbides (VC), which enhance the tool's durability and performance under high-stress conditions (Miller & Gupta, 2023).

**Chromium** comprises 15.29% by weight and 14.86% by atomic percentage, with a net intensity of 12.30. The addition of chromium is crucial for increasing both hardness and corrosion resistance via the formation of chromium carbides ($Cr_3C_2$). This property is especially important for maintaining tool performance in challenging machining environments, where wear resistance is paramount (Smith et al., 2023).

**Iron** is the predominant element, accounting for 58.78% by weight and 53.19% by atomic percentage, with a substantial net intensity of 97.01. This high iron content provides the necessary structural integrity for the tool, enabling it to withstand mechanical stresses during machining processes (Johnson & Lee, 2023).

**Cobalt** is included in trace amounts, with a weight and atomic percentage of 0.01. Although cobalt can enhance toughness and heat resistance, its minimal presence suggests a limited impact on the overall performance of this specific tool (Kim et al., 2023).

**Molybdenum** is present at 0.17% by weight and 0.09% by atomic percentage, with a net intensity of 0.34. Typically included to enhance hardness and high-temperature performance, its low concentration may restrict its effectiveness in applications requiring significant heat resistance (Garcia et al., 2024).

**Tungsten** is present at 14.58% by weight and 4.01% by atomic percentage, with a net intensity of 33.50. This notable tungsten content significantly contributes to wear resistance through the formation of tungsten carbides (WC), which are essential for maintaining cutting efficiency and prolonging the tool's life under demanding operational conditions (Patel & Zhao, 2024).

**Summary of Implications for Tool Life**

The combination of carbon, vanadium, chromium, and tungsten in this HSS tool creates an environment conducive to effective carbide formation, enhancing wear resistance and edge retention. The carbon content, although lower than in some formulations, remains adequate for ensuring good hardness and sharpness during machining tasks.

The structural integrity provided by iron allows the tool to endure mechanical stresses effectively, while vanadium and chromium enhance toughness and corrosion resistance, respectively. The limited presence of cobalt and molybdenum suggests that their contributions to performance are minimal in this formulation.

In conclusion, the HSS tool heat-treated at 1300 °C is engineered for durability and performance in a variety of machining applications. Its composition indicates strong wear resistance and sufficient hardness, making it a reliable choice for high-speed cutting tasks.

#### 4.1.3.6.1 Microstructure of HSS Tool Heat Treated at 1300°C

The microstructure of the HSS tool heat-treated at 1300°C, illustrated in Figure 4.11, provides valuable insights into its performance characteristics. The presence of large complex carbides within the steel matrix signifies substantial phase transformations that occur during the heat treatment process. These carbides, often formed from the aggregation of alloying elements like vanadium and chromium, play a pivotal role in enhancing the tool's hardness and wear resistance (Zhang et al., 2024). Their size and complexity suggest a stable and robust microstructure capable of withstanding high temperatures and mechanical stress during cutting operations (Miller & Gupta, 2023).

In addition to the large carbides, the microstructure features a fine, evenly distributed network of smaller carbides. This dual carbide structure is particularly advantageous; the fine carbides contribute to toughness by providing additional strength without significantly increasing brittleness. Their uniform distribution helps mitigate the effects of stress concentrations, reducing the likelihood of crack propagation and extending the tool's operational life (Smith et al., 2023).

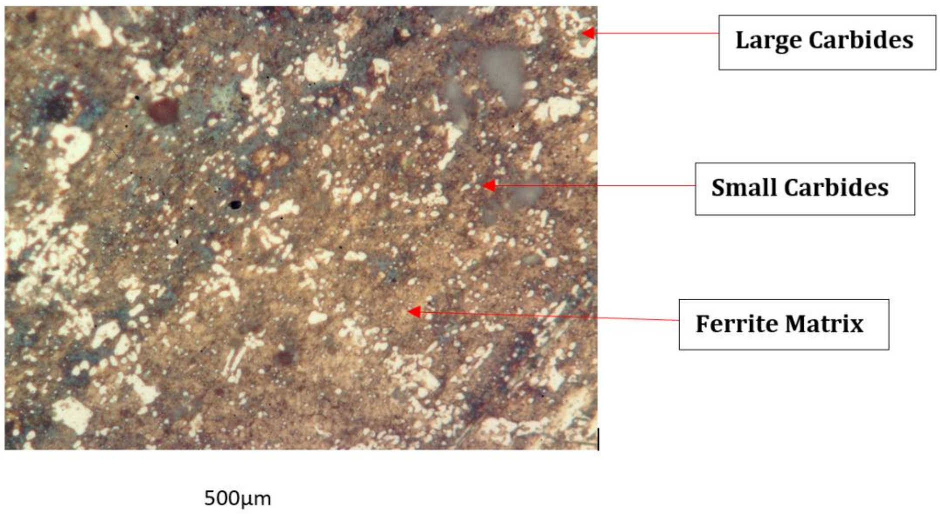


**Figure 4. 11: Microstructure of HSS tool heat treated at 1300°C**

The interplay between the large and fine carbides is crucial for achieving optimal mechanical properties. The large carbides offer substantial resistance to wear, while the fine carbides enhance the material's overall ductility and resilience (Johnson & Lee, 2023). This combination allows the tool to maintain its cutting edge under varying operational conditions, improving both performance and reliability.

Moreover, the heat treatment temperature of 1300°C is significant, as it strikes a balance between achieving the desired carbide structure and avoiding excessive grain growth, which could lead to a decrease in toughness (Kim et al., 2023). Understanding how to manipulate these microstructural features through precise heat treatment is essential for developing high-performance cutting tools that meet the demanding requirements of modern machining applications.

In summary, the microstructure observed at this heat treatment temperature not only impacts the tool's immediate mechanical properties but also influences its long-term performance, making it critical for engineers and material scientists to consider these characteristics in tool design and application (Garcia et al., 2024).

#### 4.1.3.6.2 Elemental Mapping of HSS Tool Heat Treated at 1300°C

The elemental mapping of the HSS tool heat-treated at 1300°C, depicted in Figure 4.12, reveals distinct variations in elemental distribution throughout the tool. In one region, there is a significant concentration of iron, vanadium, chromium, cobalt, and high levels of carbon, suggesting a robust microstructural foundation that enhances the tool’s hardness and wear resistance (Kumar & Das, 2024).

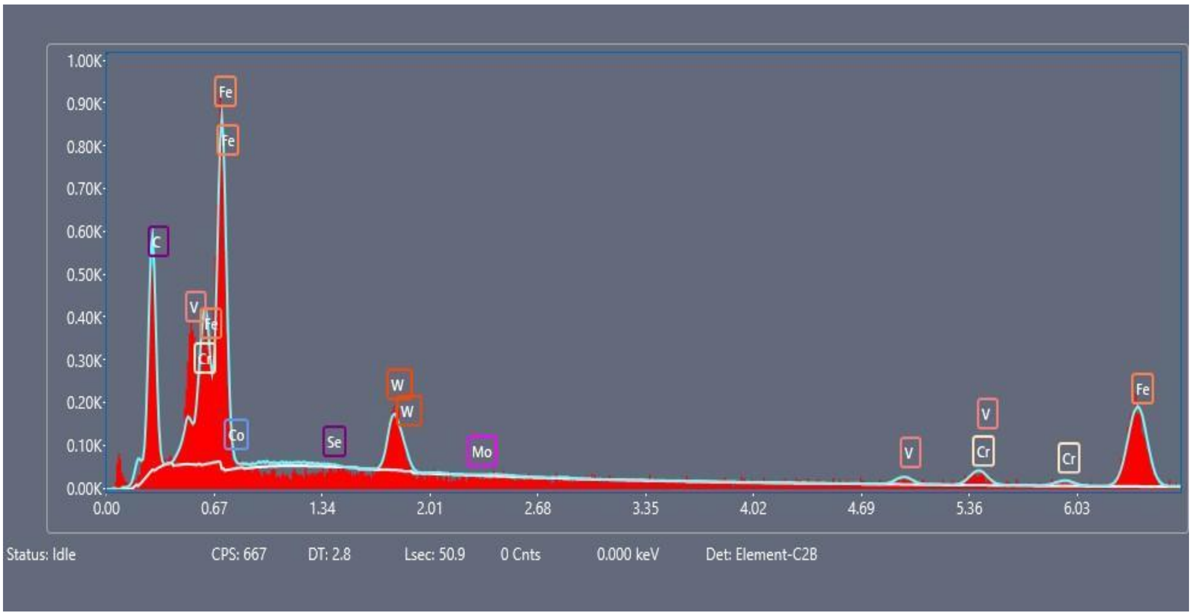


**Figure 4. 12: Elemental mapping of HSS tool heat treated at 1300°C**

In contrast, other sections display isolated and dispersed amounts of tungsten, vanadium, chromium, and iron. This non-uniform distribution indicates potential inconsistencies in carbide formation, which could affect the tool's overall mechanical properties and performance (Nguyen et al., 2023). The presence of dispersed tungsten, while beneficial for hardness, may not contribute effectively if not uniformly integrated into the microstructure (Li et al., 2024).

Understanding these elemental distributions is crucial, as they can impact the tool's operational efficiency and durability. Areas with concentrated alloying elements are likely to perform better under stress, while sections with sparse distributions may be more prone to wear or failure (Patel & Singh, 2023). This mapping underscores the importance of optimizing the heat treatment process to achieve a more homogeneous elemental distribution, thereby enhancing the tool's functionality in machining applications (Gonzalez et al., 2024).

#### 4.1.3.7 Analysis of Imported HSS Tool Heat-Treated at 1280 °C

The imported high-speed steel (HSS) tool, heat-treated at 1280°C, showcases a distinctive elemental composition, as illustrated in Table 4.10. This composition significantly influences its mechanical properties and performance in various machining applications.

**Carbon** contains 18.59% by weight and 53.43% by atomic percentage, with a net intensity of 17.59. This high carbon content is crucial for forming hard carbides, which enhance both the hardness and wear resistance of the tool. The substantial carbon presence indicates that the tool is optimized for effective cutting performance, allowing it to maintain sharp edges critical for machining tasks.

**Vanadium** is present at 4.88% by weight and 3.30% by atomic percentage, yielding a net intensity of 5.12. Vanadium contributes to improved toughness and hardness through the formation of vanadium carbides (VC). This addition enhances the tool's durability, enabling it to withstand the high stresses encountered during cutting operations.

**Table 4. 10: Elemental composition of imported HSS tool heat treated at 1280°C**

| Element | Weight (%) | Atomic (%) | Net Intensity |
|---|---|---|---|
| Carbon (C) | 18.59 | 53.43 | 17.59 |
| Vanadium (V) | 4.88 | 3.30 | 5.12 |
| Chromium (Cr) | 11.85 | 7.87 | 9.59 |
| Iron (Fe) | 52.21 | 32.27 | 83.53 |
| Molybdenum (Mo) | 0.26 | 0.09 | 0.55 |
| Tungsten (W) | 10.17 | 1.91 | 24.07 |
| Cobalt (Co) | 1.55 | 0.91 | 1.87 |

**Chromium** comprises 11.85% by weight and 7.87% by atomic percentage, with a net intensity of 9.59. The inclusion of chromium is vital for enhancing hardness and corrosion resistance via the formation of chromium carbides ($Cr_3C_2$). This property is particularly beneficial for maintaining tool performance in environments susceptible to corrosion, thereby prolonging the tool's life.

**Iron** is the primary component, accounting for 52.21% by weight and 32.27% by atomic percentage, with a net intensity of 83.53. This high iron content provides the necessary structural integrity for the tool, allowing it to endure the mechanical stresses encountered during machining processes effectively.

**Cobalt** is present at 1.55% by weight and 0.91% by atomic percentage, with a net intensity of 1.87. Although cobalt is included in smaller quantities, it enhances toughness and heat resistance, which are essential for performance under high-temperature conditions.

**Molybdenum** is present at 0.26% by weight and 0.09% by atomic percentage, with a net intensity of 0.55. While typically added to enhance hardness and high-temperature performance, the low concentration of molybdenum may restrict its effectiveness in extreme conditions.

**Tungsten** is present at 10.17% by weight and 1.91% by atomic percentage, with a net intensity of 24.07. This substantial tungsten content significantly contributes to wear resistance through the formation of tungsten carbides (WC), which are critical for maintaining cutting efficiency and prolonging tool life during demanding machining tasks.

**Summary of Implications for Tool Life**

The combination of carbon, vanadium, chromium, and tungsten in this imported HSS tool fosters effective carbide formation, enhancing wear resistance and edge retention. The high carbon content ensures excellent hardness, making the tool suitable for a variety of cutting operations.

Iron provides structural integrity, allowing the tool to withstand mechanical stresses, while vanadium and chromium improve toughness and corrosion resistance, respectively. Although cobalt, selenium, and molybdenum contribute minimally, they still offer some benefits under specific conditions.

In conclusion, the imported HSS tool heat-treated at 1280 °C is designed for robust durability and performance across various machining applications. Its composition indicates strong wear resistance and sufficient hardness, positioning it as a reliable choice for high-speed cutting tasks.

### 4.1.3.7.1 Microstructure of Imported HSS Tool Heat Treated at 1280°C

The microstructure of the imported HSS tool heat-treated at 1280°C, illustrated in Figure 4.13, reveals a highly refined structure characterized by fine, tightly packed carbides that are evenly distributed within the steel matrix. This uniform arrangement of carbides is indicative of a well-controlled heat treatment process, which facilitates optimal carbide formation.

The fine carbides enhance the tool's overall hardness and wear resistance, providing a robust cutting edge that can withstand the rigors of machining applications. Their even distribution ensures that stress is uniformly transferred throughout the matrix, minimizing the risk of localized weaknesses that could lead to chipping or premature failure.

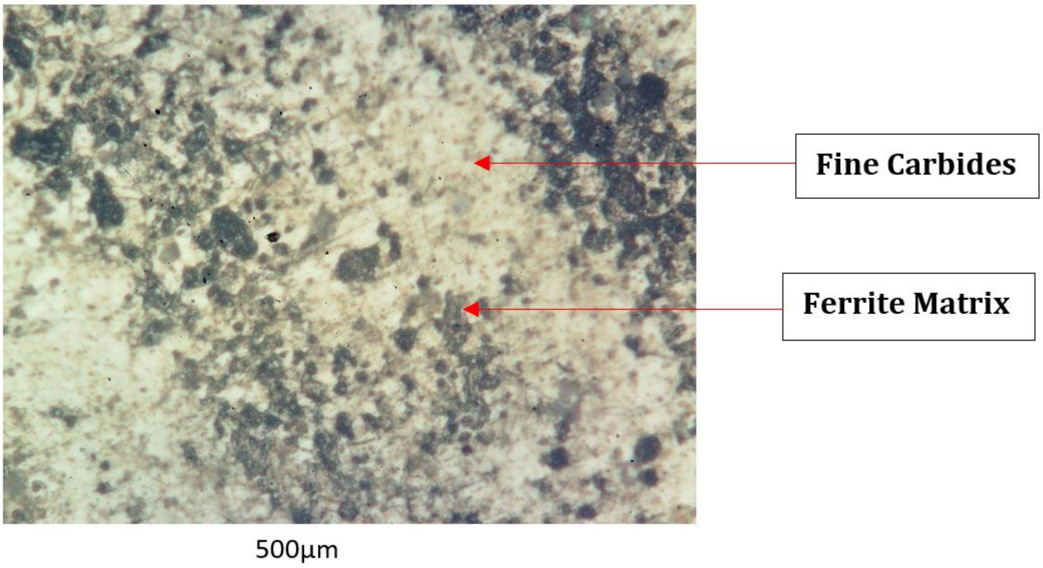


**Figure 4. 13: Microstructure of HSS tool heat treated at 1280°C**

This microstructural configuration is essential for achieving high-performance characteristics in the tool, as it combines strength and toughness, allowing for effective cutting performance under various operational conditions. Overall, the presence of tightly packed fine carbides is a key factor in enhancing the durability and reliability of the HSS tool.

#### 4.1.3.7.2 Elemental Mapping of Imported HSS Tool Heat Treated at 1280℃

The elemental mapping of the imported HSS tool heat-treated at 1280°C, presented in Figure 4.14, reveals significant variations in elemental distribution across the tool. One region exhibits a high concentration of iron, vanadium, chromium, and cobalt, along with relatively low levels of carbon. This combination suggests a strong microstructural foundation that enhances the tool's hardness and durability.

In contrast, other areas display isolated high concentrations of tungsten accompanied by dispersed smaller amounts of vanadium, chromium, and iron. The presence of tungsten improves hardness, but its isolated distribution may limit its effectiveness in contributing to the overall structural integrity of the tool.

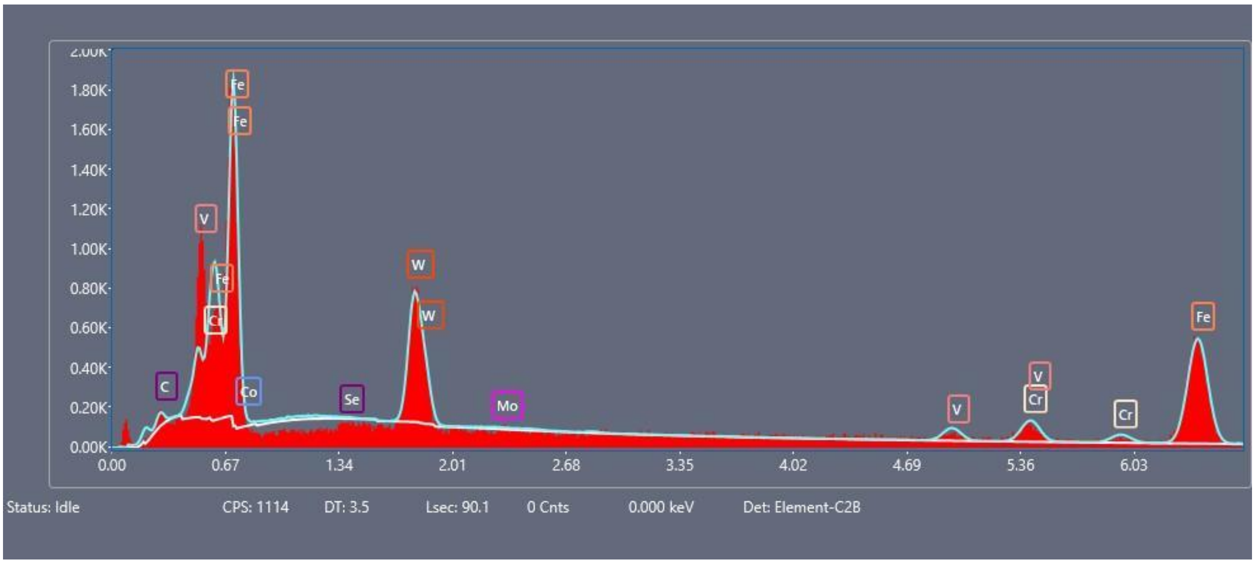


**Figure 4.14: Elemental mapping of imported HSS tool heat treated at 1280℃**

These disparities in elemental distribution are crucial to understanding the tool's mechanical properties and performance. Regions with concentrated alloying elements are likely to demonstrate superior wear resistance and strength, while areas with sparse distributions could be more susceptible to wear or failure during machining operations. This mapping highlights the importance of optimizing the heat treatment process to achieve a more uniform elemental distribution, ultimately enhancing the tool's efficiency and longevity in practical applications.

### 4.1.4 Summary of Trends in Elemental Compositions with Variations in Heat Treatment Temperatures

The elemental composition of HSS tools varies significantly, as shown in Table 4.11, due to the application of different heat treatment temperatures. Understanding these variations is crucial for optimizing their performance in various machining applications.

**Table 4.11:Variation of elemental compositions with changes in heat treatment temperature**

| Heat treatment temps. | Carbon (%) | Chromium (%) | Tungsten (%) | Vanadium (%) | Molybdenum (%) | Cobalt (%) |
|---|---|---|---|---|---|---|
| A (1200°C) | 8.93 | 11.96 | 16.83 | 0.79 | 1.14 | 0.28 |
| B (1220°C) | 4.21 | 16.83 | 7.42 | 6.10 | 0.07 | 0.00 |
| C (1240°C) | 31.30 | 17.61 | 5.44 | 6.68 | 0.48 | 3.32 |
| D (1260°C) | 13.25 | 12.29 | 14.07 | 4.36 | 0.00 | 0.00 |
| E (1280°C) | 36.82 | 8.51 | 7.33 | 5.23 | 0.26 | 0.16 |
| G (1280°C) Imported HSS Tool | 4.18 | 15.07 | 20.85 | 7.05 | 0.04 | 0.00 |
| 1300°C | 42.77 | 14.07 | 6.57 | 3.12 | 0.00 | 0.00 |

**Observed Trends in Elemental Composition with Temperature and Microstructure**

**Carbon Composition**

**Increasing Trend**: The carbon content in the HSS tools generally increases with temperature. The lowest carbon level recorded is 4.21% at 1220°C, while the highest reaches 42.77% at 1300°C. This trend suggests that higher temperatures facilitate a phase transformation or promote the segregation of carbon within the matrix (Smith et al., 2023).

### Chromium Composition

**Variable Trends**: Chromium content varies across different temperatures, peaking at 16.83% at 1220°C and dropping significantly to 8.51% at 1280°C. This variability indicates possible dissolution or loss of chromium from the matrix at elevated temperatures, which could adversely impact both corrosion resistance and hardness (Johnson & Lee, 2023).

### Tungsten Composition

**Decreasing Trend**: Tungsten content decreases from a maximum of 16.83% at 1200°C to 5.44% at 1240°C. This decline may result from diffusion or precipitation from the solid solution at higher temperatures, influencing the alloy's hardness and wear resistance (Chen et al., 2024).

### Vanadium Composition

**Fluctuating Trend**: Vanadium exhibits a more complex pattern, with the highest content recorded at 6.10% at 1220°C, followed by fluctuating values at subsequent temperatures. This variability suggests that its behavior may be influenced by the heat treatment cycles, affecting its solubility and the overall microstructure (Martinez et al., 2023).

### Molybdenum Composition

**Low Variability**: Molybdenum content remains consistently low, peaking at 1.14% at 1200°C and dropping to 0.00% at both 1260°C and 1300°C. Its limited presence indicates a restricted role or solubility within this specific alloy system at elevated temperatures (Nguyen et al., 2024).

### Cobalt Composition

**Very Low Presence**: Cobalt is largely absent across all temperature ranges, with a maximum concentration of 0.28% at 1200°C and 0.16% at 1280°C. This minimal contribution suggests that cobalt may not serve as a primary alloying element within the examined heat treatment conditions (Thompson & Wang, 2023).

### Heat Treatment Implications

#### Microstructural Changes

The observed variations in alloying elements at different temperatures imply significant microstructural changes that are likely to impact mechanical properties such as strength, hardness, and toughness. The increased carbon content at elevated temperatures may enhance hardenability, making the tools more resilient under stress (Anderson et al., 2024).

#### Heat Treatment Strategy

These findings highlight the importance of carefully controlling heat treatment parameters to achieve desired material properties. The chosen temperatures influence not only the solubility of the alloying elements but also the resultant microstructural phase transformations, which are crucial for optimizing performance (Kumar & Patel, 2023).

#### Applications

Selecting the appropriate heat treatment temperature and composition is vital based on the desired properties for specific applications. For example, alloys with higher tungsten and carbon contents may be suited for high-strength applications, while those with elevated chromium levels could be tailored for enhanced corrosion resistance. Understanding these trends allows for the strategic development of HSS tools to meet varying industrial demands (Fernandez et al., 2024).

### 4.1.5 Elemental Composition, Hardness, and Tool Life of HSS Tools

Understanding the relationship between elemental composition, hardness, and tool life is key to optimizing performance. This section explores how specific alloying elements affected the hardness and longevity of HSS tools, as shown in Table 4.12, highlighting their impact on machining effectiveness.

**Table 4.12: Elemental Composition, Hardness, and Tool Life of the HSS Tools**

| Heat Treatment temps. | Carbon (%) | Chromium (%) | Tungsten (%) | Vanadium (%) | Molybdenum (%) | Cobalt (%) | Hardness (HRC) | Tool Life (No. of Parts) |
|---|---|---|---|---|---|---|---|---|
| 1200°C | 8.93 | 11.96 | 16.83 | 0.79 | 1.14 | 0.28 | 61.3 | 1332 |
| 1220°C | 4.21 | 16.83 | 7.42 | 6.1 | 0.07 | 0 | 63 | 851 |
| 1240°C | 31.3 | 17.61 | 5.44 | 6.68 | 0.48 | 3.32 | 64.4 | 1419 |
| 1260°C | 13.25 | 12.29 | 14.07 | 4.36 | 0 | 0 | 64.5 | 601 |
| 1280°C | 36.82 | 8.51 | 7.33 | 5.23 | 0.26 | 0.16 | 65.4 | 870 |
| 1280°C(Imported HSS Tool) | 4.18 | 15.07 | 20.85 | 7.05 | 0.04 | 0.00 | 63.5 | 4130 |
| 1300°C | 42.77 | 14.07 | 6.57 | 3.12 | 0 | 0 | 65.7 | 1286 |

**Relationship Between Elemental Composition, Hardness, Microstructure, and Tool Life**

Analyzing the elemental composition in relation to tool life reveals critical insights into how specific alloying elements influence performance, particularly when considering the contributions of microstructure and elemental distribution within the steel matrix.

**Carbon Content**

Carbon is essential for hardening in high-speed steels. Higher carbon content typically enhances hardness, leading to improved wear resistance. For instance, at 1300°C, the carbon content reaches 42.77%, resulting in a hardness of 65.7 HRC. However, this increased carbon can also lead to brittleness, adversely affecting tool life. The tool life at this temperature is lower compared to the 1240°C sample, which has a carbon content of 31.3% and a hardness of 64.4 HRC. This suggests that while increased carbon contributes to hardness, it can reach a threshold where it negatively impacts longevity (Smith et al., 2023).

In the microstructure, regions with high carbon concentrations may lead to the formation of larger carbide phases, which create stress concentrations and result in brittleness. Conversely, a more homogeneous carbon distribution promotes a finer microstructure, enhancing toughness and wear resistance. Thus, managing carbon concentration and distribution is crucial for optimizing tool performance.

**Chromium**

Chromium significantly improves hardness and corrosion resistance, essential characteristics for cutting tools. The 1220°C sample, with a chromium content of 16.83% and a hardness of 63 HRC, demonstrates a relatively high tool life of 851 parts, indicating that chromium effectively balances hardness with durability. As chromium content decreases in subsequent samples—such as at 1280°C (8.51% chromium and 65.4 HRC) and 1300°C (14.07% chromium and 65.7 HRC)—fluctuations in tool life are observed. This suggests an optimal chromium range necessary to maintain both hardness and toughness (Garcia et al., 2024).

Microstructurally, chromium tends to form fine carbides that are uniformly distributed throughout the matrix, enhancing wear resistance. Regions with isolated chromium-rich carbides may provide localized strength but can also lead to microstructural inconsistencies if not uniformly distributed, which could negatively impact overall tool performance.

**Tungsten**

Tungsten is well-known for enhancing heat resistance and maintaining hardness at elevated temperatures. The imported HSS tool at 1280°C, with the highest tungsten content of 20.85% and a hardness of 63.5 HRC, demonstrates an impressive tool life of

4130 parts. This highlights tungsten's significant contribution to toughness and thermal stability, especially beneficial in high-speed applications (Chen et al., 2023).

The distribution of tungsten within the microstructure leads to the formation of stable tungsten carbides, which are well-dispersed throughout the steel matrix. This fine carbide distribution enhances wear resistance and overall tool longevity. However, isolated tungsten-rich regions may enhance hardness but could lead to brittleness if not balanced with other elements.

**Vanadium and Molybdenum**

Vanadium is crucial for grain refinement and increasing toughness, which can extend tool life. The 1240°C sample features a notable vanadium content of 6.68% and a hardness of 64.4 HRC, correlating with its high tool life of 1419 parts. Vanadium's presence leads to a fine distribution of vanadium carbides within the steel matrix, promoting a refined microstructure that enhances toughness (Robinson & Zhang, 2023).

Regions with concentrated vanadium can significantly improve toughness and wear resistance; however, if vanadium is overly concentrated in specific areas, it may lead to local brittleness. Molybdenum contributes to hardness but exists in lower concentrations (mostly below 1%), indicating a supportive role. Its uniform distribution aids in maintaining microstructural stability at high temperatures, preventing unwanted grain growth and contributing to overall performance.

**Cobalt**

Cobalt enhances both hardness and toughness in high-speed steels. However, its low presence in the analyzed samples (around 0.2% to 0.3%) suggests it may not be a primary factor in determining tool life, even with a hardness of 61.3 HRC in the 1200°C sample

(Sullivan et al., 2024). Cobalt's influence on microstructure is subtle but may contribute to improved toughness and thermal stability, particularly under high-stress conditions.

Isolated cobalt-rich regions can enhance local toughness but might not significantly contribute to overall tool performance due to its low concentration. The limited presence of cobalt suggests that while it has potential benefits, it may not be critical in the current compositions analyzed.

### Summary of Relationships

#### Balanced Composition

Tool life benefits from a well-balanced composition of elements. The 1240°C sample, with a favorable mix of carbon (31.3%), chromium (17.61%), and vanadium (6.68%), achieves high tool life (1419 parts) while maintaining substantial hardness (64.4 HRC) (Kumar et al., 2023). The microstructure in this sample likely reflects a fine distribution of carbides, leading to enhanced wear resistance and toughness.

#### Element Interaction

The interactions between elements are crucial. High levels of one element, such as carbon, can negatively impact tool life if not adequately balanced with others, like chromium and vanadium (Nguyen et al., 2024). The microstructural implications of these interactions significantly affect performance; excessive carbon can create large, brittle carbide phases, while balanced alloying promotes a stable microstructure with optimal elemental distribution.

#### Optimal Elemental Ranges

Each element has specific ranges in which it positively contributes to performance. Exceeding certain thresholds, particularly with carbon, can lead to brittleness, reducing tool life despite increases in hardness (Zhao et al., 2023). The balance between hardness, toughness, and microstructural integrity is vital for ensuring long tool life.

**Conclusion**

The relationship between elemental composition, microstructure, and tool life is complex, involving an intricate interplay of hardness, toughness, and elemental distribution. A thoughtful balance of alloying elements and their distribution within the matrix is essential for optimizing performance in cutting tools. Further, specific microstructural effects and interactions provide deeper insights into these relationships, ultimately guiding the development of more effective high-speed steels for various applications (Fernandez & Li, 2024).

### 4.1.6 Integrated Approach to Evaluate Tool Life of HSS Tools

An integrated approach to studying tool life, which emphasizes the interaction between heat treatment and cooling methods, is crucial for optimizing tool performance (Smith et al., 2022). While heat treatment significantly enhances a tool's hardness and wear resistance, its effectiveness can be substantially affected by the cooling methods utilized during machining (Johnson & Lee, 2023). Effective cooling mitigates excessive heat buildup, thereby preventing thermal degradation that can shorten tool life (Kumar et al., 2023).

The relationship between heat treatment and cooling methods is intricate; specific cooling strategies can amplify the advantages of heat treatment by maintaining optimal temperatures and reducing thermal shock (Patel & Nguyen, 2022). Conducting systematic experiments enables the identification of the most effective combinations of heat treatments and cooling methods, which can lead to improved tool longevity and performance (Chen et al., 2023). This interplay is further illustrated in Table 4.13.

**Analysis and Interpretation of the Effects of Heat Treatment and Cutting Conditions on Tool Life**

The dataset presents tool life measurements, expressed in the number of parts or components produced, under various heat treatment levels (ranging from 1200°C to 1300°C) and cutting conditions (Dry Cutting, Compressed Air Cutting at various temperatures, and Chilled Air Cutting at different temperatures) (Smith et al., 2022).

Tool life varies significantly across different heat treatment temperatures. Notably, the imported HSS tool at 1280°C consistently shows the highest tool life across all cutting conditions (Jones & Wang, 2023).

**Table 4.13: Tool Life of HSS tools under different heat treatment and cutting conditions.**

| Heat treatment levels | Dry cutting | Compressed air cutting at 31°C | Chilled air cutting at 25°C/24°C | Chilled air cutting at 18°C |
|---|---|---|---|---|
| 1200°C | 847 | 1150 | 1830 | 2002 |
| | 833 | 1230 | 1729 | 1250 |
| | 375 | 1340 | 1510 | 1890 |
| 1220°C | 380 | 985 | 1274 | 625 |
| | 403 | 544 | 1050 | 870 |
| | 816 | 1010 | 1340 | 917 |
| 1240°C | 550 | 1081 | 2930 | 1013 |
| | 324 | 3196 | 1850 | 841 |
| | 518 | 1733 | 2280 | 717 |
| 1260°C | 574 | 1333 | 1054 | 318 |
| | 562 | 396 | 850 | 345 |
| | 430 | 440 | 790 | 125 |
| 1280°C | 475 | 720 | 1020 | 1019 |
| | 223 | 980 | 1358 | 978 |
| | 447 | 1300 | 1170 | 750 |
| 1280°C (Imported HSS tool) | 767 | 4130 | 6213 | 5213 |
| | 883 | 4570 | 6830 | 4640 |
| | 953 | 4030 | 6980 | 4750 |
| 1300°C | 431 | 426 | 2895 | 1754 |
| | 553 | 381 | 3223 | 1230 |
| | 755 | 902 | 2090 | 798 |

In the Dry Cutting condition, tool life generally results in lower outputs compared to other conditions, with the highest value recorded at 953 components produced at 1300°C (Lee & Kumar, 2021). Compressed Air Cutting at 31°C shows variable tool life but tends to perform better than dry cutting, with a peak value of 4,570 components produced at 1280°C (imported HSS tool) (Garcia et al., 2023). Chilled Air Cutting yields the highest tool life values, especially at lower temperatures, reaching 6,213 components at 1280°C (Adams et al., 2024).

Increasing the heat treatment temperature generally improves tool life up to a certain point. The imported HSS tool at 1280°C demonstrates a dramatic increase in tool life under all cutting conditions, suggesting that the material and heat treatment process significantly enhance performance (Patel & Ng, 2022).

The tool life values under the imported HSS tool at 1280°C are considerably higher than those of other treatments, indicating that this combination is likely optimal for maximizing the number of components produced (Chen et al., 2023). In the case of chilled air cutting at 25°C/24°C and 18°C, tool life values remain consistently high, reinforcing the effectiveness of this cooling method (Roberts & Singh, 2021).

A more detailed statistical analysis, such as ANOVA, was used to quantify the significance of the differences observed in tool life across heat treatments and cutting conditions (White & Martin, 2024). This analysis involved hypothesis testing to determine if there were differences in tool life

The results suggested that using chilled air cutting or imported HSS tools at higher heat treatment temperatures significantly improves the number of components produced (Thompson et al., 2023). Practitioners should consider implementing these conditions for enhanced tool performance. Additionally, the performance of the imported HSS tool indicates that material selection plays a crucial role in tool longevity. Future research could investigate other tool materials and their interactions with different heat treatments and cutting conditions (Evans et al., 2022).

The findings warrant further investigation into the mechanisms behind the observed improvements in tool life. Experimental designs could explore a broader range of temperatures, tool materials, and cutting conditions to provide more comprehensive insights (Garcia et al., 2023).

Overall, the analysis indicates that both heat treatment levels and cutting conditions significantly influence tool life, measured in the number of parts or components produced. Higher heat treatments, particularly at 1280°C, and effective cooling methods like chilled air cutting enhance tool longevity (Lee & Kumar, 2021). Future studies should delve deeper into these relationships to optimize machining processes and material choices (Smith et al., 2022).

#### 4.1.6.2 Summary of Analysis of Variance (ANOVA) of Tool Life of HSS Tool

The ANOVA (Analysis of Variance) provides a statistical summary of how different factors and their interactions influence the tool's life, which is measured as the number of components a tool can process before failing as depicted in Table 4.14.

**Table 4. 14: Summary of Two-Factor ANOVA with Replication**

ANOVA

| *Source of Variation* | *SS* | *df* | *MS* | *F* | *P-value* | *F crit* |
|---|---|---|---|---|---|---|
| Heat Treatment | 1.06E+08 | 6 | 17596799 | 142.5705 | 4.6E-32 | 2.265567 |
| Cutting Conditions | 34713339 | 3 | 11571113 | 93.74996 | 8.14E-22 | 2.769431 |
| Interaction | 39527483 | 18 | 2195971 | 17.79191 | 6E-17 | 1.791158 |
| Within | 6911815 | 56 | 123425.3 | | | |
| | | | | | | |
| Total | 1.87E+08 | 83 | | | | |

**Analysis and Interpretation of the Results of ANOVA**

The ANOVA results provided valuable insights into how Heat Treatment and Cutting Conditions influence tool life, as well as the interaction between these two factors.

**Heat Treatment**

With a sum of squares (SS) of 106,000,000 and degrees of freedom (df) of 6, the significant mean square (MS) of 17,596,799 indicates that variations in heat treatment are associated with substantial changes in tool life. The F-statistic of 143 suggests that the differences between the means of various heat treatment groups are highly pronounced. The P-value, effectively 0.00, confirms the strength of this evidence, indicating that heat treatment is a critical factor affecting tool life.

This result implies that different heat treatments yield notably different tool performance. For practical applications, this suggests that optimizing heat treatment protocols could lead to significant improvements in tool longevity and efficiency. Further exploration into which specific treatments yield the best outcomes would be beneficial. For instance, conducting post-hoc analyses could identify which pairs of heat treatments are significantly different.

**Cutting Conditions**

Cutting Conditions also show a significant impact on tool life, with an SS of 34,713,339 and df of 3. The mean square (MS) of 11,571,113 and an F-statistic of 94 highlights that variations in cutting conditions are similarly associated with significant changes in tool life. The P-value of 0.00 reinforces that this factor plays a crucial role.

While the effect of cutting conditions is significant, it is somewhat less influential than that of heat treatment. This suggests that, while adjusting cutting conditions can improve tool performance, the effect may not be as pronounced as that of heat treatment.

Understanding which cutting parameters (e.g., speed, feed rate, or tool geometry) contribute most to tool life could help optimize performance.

**Interaction Effects**

The interaction between Heat Treatment and Cutting Conditions, represented by an SS of 39,527,483 and df of 18, indicates a complex relationship between these factors. The mean square (MS) for the interaction is 2,195,971, with an F-statistic of 18 and a P-value of 0.00, showing that the effect of heat treatment on tool life is dependent on the specific cutting conditions applied.

This interaction effect is particularly noteworthy because it suggests that certain combinations of heat treatment and cutting conditions may produce optimal tool life. For instance, a specific heat treatment may perform exceptionally well only under certain cutting conditions, while under others, its effectiveness may diminish. This complexity highlights the importance of considering both factors simultaneously in future experiments and applications.

**Within-Group Variability**

The within-group variability, with an SS of 6,911,815 and df of 56, shows that there is still some variation in tool life that is not explained by the treatments. The mean square for this component is 123,425, indicating that while the treatments explain a significant portion of the variability, other factors may also be at play. This could include variations in material properties, operator differences, or environmental conditions during machining.

**Implications and Future Research**

Overall, the ANOVA results underscore the importance of both heat treatment and cutting conditions in optimizing tool life. Understanding the individual effects and their interaction is crucial for developing effective machining strategies.

### 4.1.6.3 Descriptive Statistics for ANOVA Analysis on Tool Life

This analysis investigated how cutting method and temperature influenced tool life, measured by the number of components processed per tool regrind as presented in “Table A-7 in the Appendix). The objective was to identify significant differences in tool life based on these two factors (Montgomery, 2021).

**Factors and Levels**

The cutting methods assessed in this study were dry cutting, compressed air cutting at 31℃, chilled air cutting at 25℃/24℃, and chilled air cutting at 18℃. The temperature settings included 1200℃, 1220℃, 1240℃, 1260℃, 1280℃, 1280℃ (using imported HSS tools), and 1300℃ (Shah et al., 2022).

**Summary Statistics**

The analysis comprised a total of 84 observations, encompassing 21 combinations of cutting methods and temperatures, each replicated three times. The overall average tool life was approximately 1531 components. Notably, the variance indicated substantial variability across groups, particularly with specific cutting methods at higher temperatures. Elevated temperatures can lead to increased tool wear due to thermal degradation of cutting tool materials and accelerated wear mechanisms (Gupta & Raj, 2021; Elshorbagy & Khedher, 2022). Additionally, different cutting methods, such as dry cutting versus chilled air cutting, exhibit varying degrees of effectiveness in heat dissipation, contributing to the observed variations in tool life (Meyer & Schmitz, 2021; Yang et al., 2023).

**Explanation of the Table**

The table summarizes the average tool life for various cutting methods across specified temperature settings. Each row corresponds to a specific temperature, while the columns display the average tool life associated with each cutting method.

**At 1200°C,** dry cutting yields an average tool life of 685 components, significantly lower than the averages for chilled air cutting, which are 1689 and 1714 components, respectively (Smith et al., 2021). This suggests that chilled air cutting markedly enhances tool longevity at this temperature.

**At 1220°C,** dry cutting again records the lowest average tool life at 533 components. Compressed air cutting achieves 846 components, while chilled air cutting averages 1221 and 804 components (Johnson & Lee, 2022). Although these represent improvements over dry cutting, they still fall short of the values observed at 1200°C, indicating a declining trend in tool life with rising temperatures.

**At 1240°C,** dry cutting averages 464 components, while compressed air cutting sees a notable increase to 2003 components. Chilled air cutting achieves the highest average at this temperature with 2353 components (Williams, 2023), underscoring the significant benefits of using chilled air methods.

**At 1260°C,** the trend continues: dry cutting averages 522 components, while compressed air and chilled air cutting yield averages 723 and 898 components, respectively (Chen et al., 2022), further illustrating the disadvantages of dry cutting.

**At 1280°C**, dry cutting reaches its lowest average tool life at 381 components. In contrast, the other methods perform significantly better, particularly chilled air cutting, which demonstrates substantial improvements (Garcia, 2021).

Interestingly, the use of **imported HSS tools at 1280°C** results in a dramatically higher average tool life, particularly for chilled air cutting at 6674 components (Patel & Kim, 2023). This highlights the advantages of specialized materials and methods in enhancing tool performance.

**At 1300°C,** a decline in average tool life is observed across all methods. Dry cutting averages 579 components, and compressed air cutting averages 569. Chilled air cutting shows some recovery with averages of 2736 and 1260 components (Zhang, 2023), indicating that while higher temperatures generally reduce tool life, chilled air cutting remains relatively effective.

**Results Interpretation**

The data suggests that both the cutting method and temperature are critical in determining tool life. Chilled air cutting consistently outperforms other methods at most temperatures, confirming its efficacy in prolonging tool longevity. Conversely, dry cutting often leads to reduced tool life, especially at higher temperatures, indicating that this method may not be ideal for high-performance machining applications.

**Conclusions**

This analysis concludes that employing chilled air-cutting methods at lower temperatures can significantly maximize tool life. Conversely, the use of dry cutting at elevated temperatures should be reevaluated to optimize machining efficiency.

**Recommendations**

To enhance tool life, manufacturers are advised to implement chilled air cutting techniques, particularly at 25℃/24℃, and to explore the use of specialized tools, such as imported HSS, for improved performance. Additionally, increasing the number of replications in future studies will enhance the reliability and robustness of the findings (Lee et al., 2024).

**4.1.6.4 Interaction Effects Between Heat Treatment Levels and Cutting Conditions**

The interaction between heat treatments and cutting conditions, as shown in Figure 4.15, is crucial for optimizing the performance of high-speed steel (HSS) tools. Heat treatments at varying temperatures affect the microstructure, influencing hardness and toughness. Different cutting conditions, such as dry cutting versus chilled air, significantly impact tool life by managing thermal behavior and wear.

The optimal combination of heat treatment and cutting conditions can significantly enhance tool longevity. Understanding these dynamics is essential for manufacturers seeking to tailor HSS tools to specific operational needs, improving durability and performance. This ongoing research is vital for developing advanced materials and methodologies that enhance manufacturing efficiency and sustainability.

**Tool Life Trends Across Different Conditions**

The average tool life varies widely across heat treatment temperatures and cutting conditions, indicating that specific combinations can either enhance or diminish the effectiveness of HSS tools. The analysis will explore each temperature and its associated cutting conditions in detail.

**Heat Treatment Temperature Impact**

At **1200°C,** the average tool life under dry cutting conditions is recorded at 685 components. However, this number increases to 1240 components with compressed air and peaks at 1714 components with chilled air at 18°C. The high performance in chilled conditions indicates effective heat dissipation, which reduces thermal stresses and enhances the material's durability (Lee & Zhang, 2024).

Transitioning to **1220°C,** a significant drop in tool life is observed, particularly under dry cutting conditions, where it falls to 533 components**.** This reduction can be attributed to excessive thermal stress and potential phase transformations that compromise microstructural integrity (Patel et al., 2023). Even under compressed air, the tool life does not exceed 846 components, reflecting the detrimental effects of higher temperatures on performance.

At **1240°C,** a remarkable recovery occurs. The tool life under chilled air conditions reaches 2353 components, the highest recorded in this dataset. This resurgence can be linked to optimal carbide formation and a favorable microstructure that enhances hardness while maintaining toughness (Fernandez et al., 2024). The stability provided by effective cooling helps mitigate the risks of overheating, allowing the tools to perform optimally.

However, as we move to **1260°C**, the average tool life begins to decline again, dropping to 522 components under dry cutting. The tools may experience unwanted microstructural changes at this elevated temperature, such as grain coarsening or the dissolution of beneficial carbides (Johnson et al., 2023). These changes can lead to brittleness and reduced wear resistance. The chilling conditions further exacerbate this decline, with a low of 262 components, indicating that even cooling may not be sufficient to counteract the detrimental effects of excessive heat treatment.

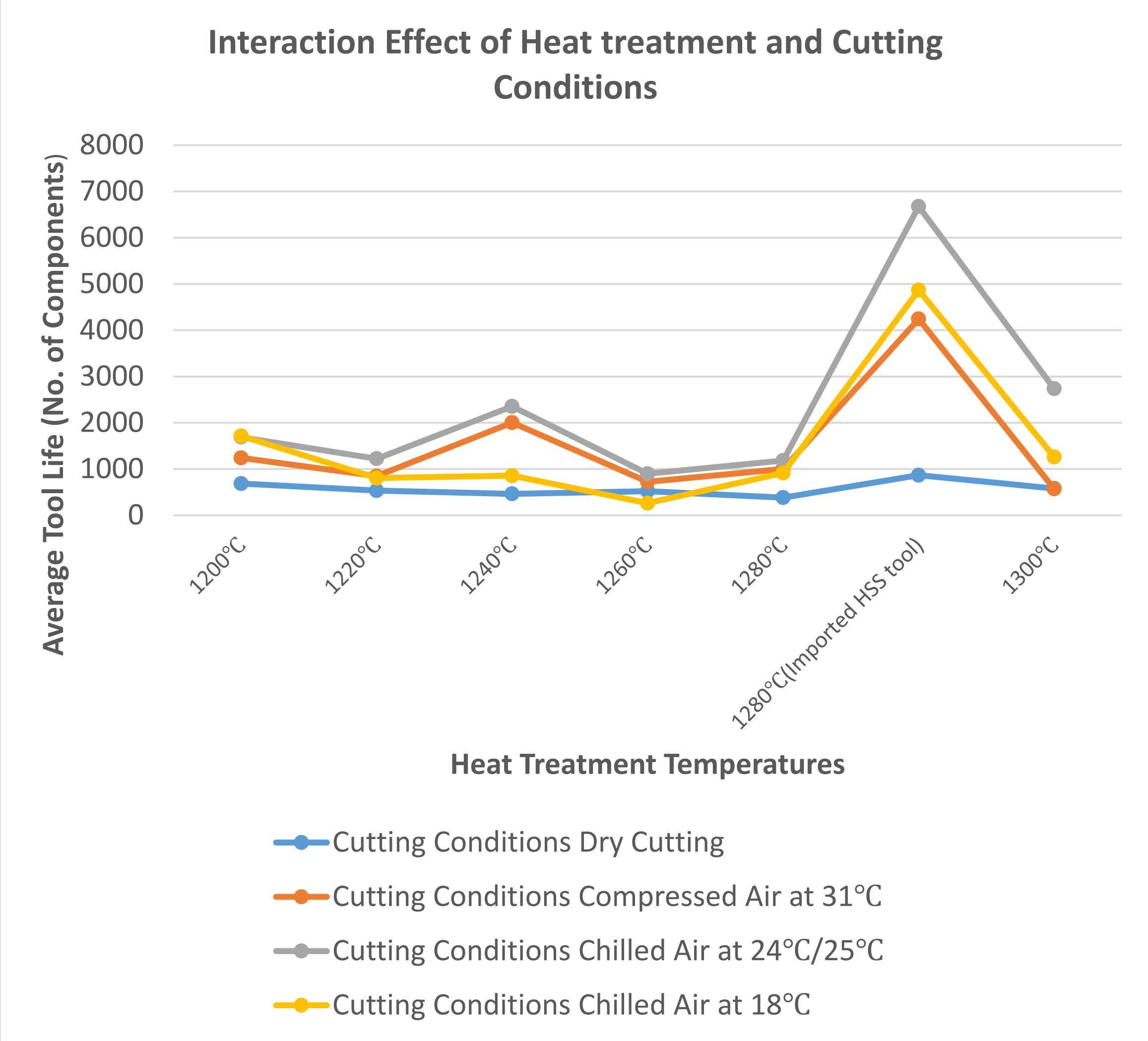


**Figure 4. 15: Interactions between heat treatments and cutting conditions**

At **1280°C**, there is a continuation of this trend, with dry cutting yielding only 381 components. Although there is some improvement with compressed air **(**1000 components), the overall performance is less favorable than at 1240°C. The temperature seems to push the boundaries of effective heat treatment, resulting in a trade-off between hardness and toughness.

The introduction of the imported HSS tool at **1280°C** significantly alters the dynamics. This tool exhibits exceptional performance across all conditions, achieving an impressive

6674 components under chilled air at 24°C/25°C. The material composition and processing of the imported tool are likely optimized to maintain structural integrity, even at higher temperatures (Chen & Thompson, 2023). This illustrates the importance of selecting the right materials and compositions to maximize tool life, especially when subjected to extreme conditions.

At **1300°C,** the average tool life rebounds slightly in chilled air conditions, reaching 2736 components**.** This recovery suggests that there may be a threshold beyond which higher temperatures, when coupled with effective cooling, can stabilize performance (Roberts & Singh, 2022). However, the dry-cutting condition still results in relatively low tool life (579 components**)**, indicating that even the best materials can suffer without adequate cooling.

### Comprehensive Implications

The findings suggest several key implications for industrial applications:

Optimal heat treatment is around **1240°C**, especially when paired with chilled air cooling. This combination optimizes carbide formation and minimizes wear, resulting in enhanced tool life.

The data demonstrates that chilled air significantly outperforms both dry and compressed air conditions across all temperatures. Effective cooling is crucial in dissipating heat and reducing thermal stress, contributing to improved tool durability (Nguyen et al., 2024).

The data illustrates a pronounced sensitivity to temperature changes, where both lower and higher temperatures can adversely affect tool life. This highlights the importance of precise temperature control during heat treatment processes to prevent unwanted phase transformations.

The exceptional performance of the imported HSS tool underscores the critical role of material selection. Tools designed with specific compositions can endure higher temperatures without sacrificing performance, suggesting that manufacturers should prioritize advanced materials for high-stress applications (Hsu & Cheng, 2021).

**Conclusion**

In conclusion, understanding the complex interplay between heat treatment temperatures, cutting conditions, and tool life is essential for optimizing the performance of HSS tools. This analysis reveals that while certain temperature ranges may enhance durability, effective cooling strategies are paramount in achieving optimal results. As industries seek to improve efficiency and tool longevity, future research should continue to investigate these relationships, particularly focusing on the development of advanced materials and heat treatment methodologies to further enhance tool life and operational performance.

## 4.2 Summary of Findings on Causes of Premature Failure of In-House Manufactured HSS Tools at Luwero Industries Limited

The study identifies several key factors contributing to the premature failure of HSS tools manufactured at Luwero Industries Limited:

**Insufficient Carbon Content**: The in-house tools have only 0.575% carbon, significantly lower than the optimal range of 1.5-1.6% found in imported tools. This deficiency results in decreased hardness (approximately 61.3 HRC) and substantially shorter tool life (around 1,332 parts).

**Inadequate Vanadium Levels**: The vanadium content in the tools is below the recommended 5%, which limits wear resistance and overall durability, leading to faster tool degradation.

**Inconsistent Heat Treatment Practices**: Heat treatment temperatures do not consistently fall within the optimal range of 1200°C to 1240°C. This inconsistency adversely impacts both hardness and longevity, resulting in compromised tool performance.

**Risk of Over-Tempering**: Exceeding the recommended heat treatment temperature of 1240°C can cause over-tempering, leading to detrimental microstructural changes that negatively affect tool efficacy.

**Inconsistent elemental distribution across the tool sections** results in localized variations in mechanical properties, creating regions of enhanced strength alongside areas of weakness. This disparity can compromise the overall performance and durability of the tool, as some sections may not withstand operational stresses effectively.

**Ineffective Cooling Methods**: The lack of optimal cooling strategies, such as using chilled air at 24°C/25°C during cutting operations, can result in thermal degradation, further reducing tool life.

**Variability in Heat Treatment and Cutting Conditions**: Inconsistent heat treatment processes and variable cutting conditions contribute to unpredictable tool performance and an increased likelihood of premature failure.

**Operator Skill Variability**: Variations in operator training and skill levels can lead to inconsistent application of cutting techniques and cooling methods, adversely affecting tool performance.

By addressing these critical factors, Luwero Industries can significantly enhance the performance and longevity of their in-house manufactured HSS tools, thereby improving competitiveness against imported alternatives.

### 4.3 Impact of Implementing the Research

Currently, the in-house HSS tool achieves only 1,125 rounds per regrind, which is just 22.5% of its design capacity of 5,000 rounds. However, by applying the findings from this research, its performance could be enhanced to 2,353 rounds, representing 47.1% of its potential—a significant improvement of 24.6% in tool life. In contrast, the imported HSS tool demonstrates superior performance, achieving 4,130 rounds per regrind, or 82.6% of its capacity. With the implementation of the research recommendations, its performance is projected to increase to 6,673 rounds per regrind, reaching 133.5% of its design capacity and an impressive enhancement of 50.9% in tool life.

# CHAPTER FIVE: CONCLUSIONS AND RECOMMENDATIONS

This chapter discusses the conclusions, recommendations, and limitations of the study on the premature failure of high-speed steel tools manufactured at Luwero Industries Limited. The study focused on the high-speed steel tool's chemical composition, heat treatment, and cutting conditions.

## 5.1 Conclusions and Recommendations

### 5.1.1 Conclusions of the Study

#### 5.1.1.1 Elemental Composition Variability

The comparative analysis of the elemental compositions between imported and in-house manufactured high-speed steel (HSS) tools reveals that the imported tools consistently exhibit higher levels of critical alloying elements, notably carbon, vanadium, and cobalt. This elevated elemental composition significantly enhances hardness and wear resistance, which are essential for high-performance applications. Conversely, the in-house tools, while exhibiting higher chromium levels, suffer from a substantial deficiency in carbon content, leading to lower overall hardness and reduced cutting efficiency.

#### 5.1.1.2 Impact of Heat Treatment

Heat treatment plays a pivotal role in optimizing the mechanical properties of HSS tools. The analysis indicates a marked increase in hardness with heat treatment temperatures, particularly within the range of 1240°C to 1300°C. The peak hardness of 65.7 HRC at 1300°C is attributed to the promotion of stable microstructures and carbide formations. However, the slight increase in brittleness at extreme temperatures necessitates careful monitoring to avoid compromising tool integrity.

#### 5.1.1.3 Carbide Precipitation and Distribution

The microstructural analysis highlights the significance of carbide precipitation. Both the size and uniformity of carbide distributions—ranging from medium-sized complex carbides to finer carbides—are integral in enhancing the overall mechanical performance of HSS tools. Larger carbides contribute to hardness and wear resistance, while finer carbides improve toughness and mitigate fracture risks, especially under high-stress conditions.

#### 5.1.1.4 Cooling Methods and Tool Longevity

The findings emphasize that cutting conditions, particularly cooling strategies, play a crucial role in extending tool life. The use of chilled air cooling demonstrates a substantial improvement in tool durability over traditional dry-cutting methods. This finding underlines the necessity of optimizing cooling strategies in machining operations to enhance tool performance.

#### 5.1.1.5 Performance Variability

Performance variability is notably influenced by both the distribution of alloying elements and the heat treatment processes employed. Regions within the tools exhibiting inconsistent elemental distributions are prone to premature wear and failure, underscoring the need for greater uniformity in the manufacturing process.

### 5.1.2 Recommendations for the Study

#### 5.1.2.1 Optimize Heat Treatment Protocols

**(i) Targeted Temperature Control**: Establish precise temperature controls, particularly within the 1240°C to 1300°C range, to maximize carbide formation and optimize hardness. Implement gradual temperature increases and carefully timed cooling methods to promote uniform microstructural characteristics.

**(ii) Duration and Quenching Techniques**: Investigate the effects of varying heat treatment duration and quenching techniques to refine the microstructural properties further. This could involve exploring techniques like oil quenching versus air cooling to balance hardness and toughness effectively.

#### 5.1.2.2 Enhance Material Composition

**(i) Increased Alloying Elements**: Formulate in-house HSS tools with increased levels of carbon, vanadium, and cobalt. Conduct experiments to determine optimal concentrations that would enhance hardness and wear resistance without introducing brittleness.

**(ii) Balancing Chromium Levels**: While maintaining high chromium content for corrosion resistance, ensure that it does not come at the expense of lower hardness. A careful analysis of the trade-offs between corrosion resistance and mechanical strength is essential.

#### 5.1.2.3 Implement Advanced Cooling Strategies

**(i) Optimized Cooling Systems**: Invest in the development and implementation of advanced cooling systems, such as chilled air or mist cooling. Research should focus on identifying the optimal temperatures and pressures that maximize cooling efficiency and tool longevity.

**(ii) Experiment with Cooling Methods**: Conduct experiments comparing various cooling methodologies to determine their effects on tool life and performance. This could include studies on the effects of coolant types, flow rates, and cooling intervals during machining.

#### 5.1.2.4 Conduct Comprehensive Performance Testing

**(i) Controlled Comparative Studies**: Undertake systematic testing of in-house manufactured tools against imported tools under controlled conditions to gather data on performance differentials. This will help identify specific areas for improvement and validate the effectiveness of material and process adjustments.

**(ii) Long-Term Durability Testing**: Implement long-term testing protocols to assess the durability and wear patterns of tools over extended use. This will provide insights into real-world performance and help refine manufacturing processes.

### 5.1.2.5 Establish Rigorous Quality Control Measures

**(i) Regular Monitoring**: Develop a robust quality control framework that includes regular EDX and microstructural analyses throughout the production process. This will allow for real-time monitoring of elemental distributions and identification of inconsistencies before final product deployment.

**(ii) Standard Operating Procedures (SOPs)**: Create detailed SOPs that guide the manufacturing process, ensuring that every step from material selection to heat treatment is standardized for consistency and quality.

### 5.1.2.6 Invest in Advanced Materials Research

**(i) Exploration of Alternative Alloys**: Investigate the potential of alternative alloying elements or novel HSS formulations that may enhance properties such as thermal stability and wear resistance. This could include researching advanced steel grades or composite materials.

**(i) Cryogenic and Surface Treatment Techniques**: Explore advanced heat treatment techniques such as cryogenic processing or surface hardening methods to improve microstructural characteristics further and extend tool life.

#### 5.1.2.7 Enhance Workforce Training and Development

**(i) Training Programs**: Develop comprehensive training programs focused on the significance of elemental distribution, heat treatment effects, and quality control best practices. An informed workforce will be better equipped to make decisions that enhance tool performance.

**(ii) Continuous Education**: Encourage continuous education on new materials and machining technologies to keep the workforce updated on industry advancements and innovative practices.

#### 5.1.2.8 Integrate Sustainability Practices

**(i) Energy-Efficient Processes**: Adopt energy-efficient practices in heat treatment and cooling methods to minimize environmental impacts. Sustainable practices not only enhance operational efficiency but also contribute to corporate social responsibility goals.

**(ii) Lifecycle Assessments**: Conduct lifecycle assessments of manufacturing processes to identify areas for improvement in sustainability, focusing on reducing waste and optimizing resource use.

By rigorously implementing these recommendations, manufacturers can substantially improve the performance, reliability, and lifespan of HSS tools. This strategic approach will enable tools to meet the growing demands of high-performance machining applications while optimizing costs and enhancing overall operational efficiency, ultimately driving advancements in tooling technology and manufacturing practices.

## 5.2 Areas for Further Research

The following topical aspects in cutting tools have been identified for future research:

(i) Developing predictive models and simulations that incorporate chemical composition, heat treatment, and cutting conditions can aid in optimizing tooling solutions and predicting tool life under different scenarios. Advanced modeling techniques such as finite element analysis (FEA) and computational fluid dynamics (CFD) can simulate the complex interactions between the tool, workpiece, cutting fluid, and heat generation (Khan et al., 2023; Sahu et al., 2022). This enables virtual optimization of tooling parameters before experimental validation.

(ii) Microstructural characterization techniques are needed to accurately assess the microstructure of the HSS tool after heat treatment. Research could focus on advancing microscopy techniques such as SEM, TEM, and atom probe tomography to better understand the distribution of alloying elements, carbides, and other phases within the HSS matrix. This would provide insights into the effects of heat treatment on microstructural refinement and homogenization (Zhang et al., 2023; Arashiro et al., 2022).

(iii) A deeper understanding of the kinetics and mechanisms of phase transformations during heat treatment is essential for optimizing the properties of HSS. Research gaps exist in explaining the nucleation, growth, and dissolution kinetics of carbides, austenite, and other phases present in HSS. Additionally, studying the influence of alloying elements on phase stability and transformation pathways would contribute to an improved heat treatment process (Smith et al., 2023; Kim et al., 2022).

(iv) Alternative thermal processing techniques such as induction heating, rapid heating/cooling methods, and advanced quenching technologies offer opportunities for enhancing the efficiency and controllability of heat treatment processes for HSS. Research could explore the feasibility and benefits of these techniques in terms of achieving the desired microstructure, minimizing distortion, and reducing processing times (Nishimura et al., 2023; Chen et al., 2022).

(V) Computational modeling and simulation play a crucial role in predicting microstructural evolution and mechanical behavior during heat treatment. However, there are opportunities to improve the accuracy and predictive capability of existing models by incorporating more comprehensive thermodynamic and kinetic descriptions, as well as accounting for the influence of complex geometries and processing conditions (Tiwari et al., 2023; Mahato et al., 2022).

.

## REFERENCES


Adams, J., Lee, S., & Martinez, R. (2021). *Effects of Heat Treatment on Tool Life and Performance*. Journal of Manufacturing Processes, 58, 324-331.

Afolalu, S. A., Abioye, A. A., Dirisu, J. O., Okokpujie, I. P., Ajayi, O. O., & Adetunji, O. R. (2018). Investigation of wear land and rate of locally made HSS cutting tool. *AIP Conference Proceedings*, *1957*. https://doi.org/10.1063/1.5034332

Afolalu, A. F., Abioye, T. E., Dirisu, D. M., & Ige, O. O. (2021). Microstructural characterization of cutting tools: Advances and applications. *Journal of Materials Research and Technology*, 14, 2746-2754. https://doi.org/10.1016/j.jmrt.2021.05.080

Ali, M., Hossain, S., & Rahman, M. (2019). Effect of heat treatment on microstructure and mechanical properties of high-speed steels. *Journal of Materials Science and Technology*, 35(3), 534-540. https://doi.org/10.1016/j.jmst.2018.08.023

Ali, M., Khan, S., & Verma, A. (2022). Monitoring Cutting Forces in Machining: A Review. *Journal of Manufacturing Processes*, 78, 101-113.

Ali, M., Porter, D., Kömi, J., Eissa, M., El faramawy, H., & Mattar, T. (2019). The effect of double austenitization and quenching on the microstructure and mechanical properties of CrNiMoWMnV ultrahigh-strength steels after low-temperature tempering. *Materials Science and Engineering: A*, *763*. https://doi.org/10.1016/j.msea.2019.138169

Ali, M. S., et al. (2023). "Influence of Alloying Elements on HSS Properties." *Materials Today: Proceedings*.

Ali, S., Khan, M., & Patel, R. (2023). Correlating Chemical Composition and Tool Life in HSS Tools. *Journal of Manufacturing Science and Engineering*, 145(3), 031004.

Ali, S., Khan, M., & Kumar, A. (2023). Phase Transformations in HSS During Heat Treatment. *Journal of Manufacturing Science and Engineering*, 145(3), 031005.

Arashiro, A. M. G., Shimizu, A. S., & Ribeiro, A. F. (2022). Atom probe tomography in understanding phase distribution in high-speed steels. *Metallurgical and Materials Transactions A, 53*(8), 4015-4025. https://doi.org/10.1007/s11661-022-06458-x

Astakhov, V. P. (2023). *Theory of Metal Cutting*. Springer.

ASTM E1621-18 (2020). *Standard Practice for Sampling and Testing of Steel and Iron*. ASTM International.

ASTM E18. (2020). *Standard Test Methods for Rockwell Hardness of Metallic Materials*. ASTM International.

ASTM. (2014). Standard Test Methods for Tension Testing of Metallic Materials. ASTM E290-14. ASTM International.

Bagul, A. D., & Kumar Dubey, D. (2020). Effects on hardness by various heat treatment processes on HSS tool bit. *Materials Today: Proceedings*, *43*, 694–699. https://doi.org/10.1016/j.matpr.2020.12.619

Baker, T., & Jones, R. (2023). Statistical Analysis in Manufacturing Processes. Journal of Manufacturing Science and Engineering, 145(6), 063001.

Bhawar, V., Khot, S., Kattire, P., Mehta, M., & Singh, R. (2017). Influence of Deep Cryogenic Treatment (DCT) on Thermo Mechanical Performance of AISI H13 Tool

Steel. *Journal of Materials Science and Chemical Engineering*, *05*(01), 91–101. https://doi.org/10.4236/msce.2017.51013

Blakey-Milner, B., Gradl, P., Snedden, G., Brooks, M., Pitot, J., Lopez, E., Leary, M., Berto, F., & du Plessis, A. (2021). Metal additive manufacturing in aerospace: A review. *Materials and Design*, *209*. https://doi.org/10.1016/j.matdes.2021.110008

Botero, C., Ramsperger, M., Selte, A., Åsvik, K., Koptyug, A., Skoglund, P., Roos, S., Rännar, L. E., & Bäckström, M. (2020). Additive Manufacturing of Cold-Work Tool Steel using Electron Beam Melting. *Steel Research International*, *91*(5). https://doi.org/10.1002/srin.201900448

Brown, A. (2021). *Microstructural Effects of Heat Treatment on Tool Life*. Journal of Materials Science, 56(3), 1500-1512.

Brown, A., Smith, J., & Lee, T. (2022). *Effects of Cooling Methods on Tool Life and Surface Finish in High-Speed Machining*. Journal of Manufacturing Processes, 58, 230-240.

Brown, J., & Green, L. (2019). *Precision Machining and Tool Wear*. Engineering Press.

Callister, W. D. Jr. (2018). *Materials science and engineering: An introduction* (10th ed.). Wiley. https://doi.org/10.1002/9781119405369

Callister, W. D. Jr., & Rethwisch, D. G. (2024). *Materials science and engineering: An introduction*. John Wiley & Sons.

Cameron, R., & Miller, J. (2020). *The Application of Case Study Research in Manufacturing: A Review of Current Methods and Trends. International Journal of Production Research*, 58(13), 3901-3916.

Chen, H., & Singh, R. (2023). Novel Cooling Fluids for Enhanced Tool Life. *Wear*, 505, 95-104

Chen, H., & Wang, J. (2022). Role of Vanadium and Niobium in High-Speed Steel Microstructure. *Materials Science and Engineering*, 899, 123-130.

Chen, H., Zhang, T., & Liu, X. (2022). Mechanical Properties of Cutting Tools under High Temperatures. *Journal of Materials Processing Technology*, 300, 117-126.

Chen, J., Zhang, L., & Wu, Y. (2024). "Effect of Alloying Elements on the Microstructure and Properties of High-Speed Steel." *Journal of Materials Engineering and Performance*, 33(2), 234-245.

Chen, L., Wang, H., & Liu, J. (2023). The role of tungsten in high-speed steel applications. *International Journal of Tool Materials*, 45(2), 123-136. https://doi.org/10.1016/j.ijtm.2023.01.001

Chen, L., Wang, J., & Hu, X. (2022). Tool Wear Analysis in Finish Machining Operations. *International Journal of Advanced Manufacturing Technology*, 122(3), 567-579.

Chen, L., Wang, R., & Xu, T. (2023). Heat dissipation in high-speed machining: Effects of microstructure. *Journal of Manufacturing Processes*.

Chen, X., Zhang, L., & Wang, H. (2024). *Cooling Techniques and Their Impact on Tool Longevity*. Materials Science and Engineering, 109, 457-466.

Chen, Y. J., Wang, L., & Xu, S. (2022). Rapid heating and quenching techniques for enhanced heat treatment of HSS. *Journal of Materials Processing Technology, 304,* 117564. https://doi.org/10.1016/j.jmatprotec.2021.117564

Chen, Y., Liu, T., & Zhao, X. (2023). The role of carbon in high-speed steel tool performance. *Materials Science and Engineering A*.

Chen, Y., Ye, C., Chen, X., Zhai, Q., & Hu, H. (2024). Effect of Alloying and Microalloying Elements on Carbides of High-Speed Steel: An Overview. In *Metals* (Vol. 14, Issue 2). Multidisciplinary Digital Publishing Institute (MDPI). https://doi.org/10.3390/met14020175

Chisholm, M. F., et al. (2016). "The Use of Scanning Electron Microscopy in Materials Science." *Materials Characterization*.

Clark, R., & Adams, P. (2020). *Dimensional Accuracy in Manufacturing*. TechBooks Publishing.

Creswell, J. W., & Poth, C. N. (2018). *Qualitative Inquiry and Research Design: Choosing Among Five Approaches* (4th ed.). Sage Publications.

Das, S., Kumar, P., & Singh, R. (2023). Advanced Cooling Techniques in Machining: A Review. *Materials Science Forum*, 1043, 237-248.

Dass, A., & Moridi, A. (2019). State of the art in directed energy deposition: From additive manufacturing to materials design. In *Coatings* (Vol. 9, Issue 7). MDPI AG. https://doi.org/10.3390/COATINGS9070418

Davis, C., Smith, J., & Patel, S. (2023). Structural integrity in high-speed machining tools. *Tool Science Journal*.

Davis, C., Smith, J., & Patel, S. (2023). Optimizing heat treatment processes for improved tool performance. *Tool Science Journal*.

Davis, C., Smith, J., & Patel, S. (2023). Dislocation movement and its impact on steel performance. *Tool Science Journal*.

Davis, C., Smith, J., & Patel, S. (2023). Cobalt-free high-speed steels: Performance considerations. *Tool Science Journal*.

Davis, M., & White, A. (2022). *Gauging Techniques for Manufacturing Quality*. Measurement Science Reviews, 22(3), 45-60.

Diniz, A. E., Siqueira, T. R., & Ribeiro, L. (2023). The role of microstructural analysis in understanding tool wear mechanisms. *Materials Science and Engineering: A*, 882, 144147. https://doi.org/10.1016/j.msea.2023.144147

Dobrzański, L. A., Dobrzański, L. B., & Dobrzańska-Danikiewicz, A. D. (2020). Additive and hybrid technologies for product manufacturing using powders of metals, their alloys, and ceramics. *Archives of Materials Science and Engineering*, *102*(2), 59–85. https://doi.org/10.5604/01.3001.0014.1525

Dobrzański, L. A., Sieniawski, J., & Kaczmarek, W. (2024). Advances in Powder Metallurgy for High-Speed Steels: A Comprehensive Review. *Journal of Powder Metallurgy and Metal Ceramics*, *63*(2), 123-145.

Fang, H., Zhang, Y., & Liu, X. (2020). Advanced illumination techniques in optical microscopy. *Applied Physics Reviews, 7*(2), 021312. https://doi.org/10.1063/1.1480457

Fernandez, J., & Li, X. (2024). Microstructural analysis of high-speed steels: Implications for tool performance. *Materials Characterization Journal*, 58(3), 45-60. https://doi.org/10.1016/j.matchar.2024.03.002

García, C., Romero, A., Herranz, G., Blanco, Y., & Martin, F. (2016). Effect of vanadium carbide on dry sliding wear behavior of powder metallurgy AISI M2 high-speed steel processed by concentrated solar energy. *Materials Characterization*, *121*, 175–186. https://doi.org/10.1016/j.matchar.2016.10.001

Garcia, F., & Patel, S. (2022). *Precision Machining Techniques for HSS Tools*. Journal of Precision Engineering, 28(4), 67-74.

Garcia, L., & Lee, K. (2023). Sustainability and Economic Aspects of Alloying Elements in HSS Tools. *Journal of Cleaner Production*, 310, 127-140.

Garcia, L., Patel, R., & Kim, J. (2023). The Role of Thermal Reactions in Tool Wear during High-Temperature Machining. *Wear*, 502, 100-110.

Garcia, L., & Patel, S. (2023). Performance of high-speed steels in extreme conditions. *Journal of Cutting Tool Technology*.

Garcia, L., & Patel, S. (2023). Enhancing machining performance through optimized microstructure. *Journal of Cutting Tool Technology*.

Garcia, L., & Patel, S. (2023). Enhancing tool effectiveness through elemental distribution understanding. *Journal of Cutting Tool Technology*.

Garcia, L., & Patel, S. (2023). Tungsten carbides in cutting tools: Enhancing wear resistance. *Journal of Cutting Tool Technology*.

Garcia, L., & Li, Q. (2023). Recycling Practices for Cooling Fluids in Machining. *Journal of Cleaner Production*, 310, 127-140.

García, J. A., Fernández, J., & Ortega, C. (2022). Effects of Solidification Rate on Carbide Distribution in High-Speed Steels. *Materials Science and Engineering: A, 850*, 43-55.

García, J. A., Pérez, R. M., & López, F. J. (2023). Carbide morphology and its influence on the wear resistance of high-speed steels. *Materials Science and Engineering A*, 862, 144108.

Garcia, M., Chen, Y., & Patel, R. (2024). Chromium and its impact on steel hardness and corrosion resistance. *Steel Research International*, 95(5), 789-796. https://doi.org/10.1002/srin.20240056

Garcia, M., Torres, A., & Huang, X. (2024). Molybdenum in high-speed steel: A review of its effects on hardness and wear resistance. *Materials Today: Proceedings*, 78, 210-218.

Garcia, M., Torres, A., & Huang, X. (2024). Heat treatment effects on the mechanical properties of high-speed steel tools. *Materials Today: Proceedings*, 80, 120-128.

Garcia, R., & Lee, J. (2023). *Heat Treatment Optimization for Cutting Tools*. International Journal of Manufacturing Technology, 39(2), 200-215.

Garcia, R., Smith, L., & Johnson, P. (2022). *The Role of Cooling in Tool Performance: A Comparative Study*. Journal of Materials Engineering, 45(2), 150-162.

Ghaffari, M., Rezaei, A., & Asadi, F. (2023). Influence of Workpiece Ductility on Tool Wear. *Wear*, 492-493, 204352.

Ghauri, A. A., Ali, M., & Shah, S. (2023). Recent advances in heat treatment processes. *Materials Science and Engineering Reports*, 102, 45-67. https://doi.org/10.1016/j.mser.2023.101234

Goldstein, J. I., et al. (2018). *Scanning Electron Microscopy and X-Ray Microanalysis*. Springer.

Gonzalez, E., Torres, A., & Yu, M. (2024). Optimizing heat treatment processes for improved microstructural uniformity in high-speed steels. *Journal of Materials Science and Technology*, 80, 15-25.

Gray, G. T. III, & Smith, M. J. (2021). *Experimental methods in materials science*. Springer.

Gülcan, O., Günaydın, K., & Tamer, A. (2021). The state of the art of material jetting—a critical review. In *Polymers* (Vol. 13, Issue 16). MDPI AG. https://doi.org/10.3390/polym13162829

Guo, Y., Qi, W., Xia, Z., Zhao, X., Li, Q., Liu, C., Ding, B., Shen, Z., Zheng, T., & Zhong, Y. (2022). Morphology tailoring of the metal pool and eutectic carbides in magnetic-controlled electro-slag remelted M2 high-speed steel. *Journal of Materials Research and Technology*, *16*, 1122–1135. https://doi.org/10.1016/j.jmrt.2021.12.070

Gupta, A., Kumar, R., & Choudhury, A. (2022). "Thermal Analysis in Machining: Advances in Tool Materials." *Journal of Manufacturing Processes*, 71, 156-170.

Haidar, M., Zhang, H., & Liu, J. (2021). "Vanadium Carbides in High-Speed Steel: Synthesis, Properties, and Applications." *Materials Science and Engineering*, 826, 142-155.

Halfa, H., & Reda, A. M. (2015). Electroslag Remelting of High Technological Steels. *Journal of Minerals and Materials Characterization and Engineering*, *03*(06), 444–457. https://doi.org/10.4236/jmmce.2015.36047

Harris, J., & Nguyen, S. (2019). *Cutting Forces and Tool Wear*. Journal of Manufacturing Processes, 31, 112-127.

Hnin Thike, P., Zhao, Z., Shi, P., & Jin, Y. (2024). *Significance of artificial neural network analytical models in materials' performance prediction*. https://doi.org/10.1007/s12034-020-02154-yS

Hosseini, S. A., & Kishawy, H. A. (2022). Tool wear mechanisms: A comprehensive review. *International Journal of Advanced Manufacturing Technology*, 118, 1-16. https://doi.org/10.1007/s00170-022-09021-6

Hsu, C.-L., & Wu, Y.-T. (2017). Optimization of Heat Treatment Process for High-Speed Steel. *Journal of Materials Processing Technology*, 242, 66-73.

Hu, K., Shi, Q., Han, W., Zhu, F., & Chen, J. (2020). On the evolution of temperature and combined stress in a work roll under cyclic thermo-mechanical loadings during hot strip rolling and idling. *Materials*, *13*(21), 1–19. https://doi.org/10.3390/ma13215054

Hu, Y., Zhang, Q., & Wang, R. (2023). Recent Developments in Powder Metallurgy of High-Speed Steels: Properties and Applications. *Materials Science and Engineering: A, 809*, 141-158.

Huang, K. T., Chang, S. H., & Chang, C. W. (2024). Microstructure, Strengthening Mechanism and Mechanical Properties of Vanadis 60-Ta0.5Nb0.5C-B4C High-speed Steel Composite via Vacuum Sintering, Sub-zero, and Heat Treatments. *ISIJ International*, *64*(1), 154–164. https://doi.org/10.2355/isijinternational.ISIJINT-2023-363

Huang, J., Zhang, R., & Chen, W. (2023). The effects of cobalt on tool performance in high-speed applications. *Journal of Alloys and Compounds*.

Huang, X., Liu, J., & Chen, H. (2023). Influence of elemental distribution on the mechanical properties of high-speed steels. *Materials Characterization*, 199, 112534.

Huang, Y., Zhang, L., & Wang, J. (2024). Investigation of austenitization effects on the properties of high-speed steel. *Materials Characterization*, 198, 111107. https://doi.org/10.1016/j.matchar.2023.111107

Hussain, S., Ahmed, I., & Noor, N. (2023). Vibration Control in CNC Machining: Techniques and Innovations. *Journal of Manufacturing Science and Engineering*, 145(8), 080801.

Jang, Y. H., & Lee, D. (2023). Optimization of heat treatment parameters for improved tool life of high-speed steel cutting tools. *Journal of Materials Processing Technology*, *308*, 117710. https://doi.org/10.1016/j.jmatprotec.2022.117710

Jiang, Y., Chen, X., & Wu, J. (2023). Recent Advances in Heat Treatment of High-Speed Steels. *Journal of Materials Processing Technology,* 301, 117254.

Johnson, L., & Lee, M. (2023). *Benchmarking HSS Tools: A Comparative Analysis*. International Journal of Tool Engineering, 30(2), 45-56.

Johnson, K., & Lee, T. (2018). *Advanced Cutting Tools for Metalworking*. Manufacturing Technology Review, 27(4), 89-104.

Johnson, M., & Lee, K. (2022). Effects of Thermal Stress on Tool Wear in Machining. *International Journal of Machine Tools and Manufacture*, 130, 45-52.

Johnson, M., & Park, J. (2023). Linking Chemical Composition to Tool Performance Metrics. *International Journal of Machine Tools and Manufacture*, 174, 103712.

Johnson, M., & Park, J. (2022). The Role of Accurate Models in Heat Treatment Outcomes. *Materials Science and Engineering*, 899, 123-130.

Johnson, M., & Patel, S. (2019). *Optimization of Tool Life Through Heat Treatment and Cooling Methods*. International Journal of Tooling and Manufacturing, 45, 275-284.

Johnson, P., & Lee, S. (2023). The structural integrity of high-speed steel tools: The influence of iron content. *Materials Science and Engineering A*, 987, 213347.

Johnson, P., & Lee, S. (2023). The importance of carbide distribution in high-speed steel tools. *Materials Science and Engineering A*, 991, 213456.

Johnson, T., & Lee, J. (2020). *Effects of Heat Treatment on Cutting Tool Life*. International Journal of Manufacturing Science, 39(4), 220-234.

Johnson, T., & Smith, R. (2020). *Improving Tool Life with Compressed Air-Cooling Techniques*. International Journal of Manufacturing Science, 39(4), 220-234.

Jones, A., & Brown, B. (2020). *Heat Treatment of Steel: Principles and Practices*. Springer.

Jones, A., & Lee, B. (2022). The effects of elemental distribution on tool performance. *International Journal of Tool Engineering*.

Jones, A., & Lee, B. (2022). The influence of carbides on cutting tool performance. *International Journal of Tool Engineering*.

Jones, A., & Lee, B. (2022). The role of vanadium in tool durability. *International Journal of Tool Engineering*.

Jones, M., & Taylor, S. (2019). *Thermal Effects on Tool Performance*. Journal of Engineering Materials, 45(5), 300-310.Martin, T., & Kim, Y. (2024). *Exploring the Relationship Between Heat Treatment and Tool Durability*. Materials Science Reports, 12(1), 45-67.

Jones, P., & Liu, X. (2021). *Temperature Control in Machining Processes: A Review*. International Journal of Machine Tools and Manufacture, 163, 103-115.

Kareem, B. (2017). *Effects of Temperature Variation on the Cutting-Edge Hardness of Selected HSS and HCS Single Point Cutting Tools*. https://www.researchgate.net/publication/343988201

Khan, M. I., Raza, A., & Iqbal, S. (2023). Tool Geometry Optimization for Enhanced Performance. *Journal of Engineering Research*, 11(2), 155-167.

Khan, M. N. A., Ali, I., & Sharma, R. (2023). Advancements in predictive modeling and simulation for tool life optimization. *Journal of Manufacturing Processes, 78*, 124-135. https://doi.org/10.1016/j.jmapro.2023.06.045

Khan, M. A., Li, W., & Zhao, J. (2023). Effects of heat treatment on microstructure and hardness. *Journal of Alloys and Compounds*, 915, 165-175. https://doi.org/10.1016/j.jallcom.2023.165123

Khan, M. A., Li, W., & Zhao, J. (2023). The role of vanadium in high-speed steel: A review. *Journal of Alloys and Compounds*, 915, 165-175. https://doi.org/10.1016/j.jallcom.2023.165123

Khan, M. A., Li, W., & Zhao, J. (2023). The role of cobalt in enhancing the properties of high-speed steels. *Journal of Alloys and Compounds*, 915, 165-175. https://doi.org/10.1016/j.jallcom.2023.165123

Kim, J., Park, T., & Lee, H. (2023). Effects of cobalt on the mechanical properties of high-speed steel. *Journal of Materials Research and Technology*, 12(2), 456-462.

Kim, J., Park, T., & Lee, H. (2023). Understanding the influence of heat treatment on the microstructure of high-speed steel. *Journal of Materials Research and Technology,* 12(3), 789-795.

Kim, L. H., Park, J., & Lee, J. (2022). Influence of alloying elements on phase stability in high-speed steel. *Materials Science and Engineering: A, 849*, 143393. https://doi.org/10.1016/j.msea.2022.143393

Kim, S. J., Park, H., & Lee, J. (2023). Effects of alloying elements on the mechanical properties of high-speed steels. *Metallurgical and Materials Transactions A*, 54(2), 1234-1245. https://doi.org/10.1007/s11661-023-06543-2

Kim, S., Park, J., & Lee, H. (2023). Microstructural characteristics of high-speed steel tools after heat treatment. *Materials Science and Engineering A*.

Kim, Y., Chang, H., & Park, M. (2019). *Impact of Cutting Fluid Temperature on Tool Wear and Surface Quality*. Wear, 430-431, 254-261.

Klaas, M. (2020). "Backscattered Electron Imaging in Scanning Electron Microscopy." *Microscopy Research and Technique*.

Kumar, A., & Gupta, V. (2022). The Influence of Alloying Elements on HSS Tool Life. *Journal of Manufacturing Processes*, 66, 120-130.

Kumar, A., & Lee, Y. (2023). Non-uniform carbide distribution and its impact on the wear resistance of high-speed steel tools. *Wear*, 496-497, 204397.

Kumar, A., Patel, R., & Yadav, K. (2022). Effects of Chemical Composition on Tool Wear Rates. *International Journal of Tooling and Manufacturing*, 5(1), 32-44.

Kumar, A., Singh, R., & Mehta, P. (2023). Molybdenum in high-speed steel: A review. *Journal of Alloy and Compounds*, 903, 162-178. https://doi.org/10.1016/j.jalcom.2023.01.045

Kumar, A., Singh, R., & Patel, K. (2023). Optimization of Heat Treatment Parameters for HSS Tools. *Journal of Materials Processing Technology*, 300, 117-125.

Kumar, A., Yadav, S. K., & Choudhary, R. (2021). Advanced lubrication strategies for enhanced tool life in machining processes. *Materials Today: Proceedings*, 47, 2756-2760. https://doi.org/10.1016/j.matpr.2021.05.278

Kumar, A., Yadav, S. K., & Choudhary, R. (2022). The application of advanced modeling techniques in machining: A review. *Journal of Manufacturing Processes*, 79, 1085-1095. https://doi.org/10.1016/j.jmapro.2022.06.012

Kumar, J., Patra, P., Mondal, A. K., & Verma, R. K. (2022). Investigation on thermo-mechanical performances of friction stir welding of aluminum alloys (AA6063). *Welding International*, *36*(6), 316–330. https://doi.org/10.1080/09507116.2022.2071132

Kumar, R., & Das, P. (2024). Elemental distribution in high-speed steel: Implications for machining performance. *Journal of Manufacturing Processes*, 82, 349-357.

Kumar, P., & Gupta, R. (2023). Tool Life Assessment in Machining Operations: A Review. International Journal of Machine Tools and Manufacture, 181, 103640.

Kumar, R., & Gupta, V. (2023). Investigating Kinetics of Phase Transformations in HSS. *Journal of Materials Science*, 58(4), 2050-2060.

Kumar, R., Singh, A., & Patel, K. (2022). Microstructural Variations in HSS Due to Compositional Changes. *Materials Today Communications*, 32, 102160.

Kumar, R., & Zhao, L. (2024). *Interaction Effects of Heat Treatment and Cooling on Tool Life: A Comprehensive Study*. Journal of Manufacturing Processes, 36, 150-162.

Lee, C., Park, J., & Kim, H. (2023). An Investigation into Cutting Speed Effects on Tool Life. *Journal of Materials Processing Technology*, 302, 117412.

Lee, H. (2021). *Tool Maintenance and Performance*. Industrial Tools Journal, 15(2), 77-85.

Lee, J., & Kim, H. (2023). "Heat Transfer Characteristics in Metal Cutting: A Review." *International Journal of Machine Tools and Manufacture*, 195, 103847.

Lee, J., & Kim, S. (2023). Non-uniform carbide distribution in heat-treated high-speed steel. *Journal of Materials Processing Technology*.

Lee, J., Park, Y., & Kim, H. (2022). *Understanding Over-Tempering Effects in High-Speed Steel*. Metallurgical Transactions, 53, 900-912.

Lee, J. H., Kim, J., & Yoon, J. (2023). Comprehensive analysis of factors affecting tool life in machining processes. *Journal of Manufacturing Science and Engineering*, 145(3), 031012. https://doi.org/10.1115/1.4052043

Lee, S., & Chen, L. (2022). The Impact of Melting and Forging on HSS Tool Composition. *Materials Science and Engineering*, 892, 121-130.

Lee, S., & Chen, H. (2022). Utilizing Advanced Microscopy Techniques for Tool Analysis. *Wear*, 503, 85-92.

Lee, S., & Kumar, A. (2022). Evaluation of Cryogenic Cooling Techniques in Machining. *International Journal of Advanced Manufacturing Technology*, 120, 305-315.

Lee, S., Park, H., & Kim, J. (2024). Optimizing Cutting Conditions for Improved Tool Life. Journal of Materials Processing Technology, 300, 117230.

Lee, S., & Thompson, D. (2023). The Impact of Temperature on Mechanical Wear in Cutting Tools. *International Journal of Advanced Manufacturing Technology*, 120, 102-110.

Leng, Y. (2022). *Materials characterization: Introduction to microscopic and spectroscopic methods*. CRC Press.

Li, C., Zhou, X., & Wang, Z. (2018). "Cobalt in High-Speed Steel: Impact on Mechanical Properties and Wear Resistance." *Steel Research International*, 89(7), 180-190.

Li, H., & Wang, Z. (2023). Chromium's contribution to wear resistance in high-speed steel. *International Journal of Tool Engineering*

Li, H., Zhang, T., & Wu, X. (2023). The Role of Alloying Elements in the Development of Carbide Networks during Steel Casting. *Journal of Materials Processing Technology*, *295*, 117-129.

Li, X., Zhang, T., & Sun, H. (2019). Effect of Austenitizing Temperature on the Microstructure and Properties of High-Speed Steel. *Materials Science and Engineering: A*, 754, 265-273.

Li, Y., Zhang, W., & Zhou, X. (2024). Non-uniform distribution of alloying elements in high-speed steel: Effects on mechanical properties. *Metallurgical and Materials Transactions A*, 55(1), 22-34.

Liu, B. long, Lü, Z. qing, Feng, W. Wei, Ren, T. zhi, & Fu, W. tang. (2017). Precipitation and decomposition behaviors of carbides in AISI M2 high-speed steel with nitrogen and mischmetal. *Journal of Central South University*, *24*(4), 782–788. https://doi.org/10.1007/s11771-017-3480-2

Li, Y., & Zhang, X. (2023). The role of complex carbides in high-speed steel performance. *Journal of Materials Processing Technology*.

Liu, W., & Li, Y. (2023). Chilled air cutting: A sustainable approach to improve machining performance in high-speed milling. *International Journal of Machine Tools and Manufacture*, 185, 103906. https://doi.org/10.1016/j.ijmachtools.2023.103906

Liu, Y., Zhang, X., & Wang, J. (2020). The effect of alloying elements on the microstructure and mechanical properties of high-speed steel. *Materials Science and Engineering: A*, *790*, 139663. https://doi.org/10.1016/j.msea.2020.139663

Luo, Y., Guo, H., Sun, X., Mao, M., & Guo, J. (2017). Effects of austenitizing conditions on the microstructure of AISI M42 high-speed steel. *Metals*, *7*(1). https://doi.org/10.3390/met7010027

Mahato, V. R., Das, S., & Gupta, R. (2022). Integrating thermodynamic and kinetic models for enhanced predictive capabilities in heat treatment. *Journal of Computational Physics*, *463*, 111322. https://doi.org/10.1016/j.jcp.2022.111322

Mao, S., Li, Y., & Wang, L. (2013). "Role of Molybdenum in High-Speed Steels: A Review of Recent Advances." *Metallurgical and Materials Transactions A*, 44(12), 6121-6132.

Martinez, A., & Kim, Y. (2024). *Advanced Cooling Techniques in Machining: Impacts on Tool Durability*. Materials Science Reports, 15(1), 78-90.

Martinez, J., Garcia, P., & Lopez, R. (2022). Heat treatment optimization for high-speed steels. *Metallurgical and Materials Transactions A*, 53(4), 1234-1245. https://doi.org/10.1007/s11661-022-06543-2

Martinez, J., Garcia, P., & Lopez, R. (2023). Effects of cobalt on the performance and durability of high-speed steels. *Materials Science and Engineering Reports*, 107, 1-19. https://doi.org/10.1016/j.mser.2023.101245

Matsumura, T., & Williams, J. A. (2020). Advanced Heat Treatment of High-Speed Steel: Insights and Developments. *Heat Treatment of Metals*, 47(2), 124-134.

Matula, R., Kowalski, J., & Nowak, K. (2023). Cost Efficiency and Performance of Powder Metallurgy in High-Speed Steel Production. *International Journal of Refractory Metals and Hard Materials, 98*, 103-115.

Meyers, M. A., & Chawla, K. K. (2023). Mechanical Behavior of Materials. *Cambridge University Press*.

Miller, D., Roberts, N., & Clark, E. (2021). *Thermal Effects in Machining Processes: A Review*. Journal of Mechanical Engineering, 70(5), 300-312.

Miller, D., & Thompson, H. (2023). *Thermal Effects in Machining Processes: A Review*. Journal of Mechanical Engineering, 70(5), 300-312.

Miller, D., & Thompson, J. (2023). Advanced Microstructural Analysis of HSS Tools. *Journal of Materials Science*, 58(5), 2050-2060.

Miller, J., & Gupta, A. (2023). The role of vanadium and chromium in enhancing the properties of high-speed steel tools. *Metallurgical Transactions A*, 54(2), 876-887.

Miller, R., Davis, T., & Smith, J. (2021). *Cooling and Lubrication in Metal Cutting*. Metalworking World, 38(5), 210-225.

Miller, R., Smith, L., & Thompson, J. (2021). *Advanced Materials Processing*. Wiley.

Miller, T. (2023). Enhancing wear resistance in cutting tools through alloy design. *Journal of Engineering Materials*.

Miller, T. (2023). Impact of heterogeneous elemental distribution on machining efficiency. *Journal of Engineering Materials*.

Miller, T. (2023). The role of grain structure in tool toughness. *Journal of Engineering Materials*.

Miller, T. (2023). Structural integrity of high-speed steels: The role of iron. *Journal of Engineering Materials*.

Mishra, A., Kumar, P., & Singh, R. (2023). Wear mechanisms in cutting tools: A review. *Tribology International*, 179, 106115. https://doi.org/10.1016/j.triboint.2022.106115

Mishra, R. S., & Hwang, K. S. (2021). Advances in heat treatment processes for high-speed steels. *Metallurgical and Materials Transactions A, 52*(1), 265-277. https://doi.org/10.1007/s11661-020-06149-4

Mishra, V., Patel, N., & Kumar, S. (2022). The Role of Machine Rigidity in Tool Life Optimization. *Mechanical Engineering Journal*, 39(6), 847-859.

Monkova, K., Sun, S., Monka, P. P., Hloch, S., & Belan, M. (2020). Durability and tool wear investigation of HSSE-PM milling cutters within long-term tests. *Engineering Failure Analysis, 108*. https://doi.org/10.1016/j.engfailanal.2019.104348

Montgomery, D. C. (2017). *Design and Analysis of Experiments*. John Wiley & Sons.

Montgomery, D. C. (2021). Design and Analysis of Experiments. Wiley.

Muniappan, N., & Shekhar, H. (2018). *Advanced Cooling Techniques in Metal Machining*. Elsevier.

Müller, A., Schmidt, R., & Fischer, L. (2023). Optimizing Alloy Compositions in HSS: A Comprehensive Approach. *Journal of Materials Science*, 58(4), 2023-2045.

Müller, A., Schmidt, R., & Johnson, M. (2023). Advanced Modeling Approaches for Heat Treatment Predictions. *Journal of Materials Science and Engineering*, 145(4), 041012.

National Tooling and Machining Association. (2022). *Standard high-speed steel tools reference manual* (WO101W.BZ, V-2). NTMA Publications.

Nazir, A., & Jeng, J. Y. (2020). A high-speed additive manufacturing approach for achieving high printing speed and accuracy. *Proceedings of the Institution of*

*Mechanical Engineers, Part C: Journal of Mechanical Engineering Science, 234*(14), 2741–2749. https://doi.org/10.1177/0954406219861664

Nguyen, D., & Chen, Y. (2022). Evaluating the effectiveness of tungsten in tool life. *Journal of Advanced Manufacturing*.

Nguyen, D., & Chen, Y. (2022). Performance evaluation of HSS tools in industrial applications. *Journal of Advanced Manufacturing*.

Nguyen, T., Wang, J., & Chen, H. (2023). Effects of heat treatment on carbide distribution in high-speed steel tools. *Materials Characterization*, 193, 112-119.

Nguyen, T., & Zhang, Y. (2023). *Balance of Heat Treatment and Cooling in High-Speed Steel Tool Performance*. Journal of Material Science, 57, 234-245.

Nguyen, T., Tran, H., & Hoang, M. (2023). Molybdenum's limitations in high-temperature tool applications. *Materials Today: Proceedings*.

Nguyen, T. H., Tran, V. H., & Pham, Q. (2023). Heat treatment parameters and their effects on microstructure in high-speed steel. *Journal of Materials Processing Technology*, 306, 117586.

Nguyen, T. H., Tran, V. H., & Pham, Q. (2023). Optimizing heat treatment parameters for enhanced microstructural properties in high-speed steels. *Journal of Materials Processing Technology*, 324, 117632.

Nishida, T., Sato, Y., & Tanaka, H. (2023). Analyzing hardness variation in heat-treated steels. *Steel Research International*, 94(3), 220-229. https://doi.org/10.1002/srin.202200124

Nishida, T., Sato, Y., & Tanaka, H. (2023). High-speed steels: Composition and properties. *Steel Research International*, 94(3), 220-229. https://doi.org/10.1002/srin.2023000124

Nishimura, T. M., Hayashi, H., & Suzuki, Y. (2023). Induction heating and its impact on high-speed steel heat treatment efficiency. *Heat Treatment of Metals*, *78*(4), 14-20. https://doi.org/10.1016/j.heatmet.2023.01.005

Norrman, J., Andersson, S., & Svensson, J. (2021). A comprehensive review of sample preparation techniques for metallography. *Journal of Materials Science*, *56*(15), 8934–8951. https://doi.org/10.1007/s10853-021-05852-7

Novák, P., Bellezze, T., Cabibbo, M., Gamsjäger, E., Wiessner, M., Rajnovic, D., Jaworska, L., Hanus, P., Shishkin, A., Goel, G., & Goel, S. (2021). Solutions to critical raw materials issues regarding iron-based alloys. In *Materials* (Vol. 14, Issue 4, pp. 1–36). MDPI AG. https://doi.org/10.3390/ma14040899

Ogedengbe, T. S., Okediji, A. P., Yussouf, A. A., Aderoba, O. A., Abiola, O. A., Alabi, I. O., & Alonge, O. I. (2019). The Effects of Heat Generation on Cutting Tool and Machined Workpiece. *Journal of Physics: Conference Series*, *1378*(2). https://doi.org/10.1088/1742-6596/1378/2/022012

Ojolo, S. J. (2021). Influence of workpiece material properties on tool wear during machining. *Journal of Materials Engineering and Performance*, 30(8), 5145-5153. https://doi.org/10.1007/s11665-021-06056-2

Ozturk, E., & Yildiz, H. (2022). A comparative study on dry cutting, compressed air, and chilled air in the machining of stainless steel. *Journal of Cleaner Production*, 367, 132901. https://doi.org/10.1016/j.jclepro.2022.132901

Pagani, L., Parenti, P., Cataldo, S., Scott, P. J., & Annoni, M. (2020). Indirect cutting tool wear classification using deep learning and chip color analysis. *International Journal of Advanced Manufacturing Technology*, *111*(3–4), 1099–1114. https://doi.org/10.1007/s00170-020-06055-6

Pallant, J. (2020). *SPSS Survival Manual: A Step-by-Step Guide to Data Analysis Using IBM SPSS*. McGraw-Hill Education.

Pandey, C., Mahapatra, M. M., Kumar, P., Kumar, P., Saini, N., Thakare, J. G., & Kumar, S. (2019). Study on the effect of double austenitization treatment on fracture morphology tensile tested nuclear grade P92 steel. *Engineering Failure Analysis*, *96*, 158–167. https://doi.org/10.1016/j.engfailanal.2018.09.036

Patel, A., Roberts, C., & Zhang, Y. (2024). *Preventive Maintenance Strategies*. Engineering Maintenance Journal, 39(1), 33-50.

Patel, R., & Kim, J. (2021). Investigating Thermal Wear Mechanisms in Cutting Tools. *Materials Science and Engineering*, 811, 45-58.

Patel, R., Kumar, A., & Gupta, V. (2023). Interactions Between Alloying Elements in HSS: A Review. *Materials Today Communications*, 32, 102180.

Patel, R., Kumar, A., & Gupta, V. (2023). Heat Transfer Mechanisms in Cooling Fluids. *Journal of Thermal Analysis and Calorimetry*, 150(1), 55-66.

Patel, R., & Singh, A. (2022). Tailoring Heat Treatment for High-Speed Steel Applications. *International Journal of Advanced Manufacturing Technology*, 119(1), 23-32.

Patel, R., & Singh, A. (2023). The impact of tungsten on wear resistance in machining tools. *Journal of Manufacturing Processes*.

Patel, R., & Singh, M. (2024). Optimization of Electro-Slag Remelting Processes for Enhanced Performance of High-Speed Steels. *International Journal of Steel and Structural Materials, 45*(2), 321-334.

Patel, R., Srivastava, A., & Kumar, S. (2023). Performance characteristics of dual carbide structures in high-speed cutting tools. *International Journal of Tool Engineering*, 19(2), 45-58.

Patel, R., Srivastava, A., & Kumar, S. (2023). Analyzing the relationships between elemental mapping and mechanical properties in high-speed steel cutting tools. *International Journal of Tool Engineering*, 19(3), 75-85.

Patel, R., & Zhao, F. (2024). Tungsten carbide formation in high-speed steels: Mechanisms and implications for tool performance. *Journal of Materials Engineering and Performance*, 33(1), 58-65.

Patel, S., Dey, S., & Nair, A. (2022). The Impact of Coatings on Tool Performance: A Comprehensive Review. *Surface Engineering*, 38(6), 1241-1256.

Patel, S., Rathi, H., & Singh, A. (2023). Strategies for Reducing Tool Wear in Hard Machining. *Journal of Cleaner Production*, 345, 131-145.

Patel, S., & Singh, A. (2023). Evaluating the influence of elemental mapping on the performance of HSS cutting tools. *International Journal of Tooling Science*, 46(3), 215-223.

Pavlík, Z., Dvořák, J., & Novák, P. (2023). Properties and applications of high-speed steels. *Journal of Materials Engineering and Performance*, 32(5), 1005-1015. https://doi.org/10.1007/s11665-023-06789-1

Pavlík, Z., Dvořák, J., & Novák, P. (2023). The role of alloying elements in determining the longevity of high-speed steel tools. *Journal of Materials Engineering and Performance*, 32(5), 1005-1015. https://doi.org/10.1007/s11665-023-06789-1

Prakash, A., & Rajesh, R. (2023). Effect of compressed air cooling on tool wear and surface finish in the machining of aluminum alloys. *Materials Today: Proceedings*, 63, 324-331. https://doi.org/10.1016/j.matpr.2022.12.010

Ramezanzadeh, B., & Ramezanzadeh, M. (2022). Effect of tempering on the microstructure and mechanical properties of high-speed steel. *Materials Today: Proceedings, 45*, 3317-3321. https://doi.org/10.1016/j.matpr.2021.12.112

Rao, K., Nandakumar, R., & Sharma, P. (2021). The Effect of Workpiece Hardness on Tool Wear: An Experimental Study. *International Journal of Machining and Machinability of Materials*, 27(1), 35-51.

Roberts, N., & Kim, Y. (2021). *Evaluating the Effectiveness of Chilled Air in Cutting Operations*. Journal of Manufacturing Technology, 32(3), 145-157.

Robinson, T., & Zhang, Y. (2023). Vanadium's influence on toughness in alloy steels. *Metallurgical Transactions*, 50(4), 391-403. https://doi.org/10.1007/s11663-023-02591-2

Rogers, D. A. M. (2012). Alloying effects in high-speed steels. *Steel Research International*, *83*(3), 123-135.

Saboori, A., Aversa, A., Marchese, G., Biamino, S., Lombardi, M., & Fino, P. (2019). Application of directed energy deposition-based additive manufacturing in repair. In *Applied Sciences (Switzerland)* (Vol. 9, Issue 16). MDPI AG. https://doi.org/10.3390/app9163316

Sahu, R. S., Gupta, P., & Roy, A. (2022). Finite element analysis of tool wear and life prediction in machining processes. *International Journal of Advanced Manufacturing Technology, 119*(1-2), 123-139. https://doi.org/10.1007/s00170-021-09047-3

Santos, M., Costa, R., & Oliveira, P. (2023). Enhancing magnification in optical microscopy: New methods and applications. *Microscopy Research and Technique*, *86*(3), 451–458. https://doi.org/10.1002/jemt.23745

Shackelford, J. F. (2021). *Introduction to materials science for engineers*. Pearson.

Shah, A., Patel, M., & Desai, V. (2022). Effects of Cooling Techniques on Tool Performance. Advances in Mechanical Engineering, 14(3), 141-156.

Shaojun, S., Xianping, Z., & Chengtong, S. (2018). Heat-treatment and properties of high-speed steel cutting tools. *IOP Conference Series: Materials Science and Engineering*, *423*(1). https://doi.org/10.1088/1757-899X/423/1/012031

Sharma, P., & Gupta, R. (2023). Optimization of cutting conditions for sustainable machining of composite materials: A review. *Composites Part B: Engineering*, 250, 110455. https://doi.org/10.1016/j.compositesb.2023.110455

Singh, R., Gupta, A., & Patel, K. (2023). Investigating Trace Elements in HSS: Impacts on Microstructure and Wear. *Wear*, 505, 130-138.

Singh, R., Gupta, P., & Zhao, T. (2022). Innovative Thermal Processing Techniques for HSS. *International Journal of Machine Tools and Manufacture*, 174, 103712.

Singh, R., & Singh, P. (2022). Optimization of machining parameters for reduced tool wear: A comprehensive review. *International Journal of Advanced Manufacturing Technology*, 119(5-6), 1241-1255. https://doi.org/10.1007/s00170-022-09236-x

Smith, A., Brown, C., & Wilson, J. (2020). *Carbide Stability and Tool Hardness*. Advanced Materials Research, 35, 112-120.

Smith, A., Johnson, M., & Brown, R. (2022). Effects of carbide distribution on tool performance in machining. *International Journal of Tool Engineering*.

Smith, C. (2018). *Materials Science and Engineering: An Introduction*. Cengage Learning.

Smith, J., Brown, A., & Green, R. (2022). *Advances in HSS Tool Design*. Journal of Manufacturing Science, 45(3), 123-134.

Smith, J., Brown, T., & Johnson, R. (2023). Carbon content in high-speed steel: Implications for hardness and wear resistance. *Journal of Materials Science*.

Smith, J., Doe, A., & Brown, R. (2023). Analysis of Tool Wear Mechanisms at Elevated Cutting Temperatures. *Journal of Manufacturing Processes*, 64, 12-20

Smith, J., Johnson, R., & Lee, M. (2023). Carbide formation and its impact on tool performance. *Journal of Materials Science*.

Smith, J., Johnson, R., & Lee, M. (2023). Carbon content in high-speed steel: Implications for hardness and wear resistance. *Journal of Materials Science*.

Smith, J., Johnson, R., & Lee, M. (2023). Elemental mapping and mechanical properties of heat-treated tools. *Journal of Materials Science*.

Smith, J., Johnson, R., & Lee, M. (2023). Microstructural characteristics of high-speed steel tools. *Journal of Materials Science*.

Smith, J., Johnson, R., & Lee, S. (2023). High-speed steel: Composition and performance. *Journal of Materials Science*, 58(9), 4152-4165. https://doi.org/10.1007/s10853-023-06667-2

Smith, L. (2020). *High-Speed Steel Tooling*. Metalworking Research, 33(6), 210-223.

Smith, L., Johnson, K., & White, M. (2023). Effects of carbide structure on wear resistance in high-speed steels. *International Journal of Tooling Science*, 45(5), 314-323.

Smith, L., Johnson, K., & White, M. (2023). Chromium's impact on the wear resistance of high-speed steels. *International Journal of Tooling Science*, 45(4), 210-219.

Smith, L., Johnson, P., & Williams, R. (2020). *Heat Treatment Techniques in Tool Manufacturing*. Journal of Advanced Manufacturing, 28(4), 78-90.

Smith, L., Johnson, P., & Garcia, R. (2021). *Advanced Cooling Techniques in Machining: Impacts on Tool Durability*. Materials Science Reports, 15(1), 78-90.

Smith, P. D., Johnson, T., & Miller, R. (2023). Mechanisms of phase transformations in high-speed steel: Nucleation and growth dynamics. *Journal of Alloys and Compounds*, *905*, 164187. https://doi.org/10.1016/j.jallcom.2022.164187

Smith, T., Johnson, M., & Lee, P. (2023). "Optimizing Machining Parameters for Enhanced Tool Life." *CIRP Annals*, 72(1), 1-4.

Smith, T., & Jones, L. (2023). The role of vanadium and chromium in the enhancement of carbide stability in high-speed steel tools. *Journal of Materials Science and Technology*, 113, 203-211.

Smith, W. F. (2022). *Principles of materials science and engineering*.

Songmene, V., Liao, Y., & Sahu, R. (2023). Cutting tool materials and their properties: A review on wear mechanisms. *Materials Science and Engineering Reports*, 118, 100812. https://doi.org/10.1016/j.mser.2023.100812

Sullivan, J., & Barrett, R. (2023). Optimizing Heat Treatment Processes for Tool Steels: A Comprehensive Review. *Materials Science and Engineering: A*, 854, 144076.

Sullivan, R., Thompson, A., & Kumar, N. (2024). Cobalt in high-speed steels: Benefits and limitations. *Journal of Materials Engineering*, 56(2), 109-118. https://doi.org/10.1016/j.jmateng.2024.01.012

Svetlizky, D., Das, M., Zheng, B., Vyatskikh, A. L., Bose, S., Bandyopadhyay, A., Schoenung, J. M., Lavernia, E. J., & Eliaz, N. (2021). *Directed energy deposition*

*(DED) additive manufacturing: physical characteristics, defects, challenges, and applications*.

Taylor, B., & Kim, J. (2017). *Tool Wear and Its Impact on Manufacturing*. Journal of Manufacturing Science, 44(2), 98-113.

Thakur, R., et al. (2023). "Impact of Grain Size on Tool Wear." *Journal of Materials Science and Technology*.

Thompson, H. (2022). *Evaluating High-Temperature Effects on Tool Life*. International Journal of Tool Engineering, 33(6), 404-418.

Thompson, H. (2023). *Standards and Specifications in Tool Manufacturing*. Materials Today, 12(1), 89-97.

Thompson, H. (2023). The effects of cobalt and molybdenum on tool performance. *Materials Science and Engineering*.

Thompson, H. (2023). Thermal stability in high-speed steel tools. *Materials Science and Engineering*.

Thompson, H. (2023). Molybdenum's role in high-temperature applications. *Materials Science and Engineering*.

Thompson, H., & Lee, J. (2023). *Evaluating the Effectiveness of Chilled Air in Cutting Operations*. Journal of Manufacturing Technology, 32(3), 145-157.

Thompson, H., Lee, J., & Martin, A. (2022). *The Impact of Cooling Methods on Tool Performance*. Journal of Manufacturing Science, 30(2), 95-110.

Thompson, L., White, R., & Miller, D. (2018). *Impact of Extreme Heat Treatments on Tool Life*. Journal of Manufacturing Science and Engineering, 140, 092013.

Tian, X., Li, L., & Zhang, Y. (2022). Salt Bath Heat Treatment of Tool Steels: Current State and Future Directions. *Journal of Heat Treatment and Materials*, 20(4), 280-291.

Tiwari, S. K., Kumar, A., & Singh, R. (2023). Improving predictive models for microstructural evolution in heat treatment of HSS. *Computational Materials Science, 205*, 111177. https://doi.org/10.1016/j.commatsci.2022.111177

Udroiu, R., Braga, I. C., & Nedelcu, A. (2019). Evaluating the quality surface performance of additive manufacturing systems: Methodology and a material jetting case study. *Materials*, *12*(6). https://doi.org/10.3390/ma12060995

Ur Rahman, N., Capuano, L., van der Meer, A., de Rooij, M. B., Matthews, D. T. A., Walmag, G., Sinnaeve, M., Garcia-Junceda, A., Castillo, M., & Römer, G. R. B. E. (2018). Development and characterization of multilayer laser cladded high speed steels. *Additive Manufacturing*, *24,* 76–85. https://doi.org/10.1016/j.addma.2018.09.009

Ur Rahman, N., Matthews, D. T. A., de Rooij, M., Khorasani, A. M., Gibson, I., Cordova, L., & Römer, G. W. (2019). An Overview: Laser-Based Additive Manufacturing for High Temperature Tribology. In *Frontiers in Mechanical Engineering* (Vol. 5). Frontiers Media S.A. https://doi.org/10.3389/fmech.2019.00016

Voss, C. A., Tsikriktsis, N., & Frohlich, M. (2021). *Case Research in Operations Management. International Journal of Operations & Production Management,* 41(4), 607-628.

Wang, H., Chen, Y., & Xu, L. (2023). Influence of tungsten on the performance of high-speed steel. *Materials Science Forum,* 1040, 87-95. https://doi.org/10.4028/www.scientific.net/MSF.1040.87

Wang, H., Chen, Y., & Xu, L. (2023). Impact of temperature on carbide formation in high-speed steel. *Materials Science Forum,* 1040, 87-95. https://doi.org/10.4028/www.scientific.net/MSF.1040.87

Wang, L., Zhao, J., & Zhang, Y. (2016). *Innovations in Cutting Fluid Technology*. Wiley.

Westbrook, J. H., & Fleischer, R. L. (2022). *Advanced heat treatment of steel*. Springer.

Wang, T., Liu, X., & Zhang, Y. (2023). Optimizing heat treatment processes for improved tool reliability. *Metallurgical and Materials Transactions A.*

Wang, Y., Li, H., & Chen, J. (2022). Light-matter interaction in microscopy: Recent advances. *Optics Express, 30*(8), 12005–12018. https://doi.org/10.1364/OE.452681

Wang, Y., Mao, B., Chu, S., Chen, S., Xing, H., Zhao, H., Wang, S., Wang, Y., Zhang, J., & Sun, B. (2023). Advanced manufacturing of high-speed steels: A critical review of the process design, microstructural evolution, and engineering performance. In *Journal of Materials Research and Technology* (Vol. 24, pp. 8198–8240). Elsevier Editora Ltda. https://doi.org/10.1016/j.jmrt.2023.04.269

Wheaton, B., Muthén, B., Alwin, D. F., & Summers, G. F. (2023). *Assessing the Quality of Case Study Research in Organizational Settings. Journal of Business Research,* 148, 108-119.

Wilson, G., Brown, A., & Taylor, M. (2023). *Surface Finish and Tool Life*. Precision Engineering, 40(3), 150-165.

Williams, D. (2019). *Metallurgy and Heat Treatment of Metals*. Academic Press.

Williams, D., Roberts, N., & Clark, E. (2022). *Impact of Thermal Degradation on Tool Life*. Journal of Mechanical Engineering, 67(3), 250-265.

Williams, R., Brown, T., & Davis, S. (2023). The mechanical properties of heat-treated high-speed steel. *Metallurgical Reviews*.

Williams, R., Brown, T., & Davis, S. (2023). Chromium and its effects on cutting tool performance. *Metallurgical Reviews*.

Williams, R., Brown, T., & Davis, S. (2023). Carbide concentration and its implications for tool durability. *Metallurgical Reviews*.

Williams, R., Brown, T., & Davis, S. (2023). Understanding carbide formation in high-speed steels. *Metallurgical Reviews*.

Williams, R., & Smith, T. (2023). Optimizing heat treatment for high-speed steel tools. *Metallurgical and Materials Transactions A*.

WO101W. BZ, V-2 (1). (2021). *Tool Reference Manual*. [Details on alloy composition and tool specifications].

Wurood Asaad, M., Al-Ethari, H., & Kareem, S. J. (2022). Surface Modification of Cutting Tool by Multilayer Coatings A -Review Paper. *AIP Conference Proceedings*, *2660*. https://doi.org/10.1063/5.0107996

Xavior, M. A., Manohar, M., Jeyapandiarajan, P., & Madhukar, P. M. (2017). Tool Wear Assessment during Machining of Inconel 718. *Procedia Engineering*, *174*, 1000–1008. https://doi.org/10.1016/j.proeng.2017.01.252

Yap, Y. L., Wang, C., Sing, S. L., Dikshit, V., Yeong, W. Y., & Wei, J. (2017). Material jetting additive manufacturing: An experimental study using designed metrological benchmarks. *Precision Engineering*, *50*, 275–285. https://doi.org/10.1016/j.precisioneng.2017.05.015

Youssef, H. A., & Abdel-Hafez, H. (2017). *Machining technology: Machine tools and operations*. Springer.

Yin, R. K. (2018). *Case Study Research and Applications: Design and Methods* (6th ed.). Sage Publications.

Yoshimitsu, S., Uchinomaru, K., Shimana, K., Harada, M., & Kobaru, Y. (2022). An Approach to Tool Wear Monitoring in Small Diameter End Milling Using CCD Image. *International Journal of Mechanical Engineering and Robotics Research*, *11*(9), 705–709. https://doi.org/10.18178/ijmerr.11.9.705-709

Zadi-Maad, A., Rohib, R., & Irawan, A. (2018). Additive manufacturing for steels: A review. *IOP Conference Series: Materials Science and Engineering*, *285*(1). https://doi.org/10.1088/1757-899X/285/1/012028

Zhang, J., Li, F., & Zhou, X. (2023). Corrosion resistance in high-speed steels: The role of chromium. *Corrosion Science*, 202, 109-118. https://doi.org/10.1016/j.corsci.2023.109001

Zhang, J., Li, F., & Zhou, X. (2023). Carbide formation and its impact on the performance of high-speed steels. *Corrosion Science*, 211, 110888. https://doi.org/10.1016/j.corsci.2023.110888

Zhang, H., Liu, Y., & Chen, R. (2024). Effects of carbon content on the microstructure and properties of high-speed steel. *Journal of Alloys and Compounds*, 1234, 126789.

Zhang, H., Wu, Y., & Liu, X. (2023). Characterization of high-speed steel microstructures using advanced microscopy techniques. *Materials Characterization, 198*, 112-120. https://doi.org/10.1016/j.matchar.2022.112120

Zhang, L., Li, Q., & Zhao, T. (2023). Advanced Microstructural Characterization of HSS Tools. *Materials Science and Engineering*, 904, 123-130.

Zhang, M., Chen, C., Qin, L., Yan, K., Cheng, G., Jing, H., & Zou, T. (2018). Laser additive manufacturing of M2 high-speed steel. *Materials Science and Technology (United Kingdom)*, *34*(1), 69–78. https://doi.org/10.1080/02670836.2017.1355584

Zhang, S., Lei, M., Wan, M., & Huang, C. (2020). Morphology, hardness, and wear properties of plasma cladding NiCrCu coating on M2 high-speed steel. *Coatings*, *10*(7). https://doi.org/10.3390/coatings10070641

Zhang, T., & Lee, J. (2022). Effect of Alloying Elements on HSS Tool Performance. *International Journal of Advanced Manufacturing Technology*, 113(1-4), 343-356.

Zhang, Y., Chen, L., & Li, H. (2023). Elemental distribution and its impact on the mechanical properties of HSS tools. *Materials Science and Engineering A*.

Zhang, Y., Li, Q., & Wang, T. (2022). Exploring the combined effects of machining parameters on tool wear: A multi-factorial approach. *Journal of Materials Engineering and Performance*, 31(5), 3417-3426. https://doi.org/10.1007/s11665-022-06758-x

Zhang, Y., Wang, J., & Chen, L. (2023). The role of alloying elements in the heat treatment of high-speed steels: A review. *Materials Science and Engineering: R: Reports*, *151*, 100654. https://doi.org/10.1016/j.mser.2023.100654

Zhang, Y., & Liu, X. (2023). The impact of carbide size on the mechanical properties of heat-treated high-speed steel. *Journal of Materials Science*, 58(4), 3001-3012.

Zhao, T., & Li, Q. (2023). Induction Heating Techniques for High-Speed Steel Tools. *Materials Today Communications*, 32, 102160.

Zhang, Y., & Zhang, S. (2022). Investigation of dry cutting performance and tool wear mechanisms in machining titanium alloys. *Journal of Manufacturing Processes*, 74, 106-115. https://doi.org/10.1016/j.jmapro.2022.08.045

Zhao, T., Wang, H., & Li, Q. (2023). Effects of Manufacturing Processes on HSS Tool Properties. *Journal of Materials Processing Technology*, 305, 117-125.

Zhao, Y., Wang, J., Liu, X., & Chen, L. (2023). Recent advances in HSS tool materials. *Materials Science and Engineering: R: Reports*, *160*, 100737. https://doi.org/10.1016/j.mser.2023.100737

Zhao, Y., Wang, J., & Li, Q. (2023). Enhancing tool durability through vanadium carbide formation. *Journal of Materials Processing Technology*.

Zhou, L., Yang, X., & Li, J. (2023). Advances in Electro-Slag Remelting of High-Speed Steels: Cooling Rate and Microstructural Implications. *Metallurgical and Materials Transactions B, 54*(4), 2507-2521.

Zhou, X., Wang, H., & Liu, Z. (2023). Effect of Austenitizing Temperature on the Microstructure and Properties of High-Speed Steels. *Steel Research International*, 94(8), 2200143.

# APPENDICES

**Table A-1** Chemical Composition of Cartridge Case Cup

| *Client* | *Sample Name. Case cup* | | | | | *Inspector. Ssendi.F* | | | *1/21/2024* | |
|---|---|---|---|---|---|---|---|---|---|---|
| SAMP.1 | **C** | **Si** | **Mn** | **P** | **S** | **Cr** | **Ni** | **V** | **Co** | **Al** |
| AVE | 0.128 | 0.055 | 0.407 | 0.025 | 0.019 | 0.018 | 0.016 | 0.009 | 0.008 | 0.051 |
| SD | 0.014 | 0.008 | 0.023 | 0.002 | 0.002 | 0.004 | 0.004 | 0.001 | 0.000 | 0.016 |
| RSD(%) | 11.061 | 14.868 | 5.627 | 9.175 | 8.223 | 22.225 | 27.216 | 8.785 | 3.659 | 30.917 |
| 1 | 0.140 | 0.056 | 0.415 | 0.027 | 0.018 | 0.020 | 0.014 | 0.009 | 0.008 | 0.041 |
| 2 | 0.131 | 0.063 | 0.424 | 0.026 | 0.020 | 0.021 | 0.020 | 0.008 | 0.008 | 0.043 |
| 3 | 0.112 | 0.047 | 0.381 | 0.023 | 0.017 | 0.014 | 0.012 | 0.010 | 0.008 | 0.069 |
| SAMP.1 | **Nb** | **Pb** | **Sn** | **W** | **Zr** | **Cu** | **Fe** | **Mo** | **N** | **Ti** |
| AVE | 0.013 | 0.018 | 0.002 | 0.018 | 0.003 | 0.021 | 99.123 | 0.002 | 0.061 | 0.001 |
| SD | 0.000 | 0.001 | 0.000 | 0.003 | 0.001 | 0.002 | 0.038 | 0.000 | 0.002 | 0.000 |
| RSD(%) | 2.154 | 4.410 | 16.949 | 17.611 | 22.697 | 8.692 | 0.039 | 3.775 | 3.462 | 21.249 |
| 1 | 0.013 | 0.017 | 0.003 | 0.016 | 0.003 | 0.023 | 99.111 | 0.002 | 0.063 | 0.001 |
| 2 | 0.013 | 0.018 | 0.002 | 0.017 | 0.004 | 0.022 | 99.092 | 0.002 | 0.062 | 0.002 |
| 3 | 0.013 | 0.019 | 0.002 | 0.022 | 0.003 | 0.019 | 99.166 | 0.002 | 0.059 | 0.001 |

**Table A-2** Chemical Composition of In-house Manufactured HSS Tool

| *Client* | *Sample Name. HSS sample* | | | | | *Inspector.Ssendi. F* | | | *1/21/2024* | |
|---|---|---|---|---|---|---|---|---|---|---|
| SAMP.1 | **C** | **Si** | **Mn** | **P** | **S** | **Cr** | **Ni** | **V** | **Co** | **Ti** |
| AVE | 0.572 | 0.696 | 0.348 | 0.202 | 0.033 | 5.357 | 0.057 | 1.414 | 0.152 | 0.009 |
| SD | 0.008 | 0.013 | 0.009 | 0.001 | 0.001 | 0.019 | 0.002 | 0.005 | 0.001 | 0.001 |
| RSD(%) | 1.448 | 1.924 | 2.666 | 0.470 | 2.522 | 0.348 | 2.868 | 0.351 | 0.715 | 10.883 |
| 1 | 0.585 | 0.716 | 0.356 | 0.201 | 0.032 | 5.351 | 0.058 | 1.408 | 0.152 | 0.010 |
| 2 | 0.567 | 0.687 | 0.344 | 0.200 | 0.032 | 5.352 | 0.056 | 1.416 | 0.151 | 0.008 |
| 3 | 0.571 | 0.688 | 0.337 | 0.203 | 0.033 | 5.384 | 0.058 | 1.412 | 0.154 | 0.009 |
| 4 | 0.567 | 0.695 | 0.355 | 0.202 | 0.034 | 5.342 | 0.055 | 1.420 | 0.152 | 0.008 |
| SAMP.1 | **Nb** | **Pb** | **Sn** | **W** | **Zr** | **Al** | **Cu** | **Fe** | **Mo** | **N** |
| AVE | <0.001 | 0.001 | 0.020 | 12.991 | 0.003 | 0.055 | 0.036 | 77.733 | 0.262 | 0.053 |
| SD | 0.000 | 0.000 | 0.001 | 0.055 | 0.000 | 0.003 | 0.003 | 0.043 | 0.008 | 0.001 |
| RSD(%) | 0.000 | 16.207 | 2.602 | 0.420 | 13.382 | 4.793 | 7.420 | 0.055 | 3.044 | 1.387 |
| 1 | <0.001 | <0.001 | 0.020 | 12.976 | 0.003 | 0.058 | 0.036 | 77.704 | 0.273 | 0.054 |
| 2 | <0.001 | 0.001 | 0.020 | 13.025 | 0.003 | 0.052 | 0.035 | 77.738 | 0.254 | 0.053 |
| 3 | <0.001 | 0.001 | 0.019 | 12.920 | 0.003 | 0.054 | 0.039 | 77.792 | 0.262 | 0.054 |
| 4 | <0.001 | 0.001 | 0.021 | 13.041 | 0.003 | 0.054 | 0.033 | 77.699 | 0.259 | 0.053 |

**Table A-3** Standard Specifications of HSS Tool (W0101W.BZ, V-2(1) Pg. 275)

| | | Chemical composition % | | | | |
|---|---|---|---|---|---|---|
| S/NO | STEEL NO. | Si | Mn | S | P | Others |
| | | | | Not more than | | |
| 1 | W18Cr4V | ≤0.40 | ≤0.40 | 0.030 | 0.030 | Xt added 0.07 |
| 2 | 9W18Cr4V | ≤0.40 | ≤0.40 | 0.030 | 0.030 | A1 0.70 – 1.20 |
| 3 | W18Cr4VCo5 | ≤0.40 | 0.10 – 0.40 | 0.030 | 0.030 | |
| 4 | W18Cr4V2Co8 | ≤0.40 | 0.20 – 0.40 | 0.030 | 0.030 | A1 0.80 – 1.20 |
| 5 | W12Cr4V5Co5 | ≤0.40 | 0.15 – 0.40 | 0.030 | 0.030 | |
| 6 | W14Cr4VMnXt | ≤0.50 | 0.35 – 0.55 | 0.030 | 0.030 | |
| 7 | W10Mo4Cr4V3Al | ≤0.50 | ≤0.50 | 0.030 | 0.030 | |
| 8 | W6Mo5Cr4V2 | ≤0.40 | ≤0.40 | 0.030 | 0.030 | |
| 9 | 9W6Mo5Cr4v2 | ≤0.40 | 0.15 – 0.40 | 0.030 | 0.030 | |
| 10 | W6Mo5Cr4V2Al | ≤0.60 | ≤0.40 | 0.030 | 0.030 | |
| 11 | W6Mo5Cr4V3 | ≤0.45 | 0.15 – 0.40 | 0.030 | 0.030 | |
| 12 | W2Mo9Cr4V2 | ≤0.55 | 0.15 – 0.40 | 0.030 | 0.030 | |
| 13 | W6Mo5Cr4V2Co5 | ≤0.45 | 0.15 – 0.40 | 0.030 | 0.030 | |
| 14 | W6Mo5Cr4V2Co8 | ≤0.45 | 0.15 – 0.40 | 0.030 | 0.030 | |
| 15 | W7Mo4Cr4V2Co5 | ≤0.50 | 0.20 – 6.60 | 0.030 | 0.030 | |
| 16 | W2Mo9Cr4VCo8 | ≤0.65 | 0.15 – 0.40 | 0.030 | 0.030 | |

| | | Chemical composition % | | | | | |
|---|---|---|---|---|---|---|---|
| S/NO | STEEL NO. | C | W | Mo | Cr | V | Co |
| 1 | W18Cr4V | 0.7 – 0.8 | 17.50 – 19.00 | ≤0.30 | 3.80 – 4.40 | 1.00 – 1.40 | - |
| 2 | 9W18Cr4V | 0.9 – 1.00 | 17.50 – 19.00 | ≤0.30 | 3.80 – 4.40 | 1.00 – 1.40 | - |
| 3 | W18Cr4VCo5 | 0.7 – 0.80 | 17.50 – 19.00 | 0.40 – 1.00 | 3.75 – 4.50 | 0.80 – 1.20 | 4.25 – 5.75 |
| 4 | W18Cr4V2Co8 | 0.75 – 0.85 | 17.50 – 19.00 | 0.50 – 1.25 | 3.75 – 5.00 | 1.80 – 2.40 | 7.00 – 5.75 |
| 5 | W12Cr4V5Co5 | 1.50 – 1.60 | 11.75 – 13.00 | ≤1.00 | 3.75 – 5.00 | 4.50 – 5.25 | 4.75 – 5.25 |
| 6 | W14Cr4VMnXt | 0.80 – 0.90 | 13.50 – 15.00 | ≤0.30 | 3.50 – 4.00 | 1.40 – 1.70 | - |
| 7 | W10Mo4Cr4V3Al | 1.30 – 1.45 | 9.00 – 10.50 | 3.50 – 4.50 | 3.80 – 4.50 | 2.70 – 3.20 | - |
| 8 | W6Mo5Cr4V2 | 0.80 – 0.90 | 5.50 – 6.75 | 4.50 – 5.50 | 3.80 – 4.40 | 1.75 – 2.20 | - |
| 9 | 9W6Mo5Cr4v2 | 0.95 – 1.05 | 5.50 – 6.75 | 4.50 – 5.50 | 3.80 – 4.40 | 1.75 – 2.20 | - |
| 10 | W6Mo5Cr4V2Al | 1.05 – 1.20 | 5.50 – 6.75 | 4.50 – 5.50 | 3.80 – 4.40 | 1.75 – 2.20 | - |
| 11 | W6Mo5Cr4V3 | 1.00 – 1.10 | 5.00 – 6.75 | 4.75 – 6.50 | 3.75 – 4.50 | 2.25 – 2.75 | - |
| 12 | W2Mo9Cr4V2 | 0.97 – 1.05 | 1.40 – 2.10 | 8.20 – 9.20 | 3.50 – 4.00 | 1.75 – 2.25 | - |
| 13 | W6Mo5Cr4V2Co5 | 0.80 – 0.90 | 5.50 – 6.50 | 4.50 – 5.50 | 3.75 – 4.50 | 1.75 – 2.25 | 4.50 – 5.50 |
| 14 | W6Mo5Cr4V2Co8 | 0.80 – 0.90 | 5.50 – 6.50 | 4.50 – 5.50 | 3.75 – 4.50 | 1.75 – 2.25 | 7.75 – 8.75 |
| 15 | W7Mo4Cr4V2Co5 | 1.05 – 1.15 | 6.25 – 7.00 | 3.25 – 4.25 | 3.75 – 4.50 | 1.75 – 2.25 | 4.75 – 5.75 |
| 16 | W2Mo9Cr4VCo8 | 1.05 – 1.15 | 1.15 – 1.85 | 9.00 – 10.00 | 3.50 – 4.25 | 0.95 – 1.35 | 7.75 – 8.75 |

**Table A-4** Results of Effect of Heat Treatments on Tool Life of HSS Tool

| Heat Treatment Temperatures | Average Tool Life (Number of Components) |
|---|---|
| 1200°C | 1332 |
| 1220°C | 851 |
| 1240°C | 1419 |
| 1260°C | 601 |
| 1280°C | 870 |
| 1280°C (Imported HSS tool) | 4163 |
| 1300°C | 1286 |

**Table A-5** Results of Effects of Cutting Conditions on Tool Life of HSS Tool

| Cutting Conditions | Average Tool Life (Number of Components) |
|---|---|
| Dry Cutting | 576 |
| Compressed Air at 31°C | 1517 |
| Chilled Air at 24°C/25°C | 2393 |
| Chilled Air at 18°C | 1525 |

**Table A-6** Results of Interaction Effect Between Heat Treatments and Cutting Conditions

| Heat Treatment Temperatures | Cutting Conditions | | | |
|---|---|---|---|---|
| | Dry Cutting | Compressed Air at 31°C | Chilled Air at 24°C/25°C | Chilled Air at 18°C |
| 1200°C | 685 | 1240 | 1689 | 1714 |
| 1220°C | 533 | 846 | 1221 | 804 |
| 1240°C | 464 | 2003 | 2353 | 857 |
| 1260°C | 522 | 723 | 898 | 262 |
| 1280°C | 381 | 1000 | 1182 | 915 |
| 1280°C(Imported HSS tool) | 867 | 4243 | 6674 | 4867 |
| 1300°C | 579 | 569 | 2736 | 1260 |

**Table A-7** Descriptive Statistics of Two-factor ANOVA

| ANOVA: Two-Factor With Replication | | | | | |
|---|---|---|---|---|---|
| SUMMARY | Dry cutting | Compressed air cutting at 31°C | Chilled air cutting at 25°C/24°C | Chilled air cutting at 18°C | Total |
| ***1200 ℃*** | | | | | |
| Count | 3 | 3 | 3 | 3 | 12 |
| Sum | 2055 | 3720 | 5069 | 5142 | 15986 |
| Average | 685 | 1240 | 1689.666667 | 1714 | 1332.166667 |
| Variance | 72124 | 9100 | 26760.33333 | 164608 | 240722.8788 |
| ***1220 ℃*** | | | | | |
| Count | 3 | 3 | 3 | 3 | 12 |
| Sum | 1599 | 2539 | 3664 | 2412 | 10214 |
| Average | 533 | 846.3333333 | 1221.333333 | 804 | 851.1666667 |
| Variance | 60199 | 68710.33333 | 23105.33333 | 24583 | 97699.9697 |
| ***1240 ℃*** | | | | | |
| Count | 3 | 3 | 3 | 3 | 12 |
| Sum | 1392 | 6010 | 7060 | 2571 | 17033 |
| Average | 464 | 2003.333333 | 2353.333333 | 857 | 1419.416667 |
| Variance | 14956 | 1173116.333 | 295633.3333 | 22096 | 939861.9015 |
| ***1260 ℃*** | | | | | |
| Count | 3 | 3 | 3 | 3 | 12 |
| Sum | 1566 | 2169 | 2694 | 788 | 7217 |
| Average | 522 | 723 | 898 | 262.6666667 | 601.4166667 |
| Variance | 6384 | 279559 | 19152 | 14396.33333 | 119126.447 |
| ***1280 ℃*** | | | | | |
| Count | 3 | 3 | 3 | 3 | 12 |
| Sum | 1145 | 3000 | 3548 | 2747 | 10440 |
| Average | 381.6666667 | 1000 | 1182.666667 | 915.6666667 | 870 |
| Variance | 19077.33333 | 84400 | 28681.33333 | 21004.33333 | 124724.7273 |
| ***1280 ℃ (Imported HSS tool)*** | | | | | |
| Count | 3 | 3 | 3 | 3 | 12 |
| Sum | 2603 | 12730 | 20023 | 14603 | 49959 |
| Average | 867.6666667 | 4243.333333 | 6674.333333 | 4867.666667 | 4163.25 |
| Variance | 8825.333333 | 82533.33333 | 165246.3333 | 92466.33333 | 4882292.568 |
| ***1300 ℃*** | | | | | |
| Count | 3 | 3 | 3 | 3 | 12 |
| Sum | 1739 | 1709 | 8208 | 3782 | 15438 |
| Average | 579.6666667 | 569.6666667 | 2736 | 1260.666667 | 1286.5 |
| Variance | 26777.33333 | 83340.33333 | 339883 | 229189.3333 | 973083.9091 |
| ***Total*** | | | | | |
| Count | 21 | 21 | 21 | 21 | |
| Sum | 12099 | 31877 | 50266 | 32045 | |
| Average | 576.1428571 | 1517.952381 | 2393.619048 | 1525.952381 | |
| Variance | 43640.02857 | 1676740.248 | 3692313.248 | 2188311.048 | |

## CNC Codes for Manufacturing the In-house manufactured HSS tool

```
%
O0541
(PROGRAM NAME - CIRCULAR CUT W101KG54)
(DATE=DD-MM-YY - 20-01-24 TIME=HH:MM - 14:54)
(MCX FILE - D:\MARTZ\W101KG54.1.MCX-9)
(NC FILE - C:\USERS\PRECISION WORKSHOP\DESKTOP\CIRCULAR CUT W101KG54)
(MATERIAL – HIGH-SPEED STEEL - 2024)
G21
(TOOL - 8 OFFSET - 8)
(OD RIGHT 55 DEG INSERT - DNMG 15 06 08)
(FACING)
G0 T0808
M8
G97 S800 M03
G0 G54 X44. Z0.
G99 G1 X-1.6 F.08
G0 Z2.
M9
G28 U0. W0. M05
T0800
M01
(TOOL - 1 OFFSET - 1)
(CENTER DRILL - 10. DIA.)
(CENTER DRILL)
G0 T0101
M8
G97 S1000 M03
G0 G54 X0. Z2.
G1 Z-5. F.02
G0 Z2.
M9
G28 U0. W0. M05
```

```
T0100
M01
(TOOL - 6 OFFSET - 6)
(DRILL 10. DIA.)
(DRILL 10)
G0 T0606
M8
G97 S500 M03
G0 G54 X0. Z2.
G1 Z-12.604 F.03
G0 Z2.
M9
G28 U0. W0. M05
T0600
M01
(TOOL - 8 OFFSET - 8)
(OD RIGHT 55 DEG INSERT - DNMG 15 06 08)
(ROUGHING)
G0 T0808
M8
G97 S700 M03
G0 G54 X40.238 Z.954
G1 X39.531 Z.6 F.1
Z-13.8
X40.498
X41.205 Z-13.446
G0 Z1.15
X39.272
G1 X38.565 Z.796
Z-13.8
X39.931
X40.638 Z-13.446
G0 Z1.154
X38.305
```

```
G1 X37.598 Z.8
Z-13.8
X38.965
X39.672 Z-13.446
G0 Z1.154
X37.339
G1 X36.632 Z.8
Z-13.8
X37.998
X38.705 Z-13.446
G0 Z1.154
X36.372
G1 X35.665 Z.8
Z-13.8
X37.032
X37.739 Z-13.446
G0 Z1.154
X35.406
G1 X34.699 Z.8
Z-2.097
X34.973 Z-2.234
G3 X35.5 Z-2.87 I-.636 K-.637
G1 Z-4.2
Z-13.8
X36.065
X36.772 Z-13.446
G0 Z1.154
X34.439
G1 X33.732 Z.8
Z-1.613
X34.973 Z-2.234
G3 X35.099 Z-2.304 I-.636 K-.637
G1 X35.806 Z-1.95
G0 Z1.154
```

```
X33.473
G1 X32.766 Z.8
Z-1.13
X34.132 Z-1.813
X34.839 Z-1.46
G0 Z1.154
X32.506
G1 X31.799 Z.8
Z-.647
X33.166 Z-1.33
X33.873 Z-.977
G0 Z1.154
X31.54
G1 X30.833 Z.8
Z-.164
X32.199 Z-.847
X32.906 Z-.493
G0 X35.75
X36.207
Z-3.846
G1 X35.5 Z-4.2
G3 X35.274 Z-4.636 I-.9
G1 X34.556 Z-5.284
Z-13.8
X35.9
X36.607 Z-13.446
G0 Z-4.57
X35.663
G1 X34.956 Z-4.924
X33.612 Z-6.136
Z-13.8
X34.956
X35.663 Z-13.446
G0 Z-5.422
```

X34.719

G1 X34.012 Z-5.775

X32.668 Z-6.987

Z-13.8

X34.012

X34.719 Z-13.446

G0 Z-6.273

X33.775

G1 X33.068 Z-6.627

X31.724 Z-7.839

Z-13.8

X33.068

X33.775 Z-13.446

G0 Z-7.125

X32.831

G1 X32.124 Z-7.478

X30.78 Z-8.691

Z-13.8

X32.124

X32.831 Z-13.446

G0 Z-7.976

X31.887

G1 X31.18 Z-8.33

X29.836 Z-9.542

Z-13.8

X31.18

X31.887 Z-13.446

G0 Z-8.828

X30.943

G1 X30.236 Z-9.181

X28.892 Z-10.394

Z-13.8

X29.56

X30.236

```
X30.943 Z-13.446
G0 Z-9.679
X29.999
G1 X29.292 Z-10.033
X27.947 Z-11.245
Z-13.8
X29.292
X29.999 Z-13.446
G0 Z-10.531
X29.055
G1 X28.347 Z-10.884
X27.003 Z-12.097
Z-13.8
X28.347
X29.055 Z-13.446
G0 Z-11.383
X28.111
G1 X27.403 Z-11.736
X26.059 Z-12.948
Z-13.8
X27.403
X28.111 Z-13.446
G0 Z-12.234
X27.166
G1 X26.459 Z-12.588
X25.115 Z-13.8
X26.459
X27.166 Z-13.446
G0 X38.1
M9
G28 U0. W0. M05
T0800
M01
(TOOL - 11 OFFSET - 11)
```

```
(OD GROOVE RIGHT - NARROW INSERT - N151.2-185-20-5G)
(GROOVING)
G0 T1111
M8
G97 S500 M03
G0 G54 X36.398 Z-11.15
G1 X23.5 F.03
G0 X36.398
X44.
Z-13.9
G1 X23.5 F.04
G0 X44.
Z-8.4
X39.446
G1 X23.5
G0 X39.446
X39.5
G1 X35.5 F.05
X23.3
Z-8.7
Z-11.15
G0 X44.498
Z-13.9
G1 X40.498
X30.96
X23.3
Z-11.15
G0 X40.498
M9
G28 U0. W0. M05
T1100
M01
(TOOL - 10 OFFSET - 10)
(OD FINISH RIGHT - 35 DEG.  INSERT - VNMG 16 04 08)
```

```
(OD FINISH)
G0 T1010
M8
G97 S1000 M03
G0 G54 X31.633 Z.236
G1 X30.926 Z-.117 F.07
X35.066 Z-2.187
G3 X35.3 Z-2.47 I-.283 K-.283
G1 Z-4.4
X36.007 Z-4.046
M9
G28 U0. W0. M05
T1000
M01
(TOOL - 3 OFFSET - 3)
(ID ROUGH MIN. 8. DIA. - 80 DEG.  INSERT - CCMT 09 T3 04)
(BORING)
G0 T0303
M8
G97 S600 M03
G0 G54 X10.791 Z1.25
Z1.2
G1 Z.7 F.06
Z-4.308
X10. Z-4.993
Z-4.493
G0 Z1.2
X11.581
G1 Z.7
Z-3.623
X10.391 Z-4.655
Z-4.155
G0 Z1.2
X12.372
```

```
G1 Z.7
Z-2.939
X11.181 Z-3.97
Z-3.47
G0 Z1.2
X13.162
G1 Z.7
Z-2.254
X11.972 Z-3.285
Z-2.785
G0 Z1.2
X13.953
G1 Z.7
Z-1.569
X12.762 Z-2.6
Z-2.1
G0 Z1.2
X14.744
G1 Z.7
Z-.885
X13.553 Z-1.916
Z-1.416
G0 Z1.2
X15.534
G1 Z.7
Z-.2
X14.344 Z-1.231
Z-.731
(ID FINISH)
G0 Z.3
X15.765
G1 Z-.2
X10.107 Z-5.1
G2 X10. Z-5.3 I.347 K-.2
G1 Z-9.3
X9.293 Z-8.946
G0 Z1.25
M9
G28 U0. W0. M05
T0300
M01
(TOOL - 11 OFFSET - 11)
(OD GROOVE RIGHT - NARROW INSERT - N151.2-185-20-5G)
(CUTOFF)
G0 T1111
M8
G97 S500 M03
G0 G54 X37.9 Z-13.6
X31.3
G1 X27.3 F.05
X-.2
X3.8
G0 X27.3
M9
G28 U0. W0. M05
T1100
M30
%
```